Pulsar/Stellar wind collision in 3D and The origin of the X-ray-emitting object moving away from PSR B1259-63

Barkov M.V.

INASAN, Russia

Theoretical slides

Numerical slides

Observational slides

The origin of the X-ray-emitting object moving away from PSR B1259-63

(Pavlov et al 2015)

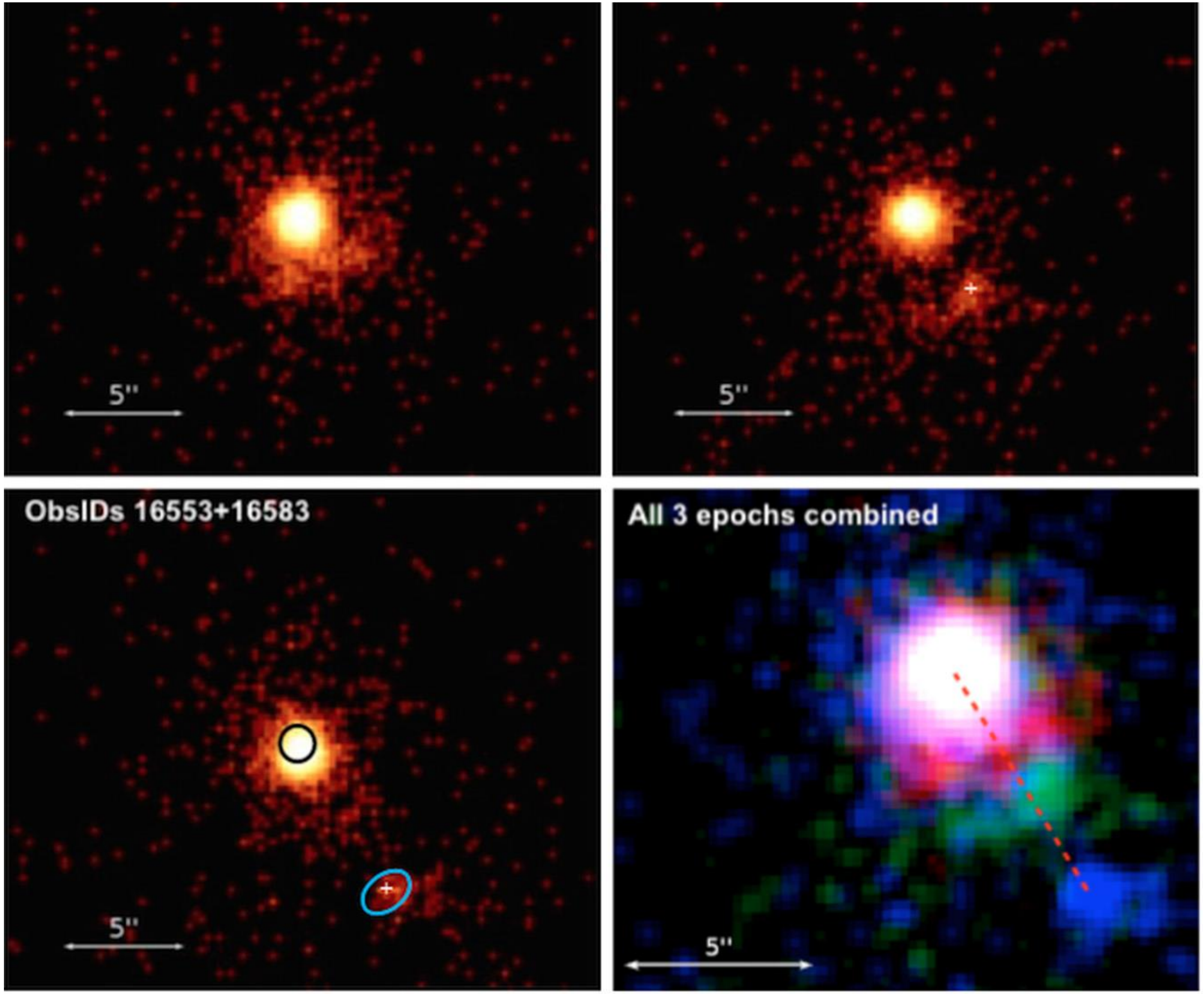

$L_{sd}=8\times10^{35}$ erg/s

$L_x=10^{31}$ erg/s

If it is thermal X-ray:
$M_c=10^{29}$ g
$T_{orb}\ dM_{wind}/dt < 10^{26}$ g

The origin of the X-ray-emitting object moving away from PSR B1259-63

(Pavlov et al 2015)

If it is thermal X-ray:
$M_c=10^{29}$ g
$L_k = 10^{40}$ erg/s
$T_{orb}\, dM_{wind}/dt < 10^{26}$ g
$L_{star} = 3\times10^{37}$ erg/s

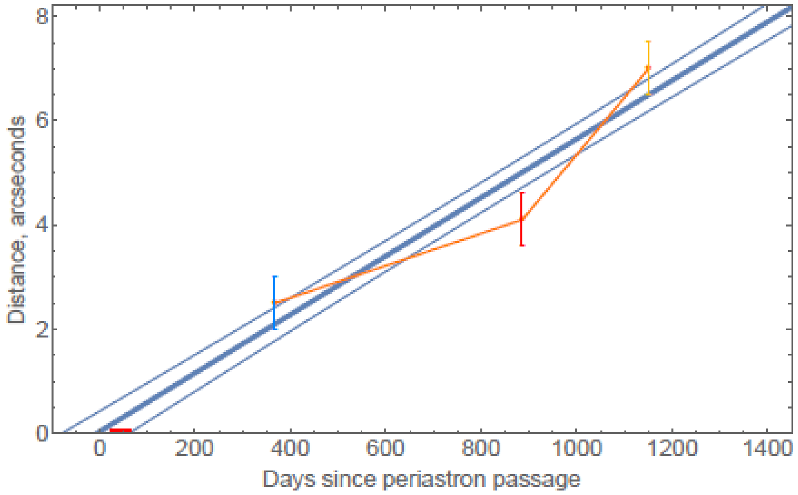

Linear fit: V = (0.07+/-0.01)c

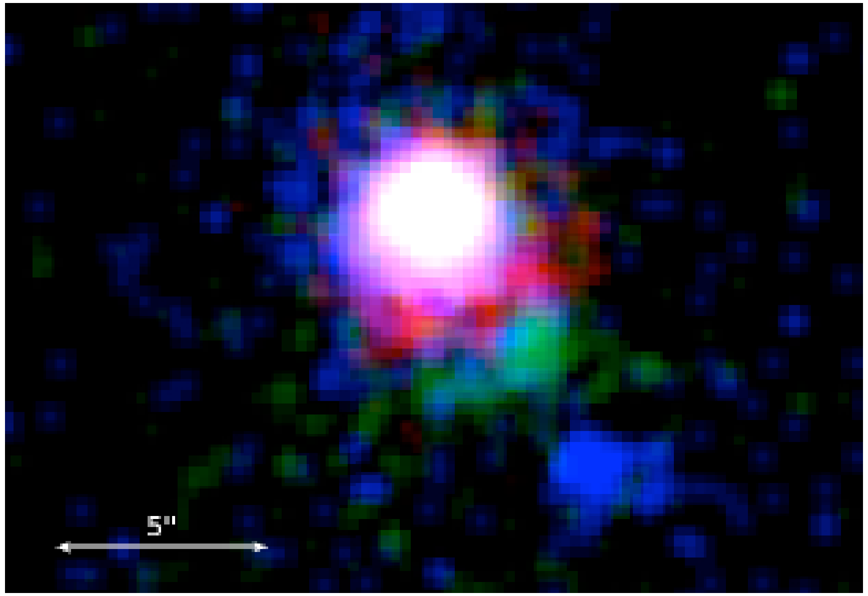

Between 3rd and 4th observations the extended structure moved by 2.5'' ±0.5''.

This corresponds to the apparent proper motion

V=(0.13±0.03)c
at d = 2.3 kpc

Apparent acceleration (?)
90±40 cm s^{-2}

Binary Systems in VHE Regime

Object	PSR B1259	LS 5039	J0632	J2032	J1086	LS I +61 303	Cyg X-1
Type	O8+Pulsar	O6+?	Be+?	B0+Pulsar	O6+?	Be+?	O9+BH
L_s, erg/s	3×10^{37}	7×10^{38}	10^{38}	10^{38}	7×10^{38}	10^{38}	1.3×10^{39}
Orbit Size, cm	$10^{13} - 10^{14}$	$10^{12} - 3 \times 10^{12}$	$10^{13} - 7 \times 10^{13}$	$10^{13} - 5 \times 10^{14}$	$\sim 10^{13}$	$2 \times 10^{12} - 10^{13}$	3×10^{12}
Eccentricity	0.87	0.31	0.83	0.97	0.25?	0.72	0
Inclination	35	10-75	10?	20-50	???	~30	~30
HE Instrument	EGRET Fermi	EGRET Fermi	Fermi	Fermi	Fermi	EGRET Fermi	AGILE
GeV detection	LC+Spctr	LC+Spctr	LC+Spctr	LC+Spectr	LC+Spctr	LC+Spctr	Point
VHE Instrument	HESS	HESS	HESS, MAGIC VERITAS	VERITAS, MAGIC	HESS	MAGIC VERITAS	MAGIC HESS
TeV detection	~20σ	~100σ	~50σ	~20σ	~10σ	~10σ	4σ
signal	periodic	Periodic, variable	periodic	flare	periodic	Periodic, variable	flare

Binary Systems orbits

Dubus et al 2013

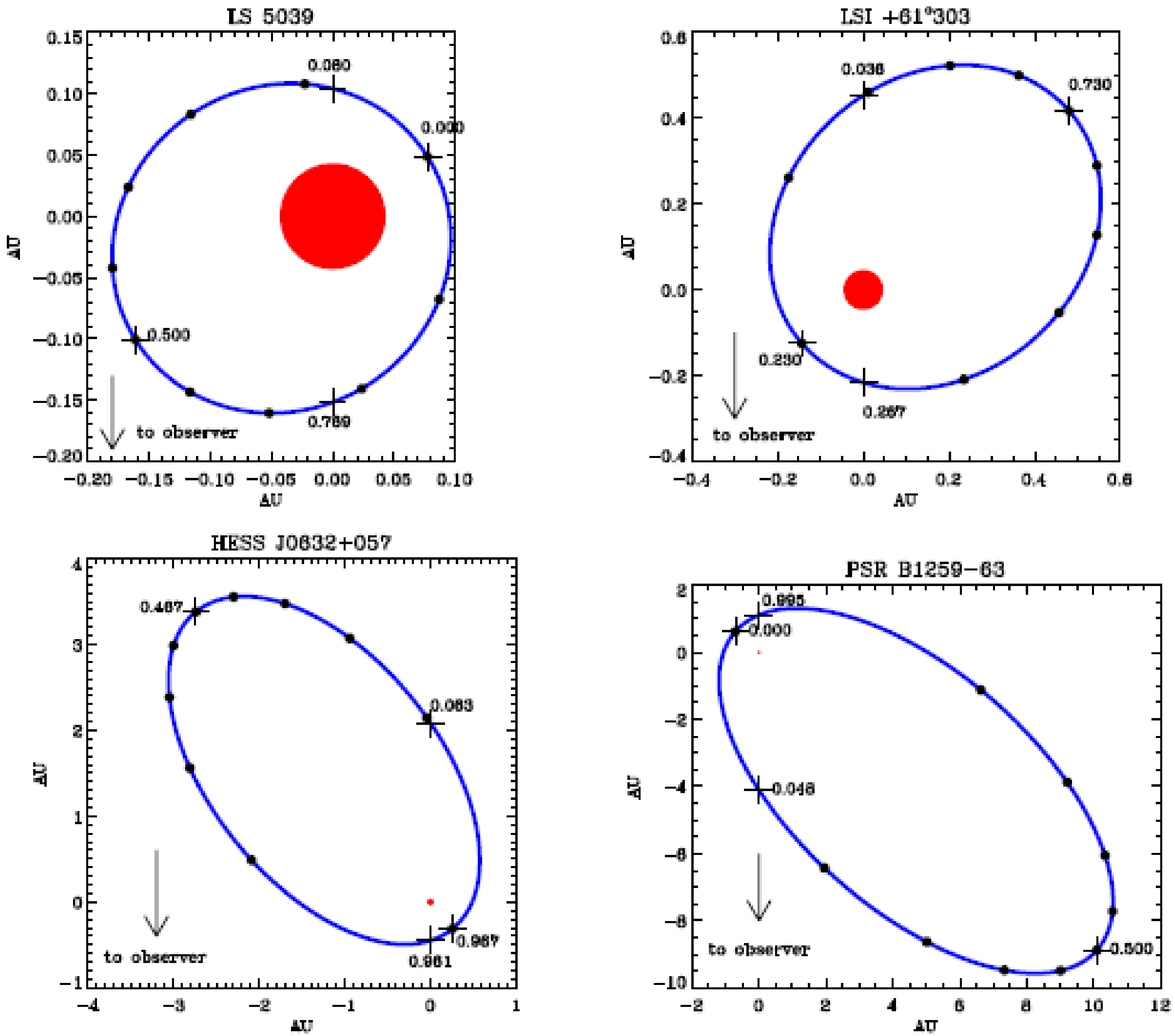

H.E.S.S.

The best studied system in VHE is LS5039

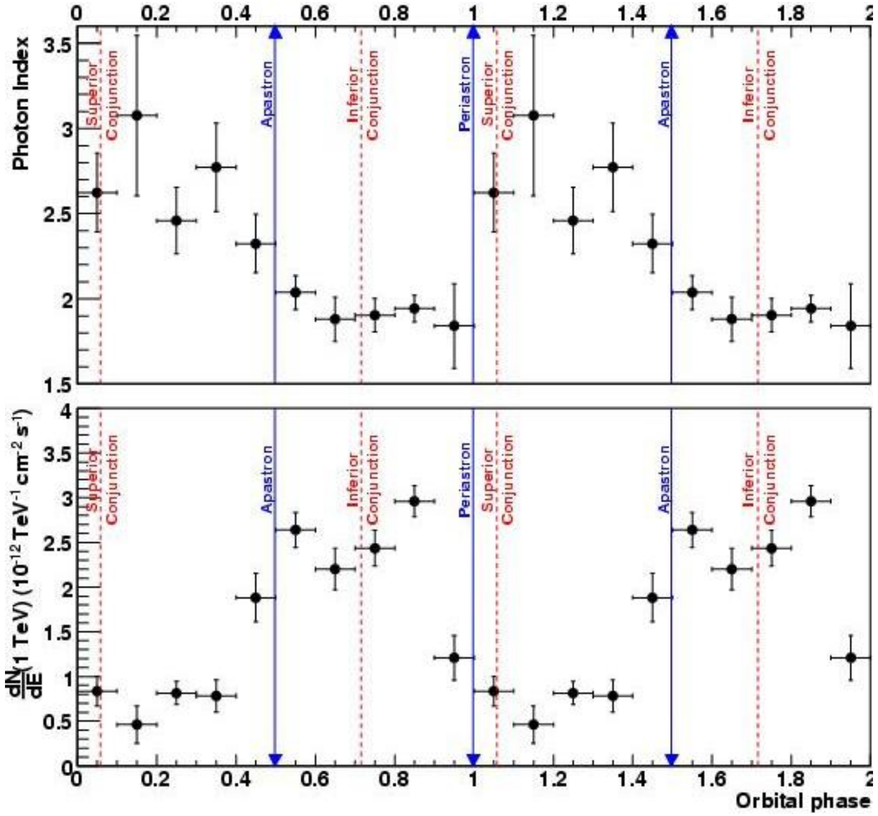

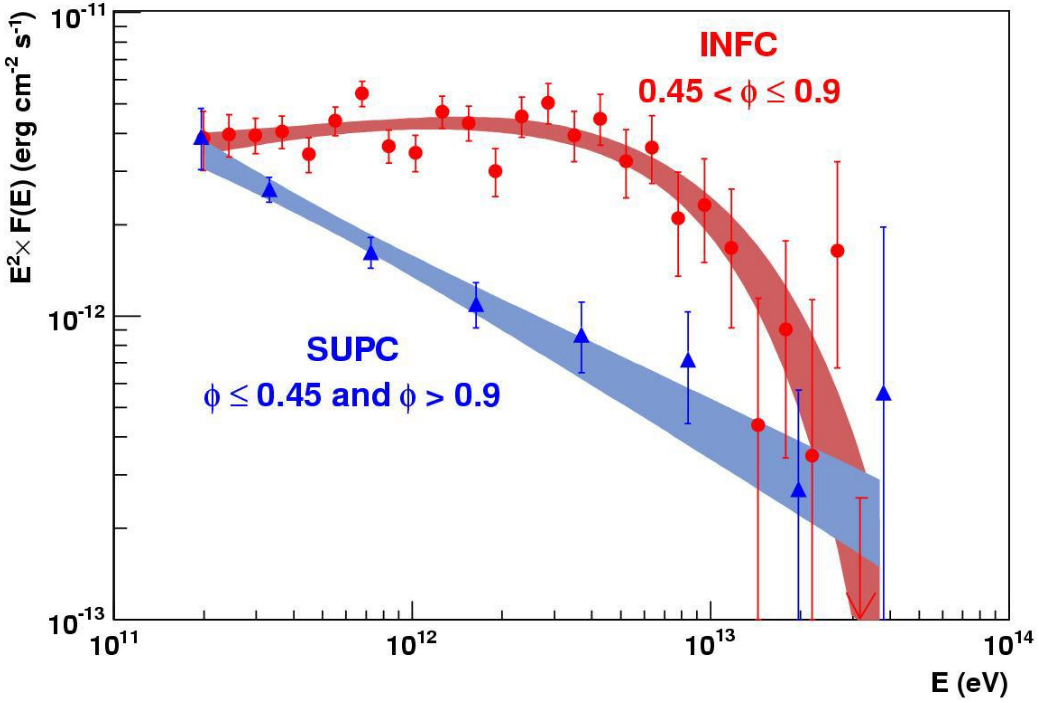

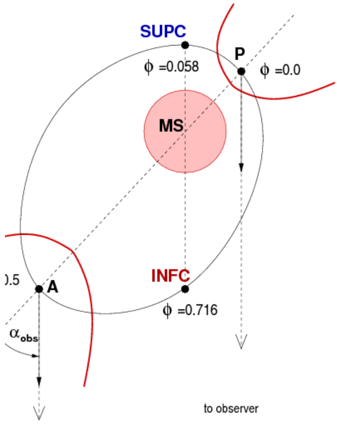

Fermi Observations of LS 5039

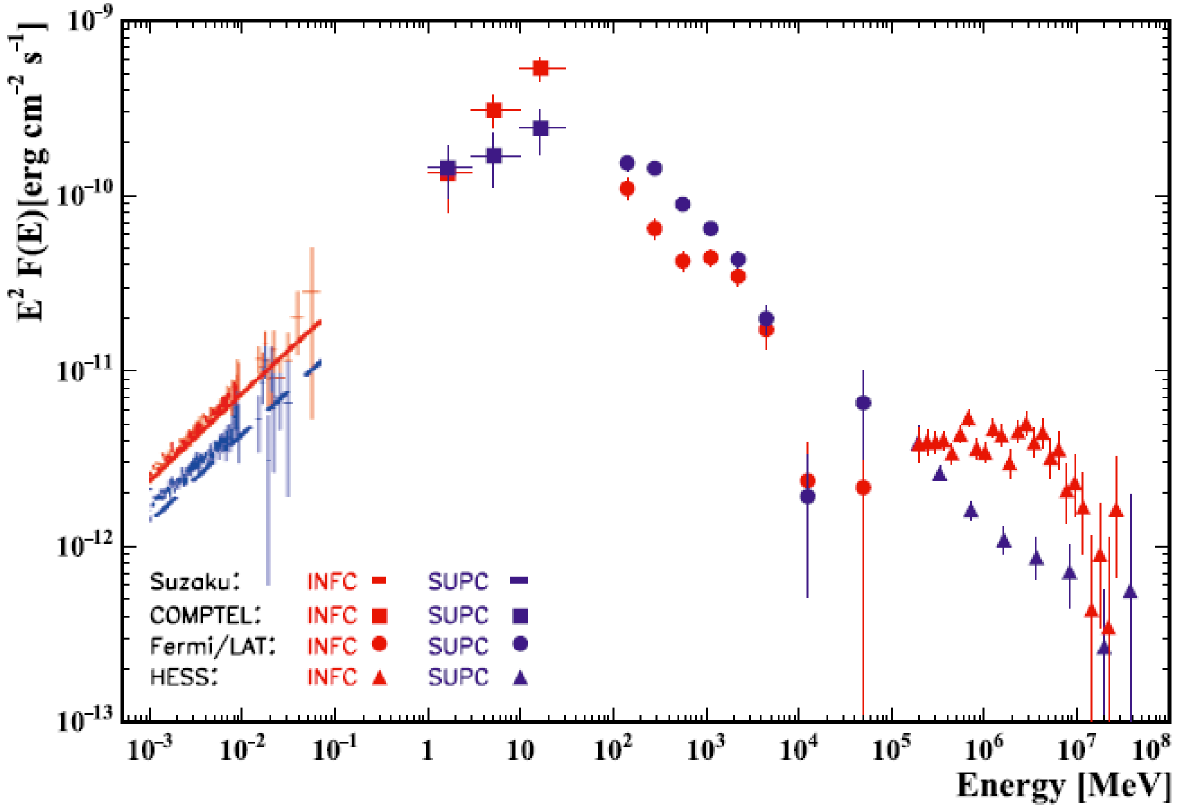

Spectrum with a HE cutoff @ a few GeV

L_{GeV}=$2 \times 10^{35}\ erg/s$

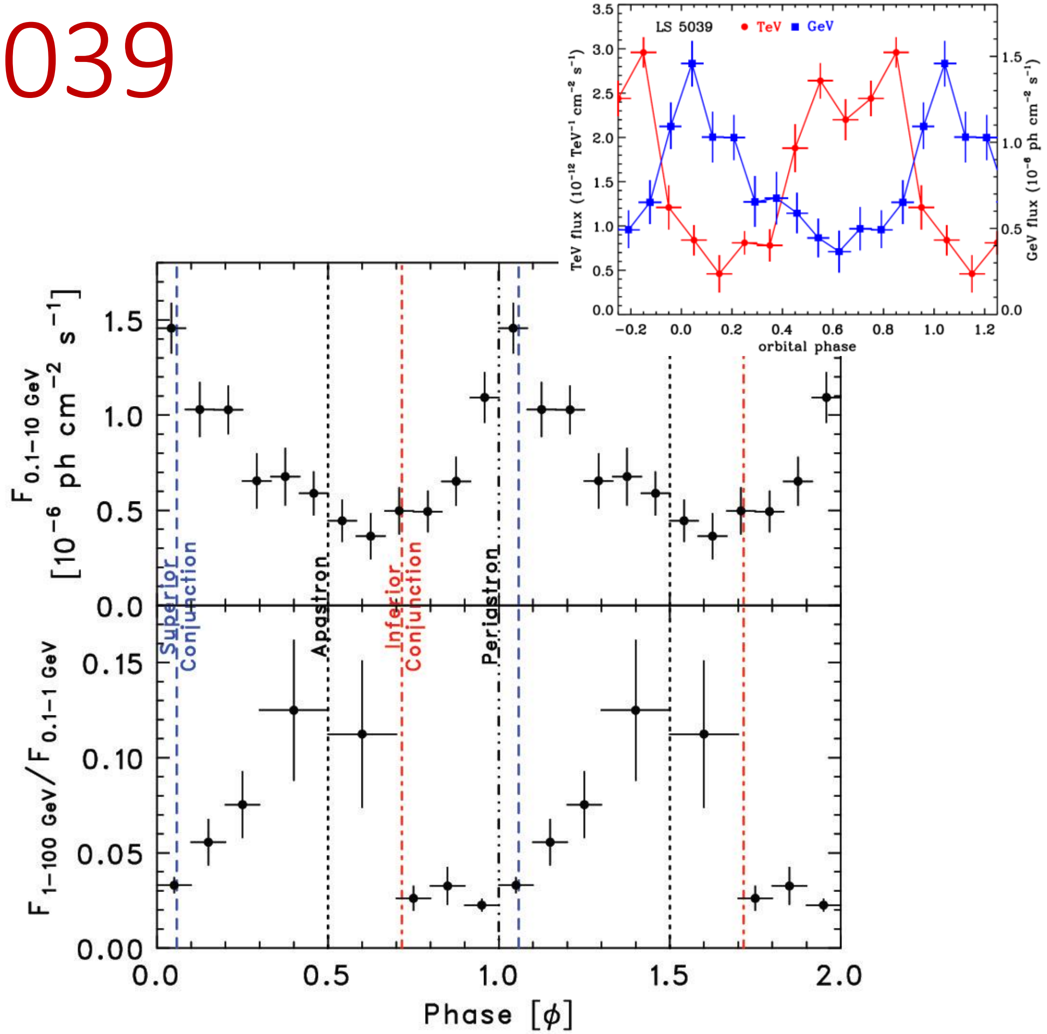

Lightcurve in GeV has a maximum close to the periastron

What are the Scenarios?

Binary Pulsar

Jet from spherical accretion to BH

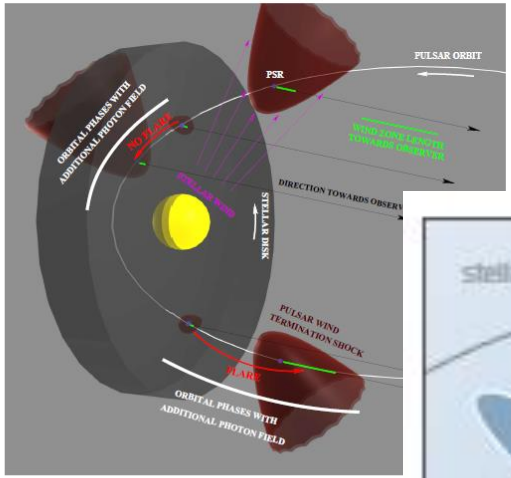

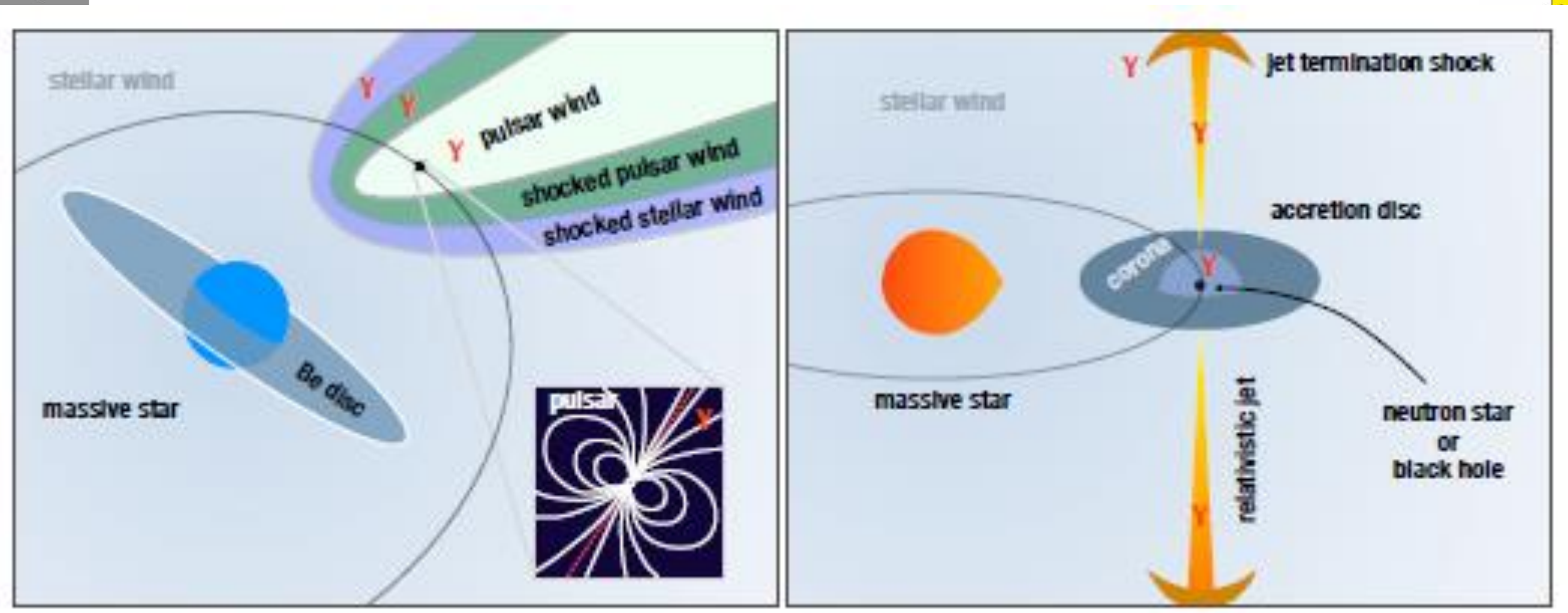

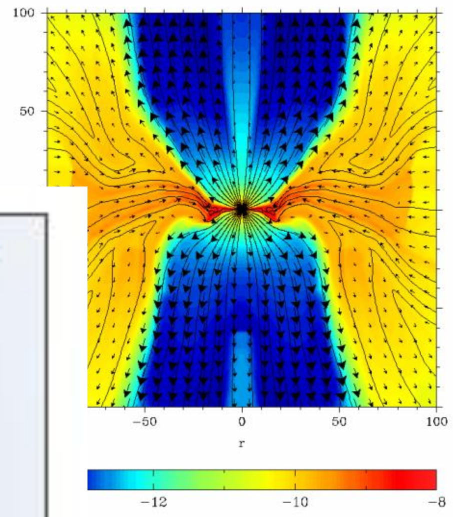

(Khangulyan et al 2012)

(MVB & Khangulyan 2012)

The parameters of the system LS5039

Table : Casares et al. 2005 and Sarty et al 2011

Description	Designation	Value
Mass of star	M_s	$26 M_\odot$
Radius of star	R_s	$9.3 R_\odot$
Temperature of the star	T_s	39, 000 K
Stellar Wind termination velocity	V_∞	2, 400 km/s
Stellar Wind loss rate	$\dot{M}_s$	$4 \times 10^{-7} \mathrm{M}_\odot \mathrm{yr}^{-1}$
Orbital period	P_s	3.9 day
Eccentricity of the orbit	e	0.24
The mass of the BH	M_{BH}	$3 M_\odot$
Semimajor axis	a_o	$3.5 R_s$

Jet lunched by spherical accretion of magnetized wind to rotating BH

ρ ρ

$\frac{B_\varphi}{B_p}$ $\frac{P_g}{P_m}$

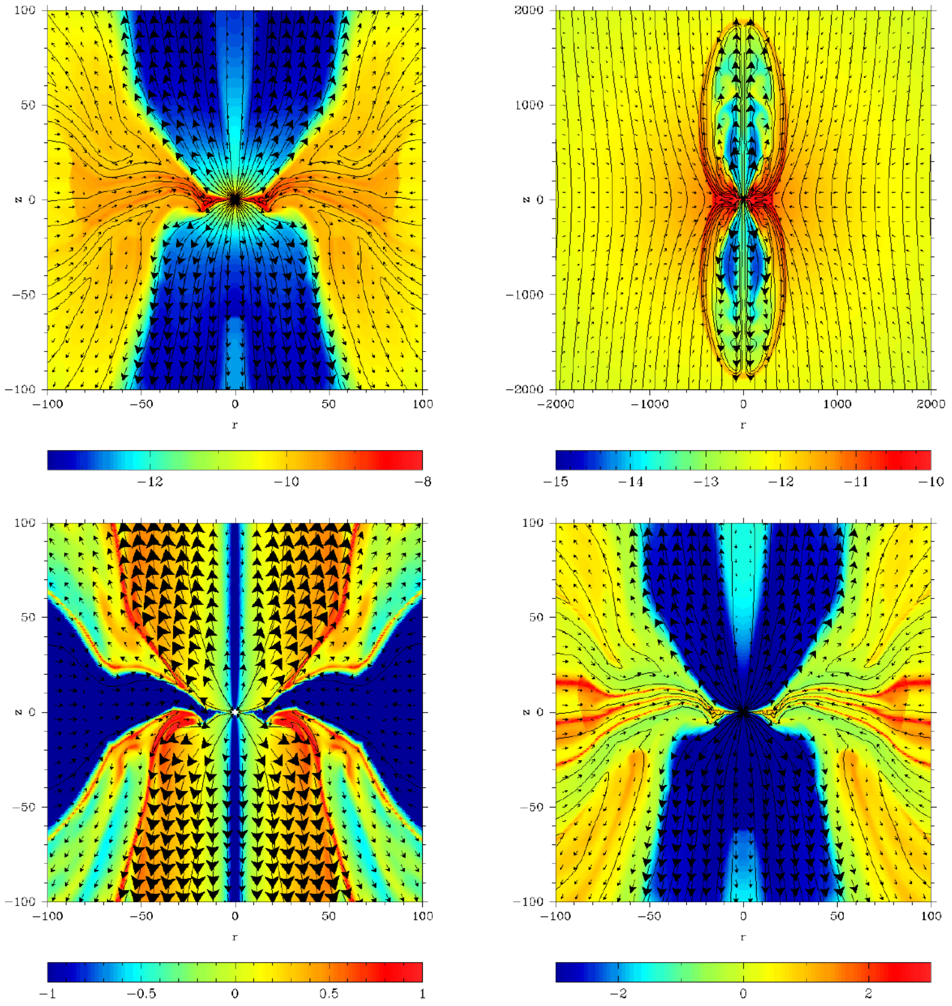

(MVB & Khangulyan 2012)

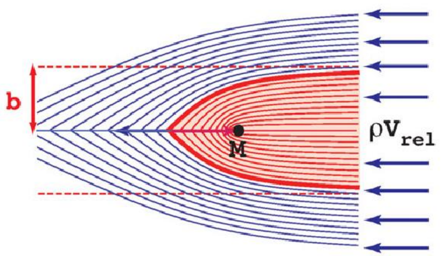

Owocki et al 2011

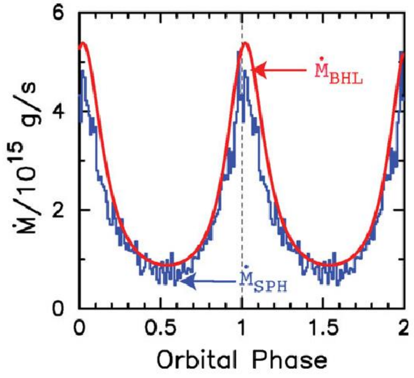

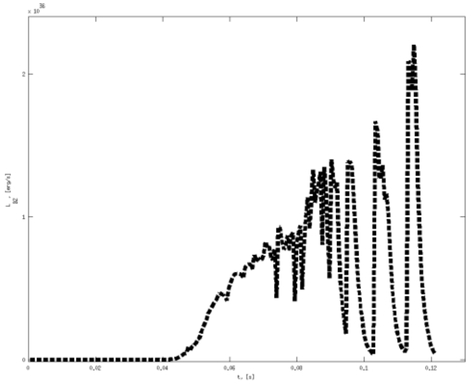

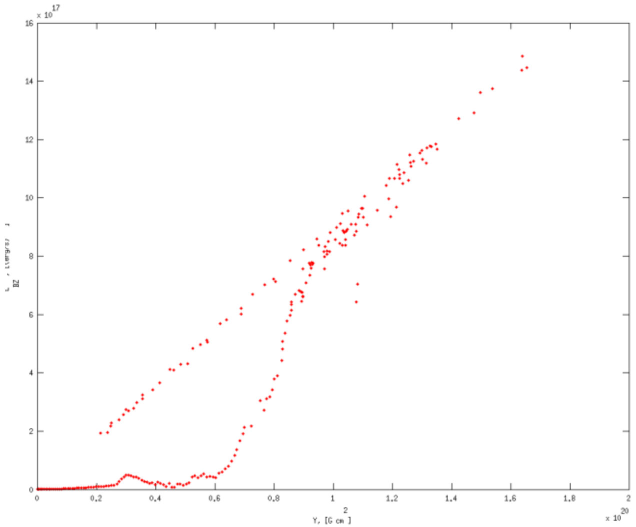

Jet formation from spherical accretion of magnetized wind to rotating BH

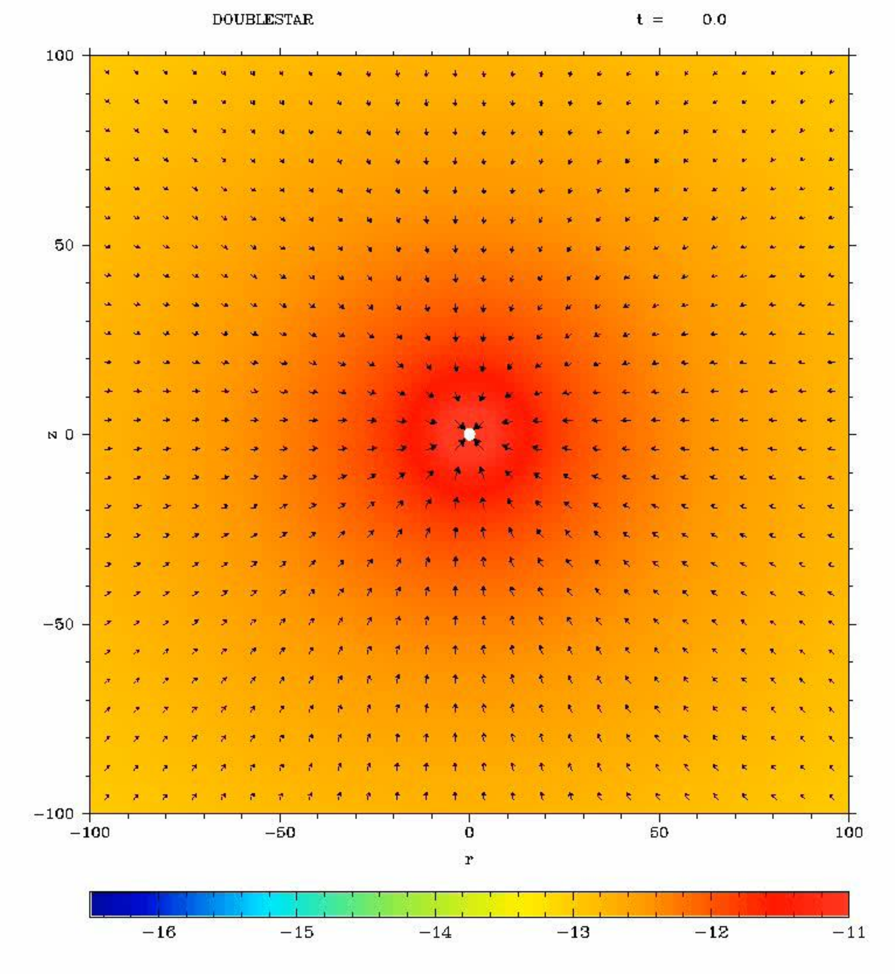

(MVB & Khangulyan 2012)

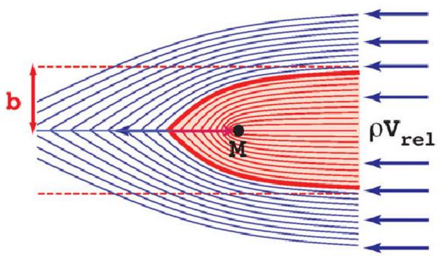

Owocki et al 2011

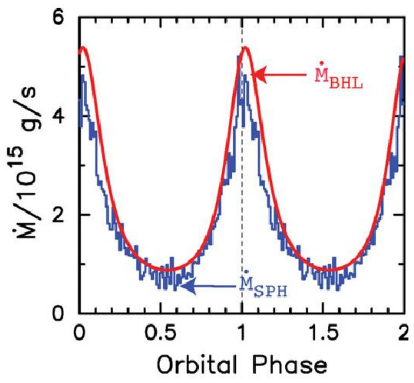

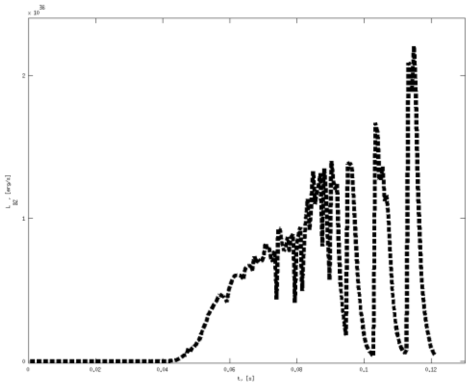

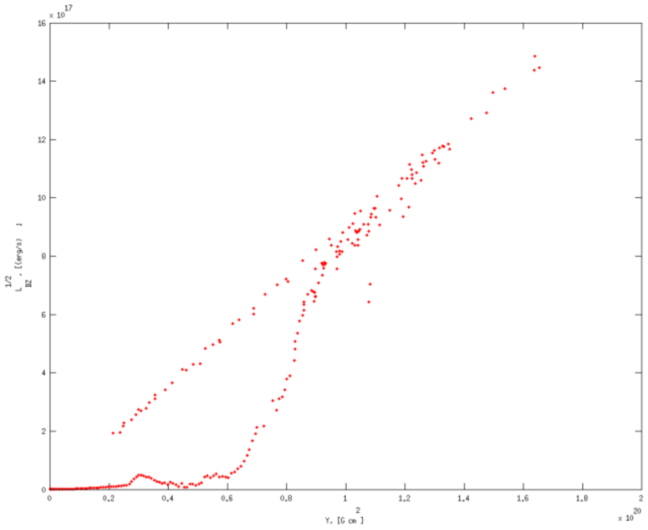

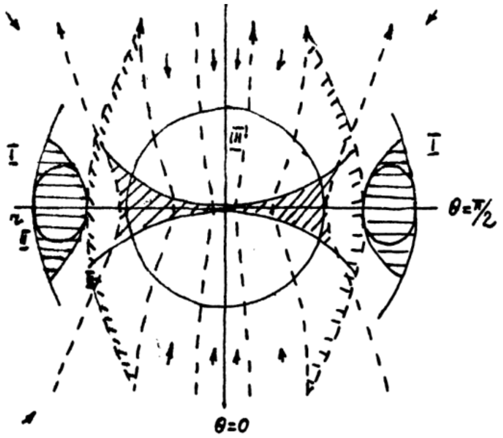

Bisnovatyi-Kogan&Ruzmaikin 1976

Stellar wind collision

$$r_{\mathrm{WR}} = \frac{1}{1+\eta^{1/2}}\,D, \quad r_{\mathrm{OB}} = \frac{\eta^{1/2}}{1+\eta^{1/2}}\,D$$

$$\eta = \frac{\dot{M}_{\mathrm{OB}} V^{\infty}_{\mathrm{OB}}}{\dot{M}_{\mathrm{WR}} V^{\infty}_{\mathrm{WR}}}$$ (non-relativistic)

cally by Girard & Willson (1987). The results of the calculations may be approximated by the following analytic equation (L. M. Ozernoy 1991, private communication)

$$\theta \simeq 2.1\left(1 - \frac{\eta^{2/5}}{4}\right)\eta^{1/3} \quad \text{for } 10^{-4} \le \eta \le 1 \qquad (3)$$

Eichler & Usov 1993

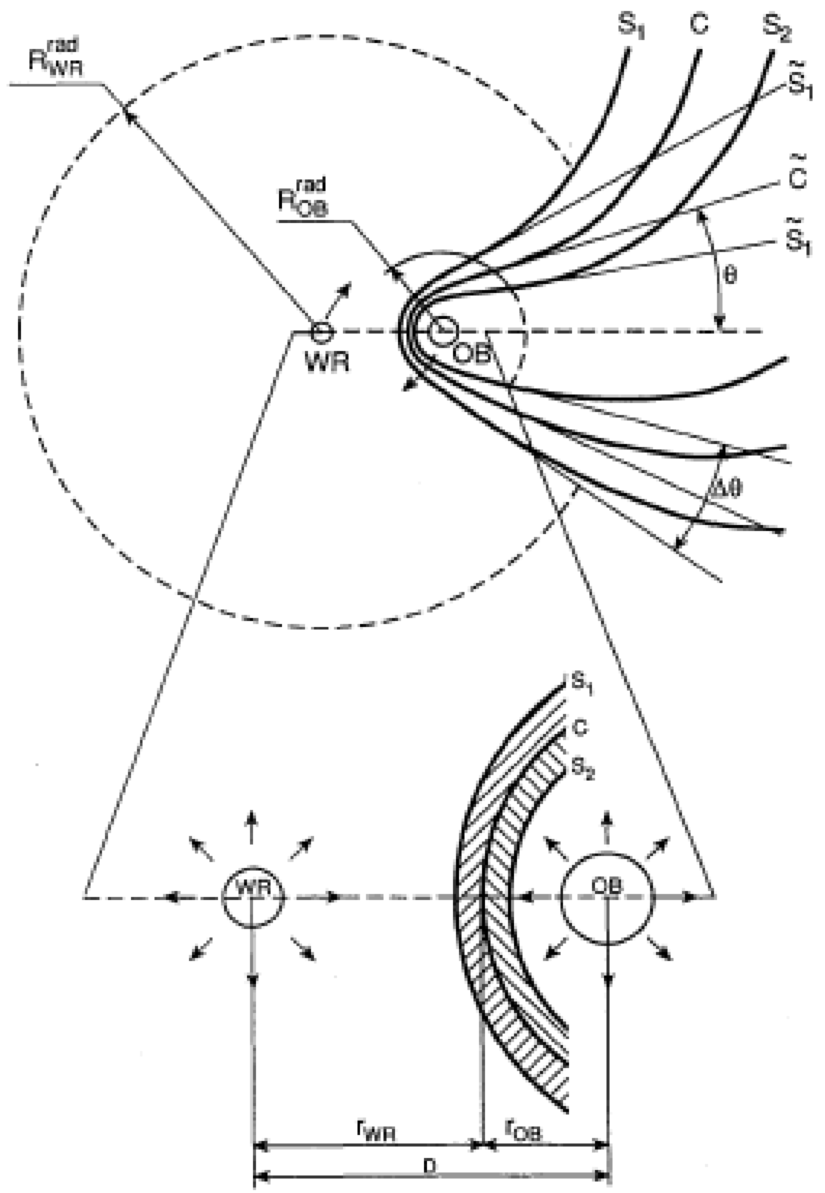

Stellar wind collision

(Romero et al. 2007) SPH Newton, LS I+61 303

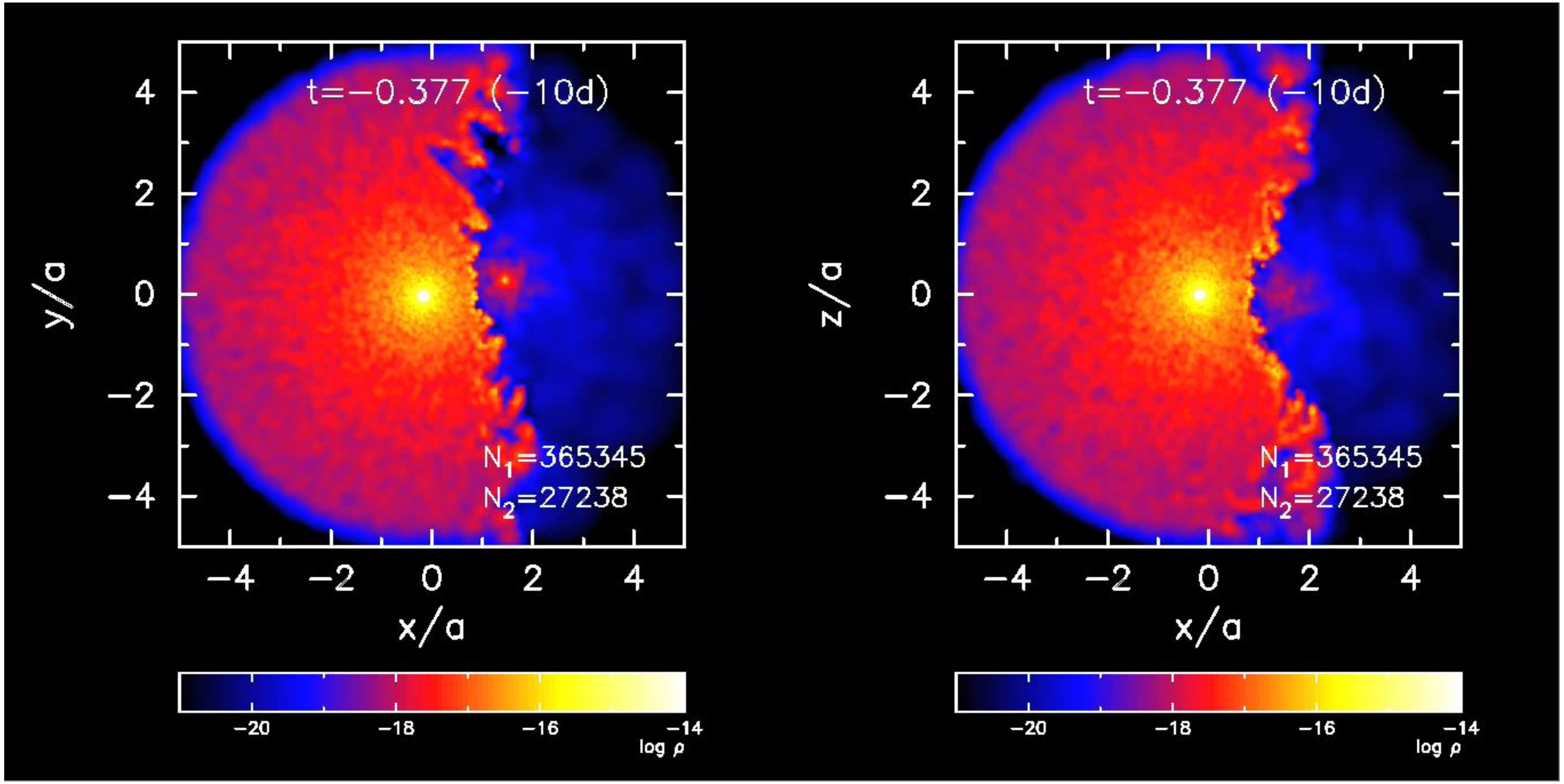

Stellar wind collision

$$\eta = \frac{L_{sd}}{\dot{M} v_w c}$$

(Bogovalov et al. 2008,2012) 2D RHD, RMHD

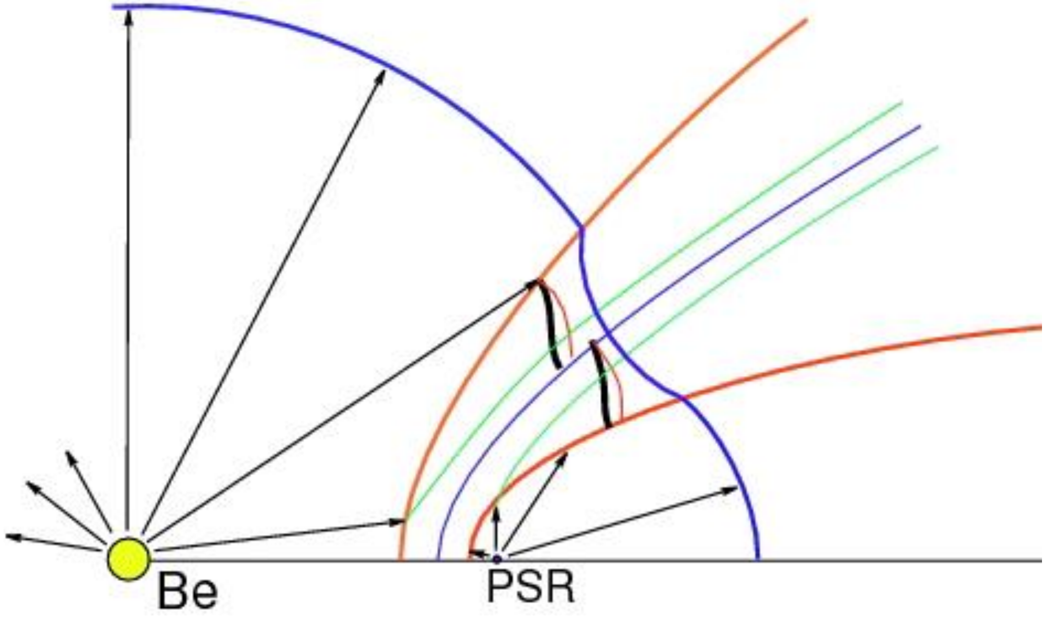

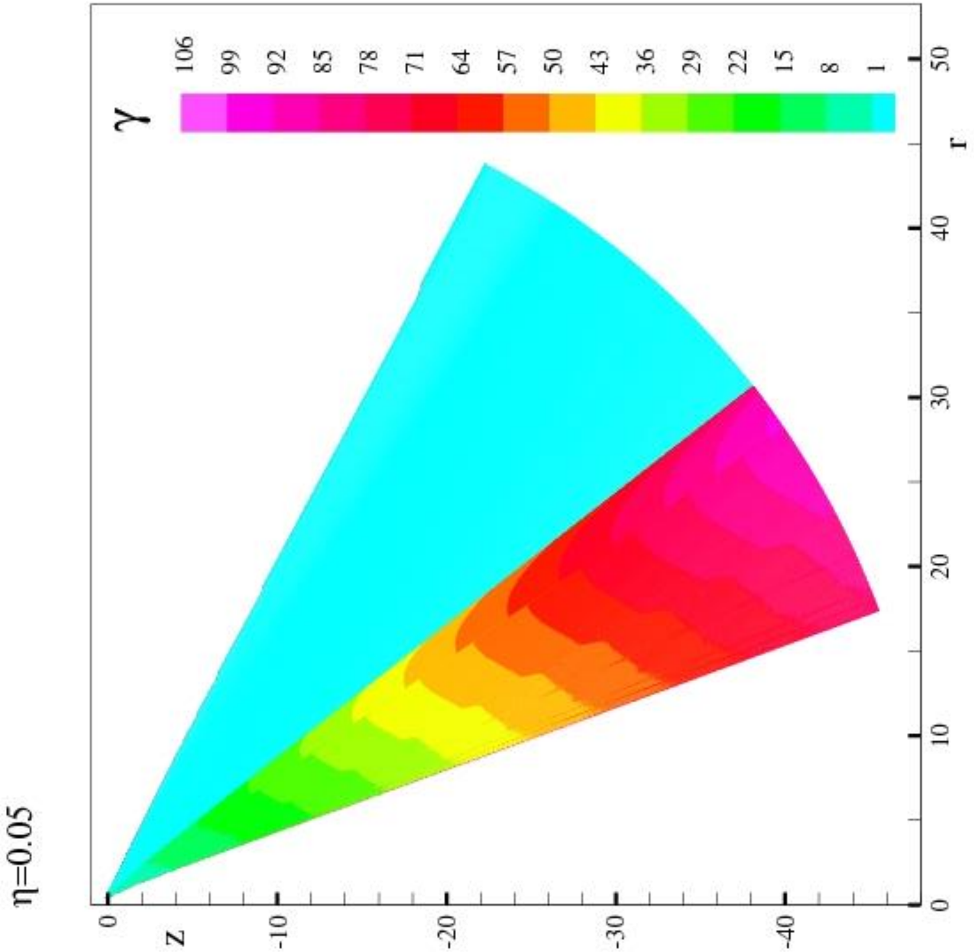

How to form back shock without orbital motion?

- $\eta = 0.001$ $\eta = 0.05$

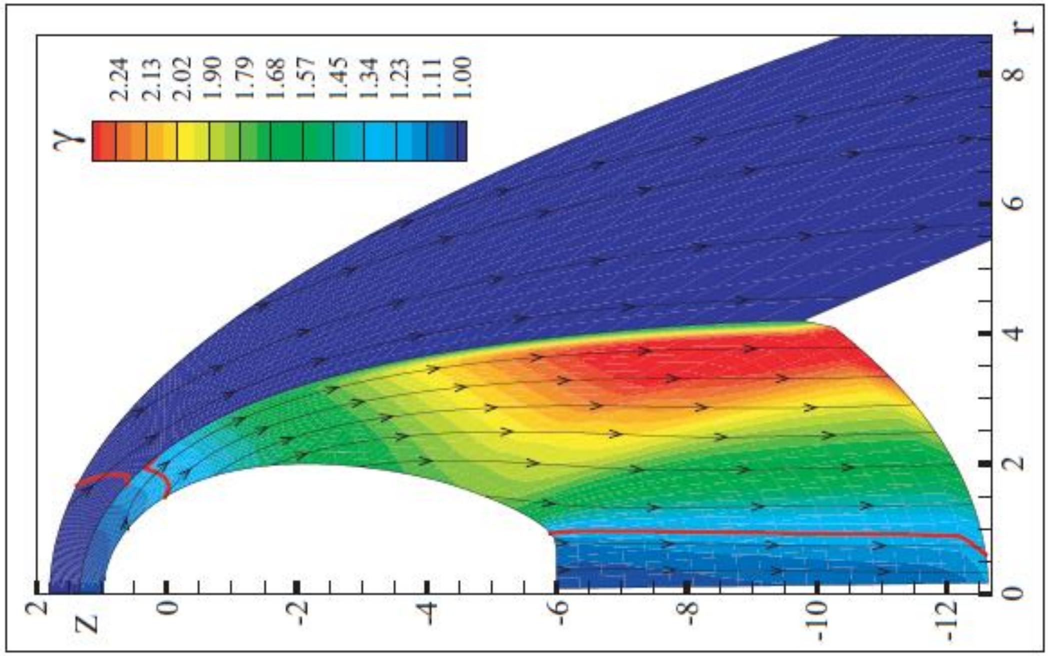

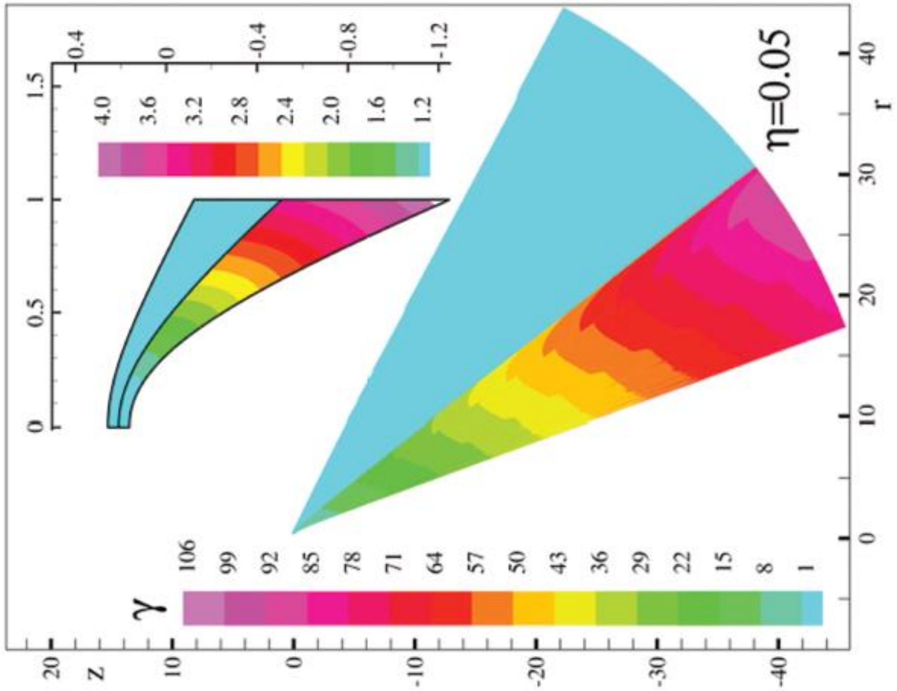

How to form back shock without orbital motion?

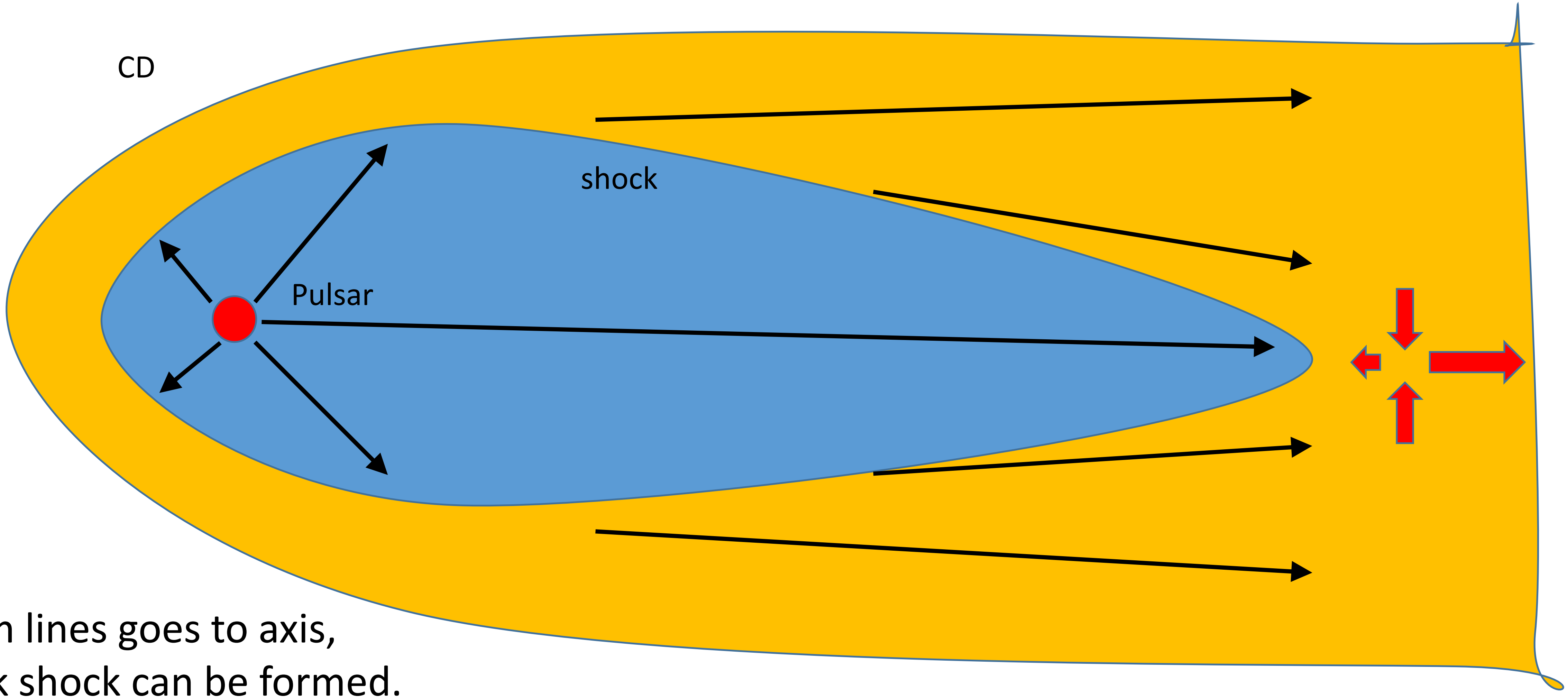

If stream lines goes to axis,
the back shock can be formed.

Stellar wind collision + orbital motion

(Bosch-Ramon & MVB 2011)

$$x \sim 3\eta^{1/2} v_w / 2\Omega$$

$$v_{exp} \sim 10^9 L_{sd37}^{1/2} \dot{M}_{-6.5}^{-1/2} cm/s$$

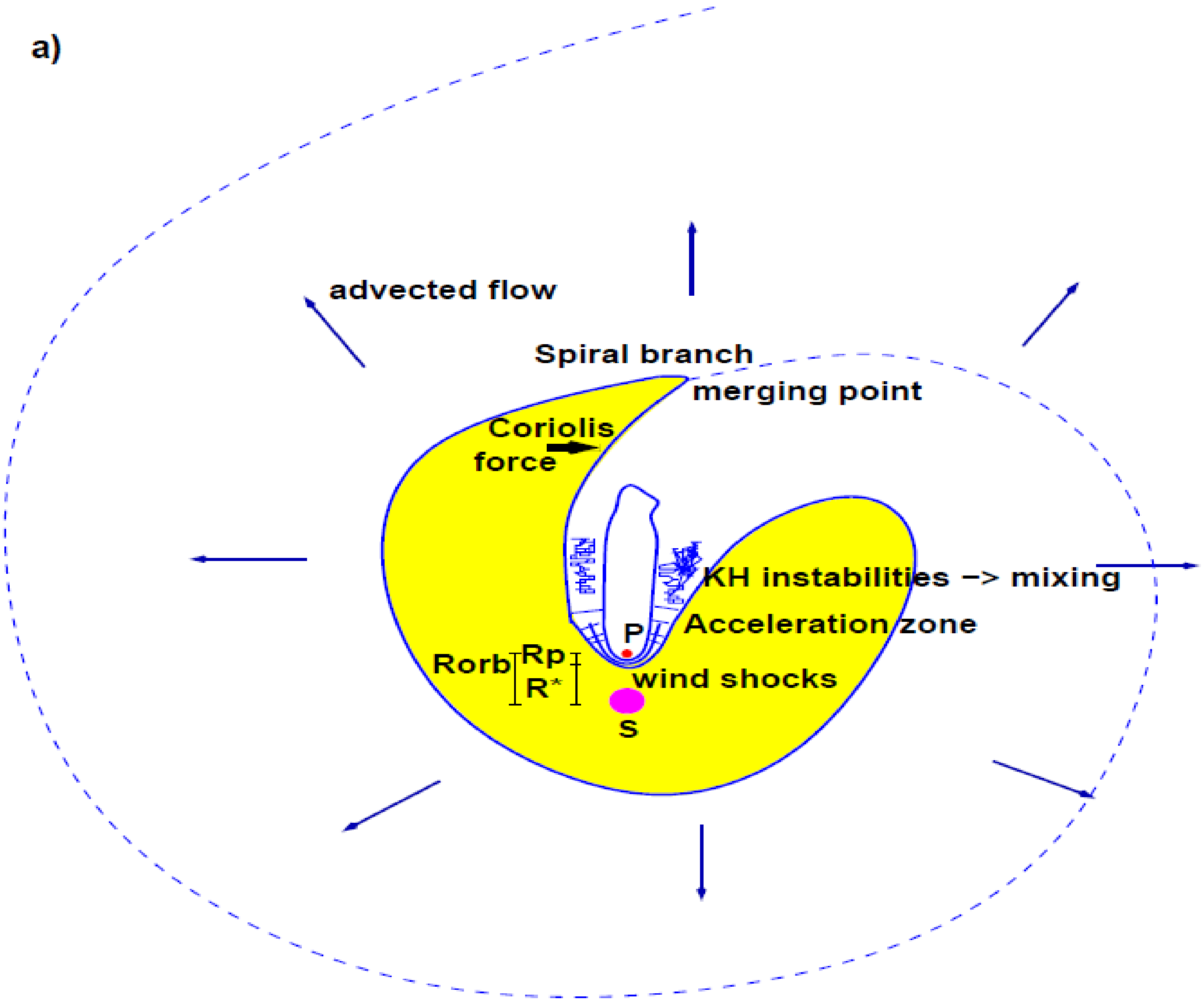

Stellar wind collision + orbital motion

(Bosch-Ramon & MVB 2011)

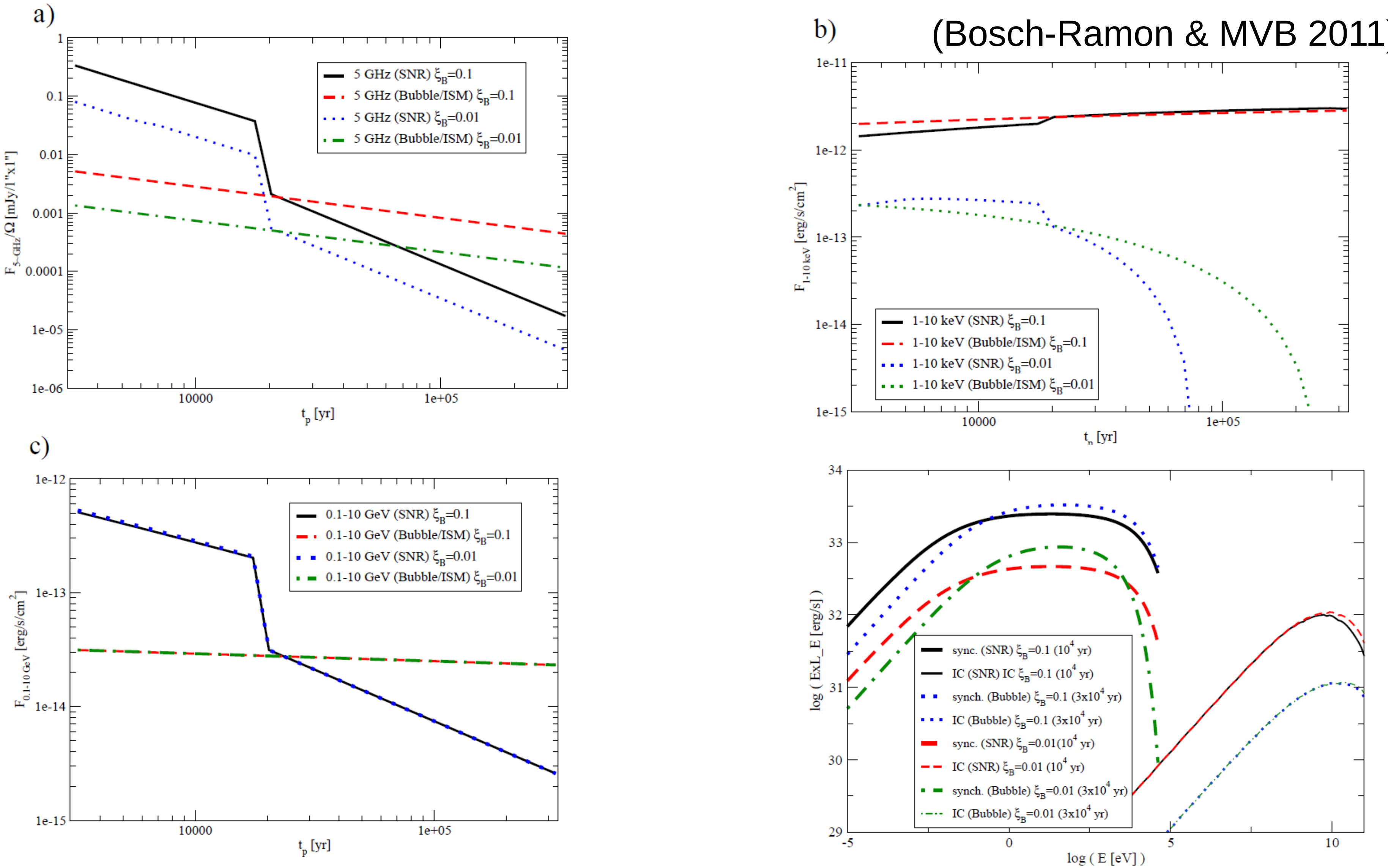

Density and tracer (Newton HD)

$$\eta = \frac{L_{sd}}{\dot{M} v_w c}$$

(Lamberts et al. 2012)
Outflow is stable.

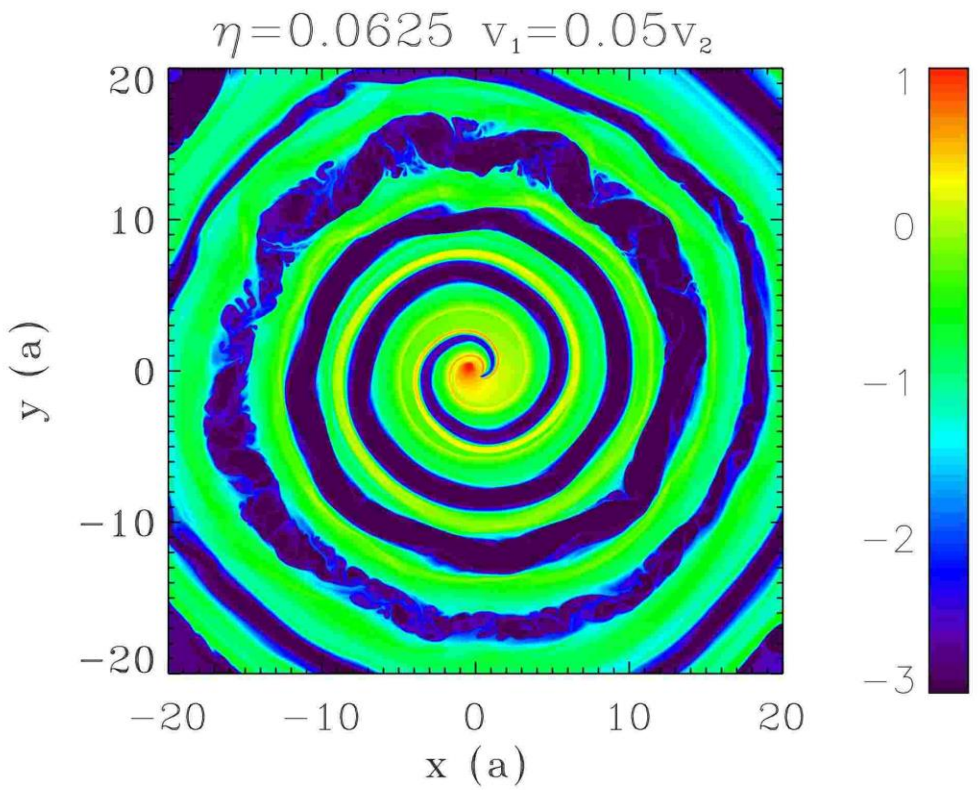

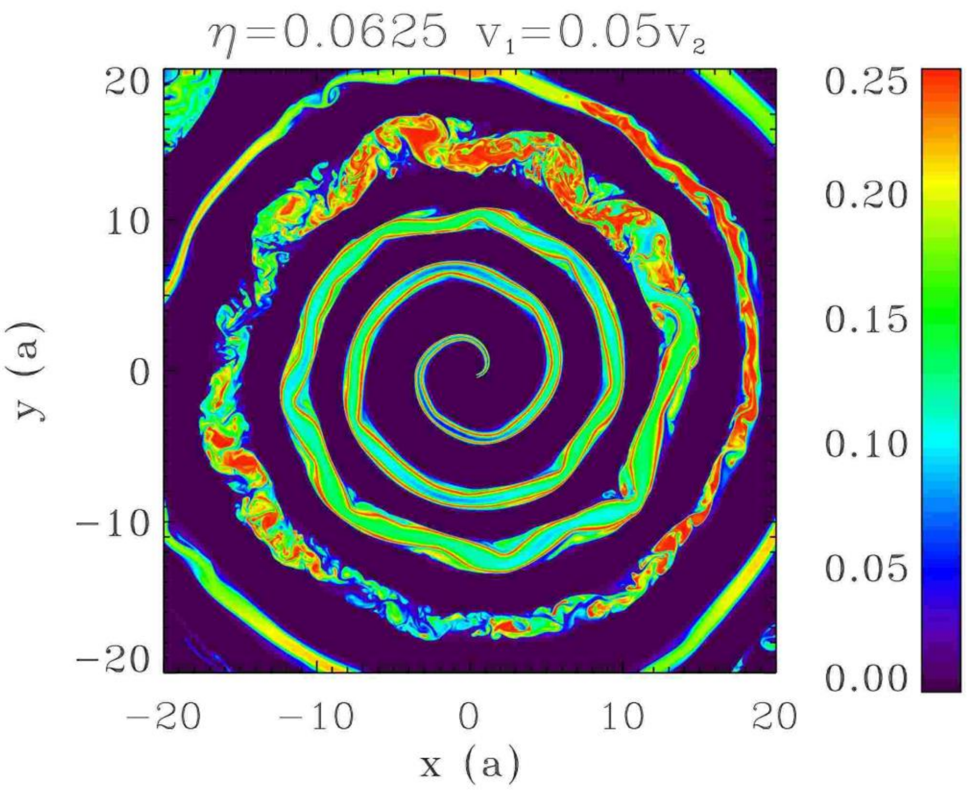

Density Γ= 2; η = 0.6

$$\eta = \frac{L_{sd}}{\dot{M} v_w c}$$

(Bosch-Ramon, MVB, Khangulyan and Perucho 2012)
2D RHD, PLUTO with AMR Chombo

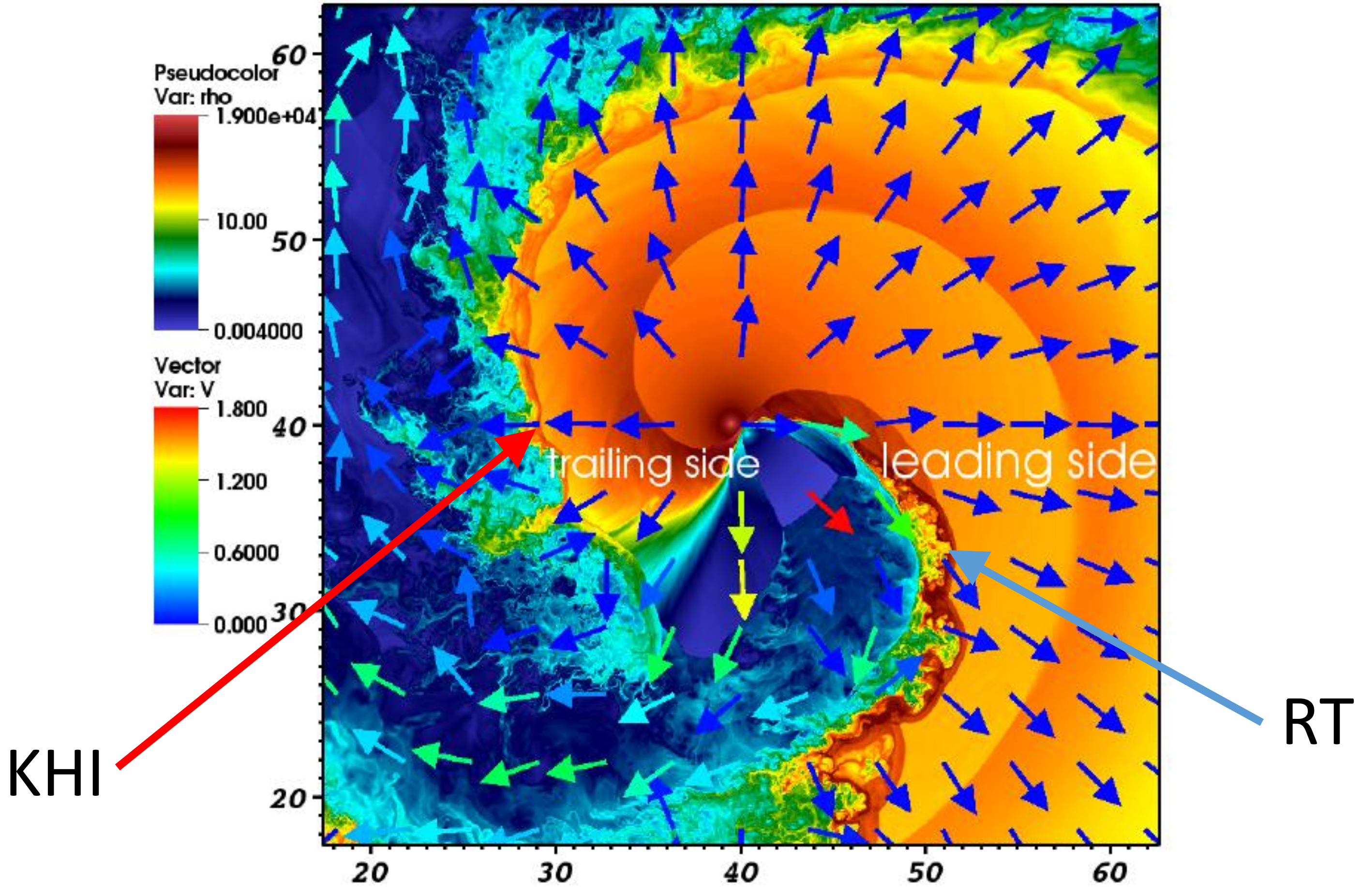

(Lamberts et al. 2013) RHD
Outflow is unstable.

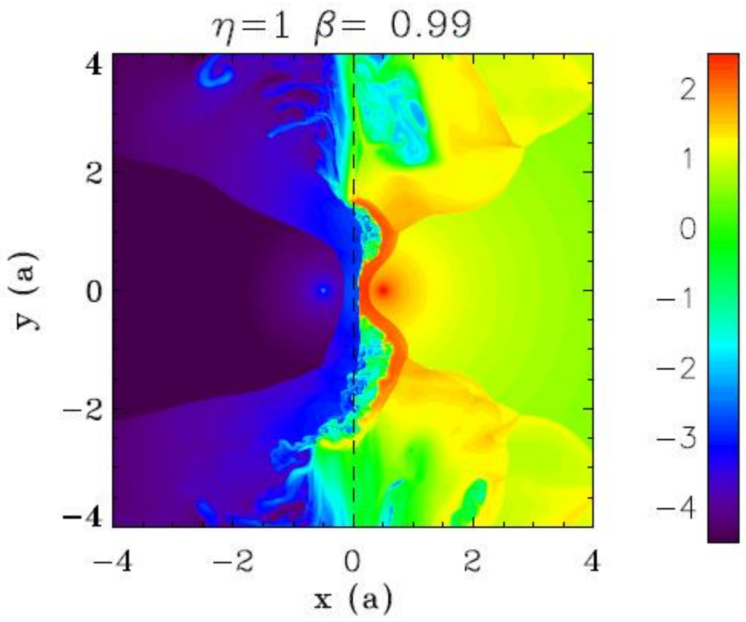

Density Γ= 2; η = 0.6

$$\eta = \frac{L_{sd}}{\dot{M} v_w c}$$

(Bosch-Ramon, MVB, Khangulyan and Perucho 2012)
2D RHD, PLUTO with AMR Chombo

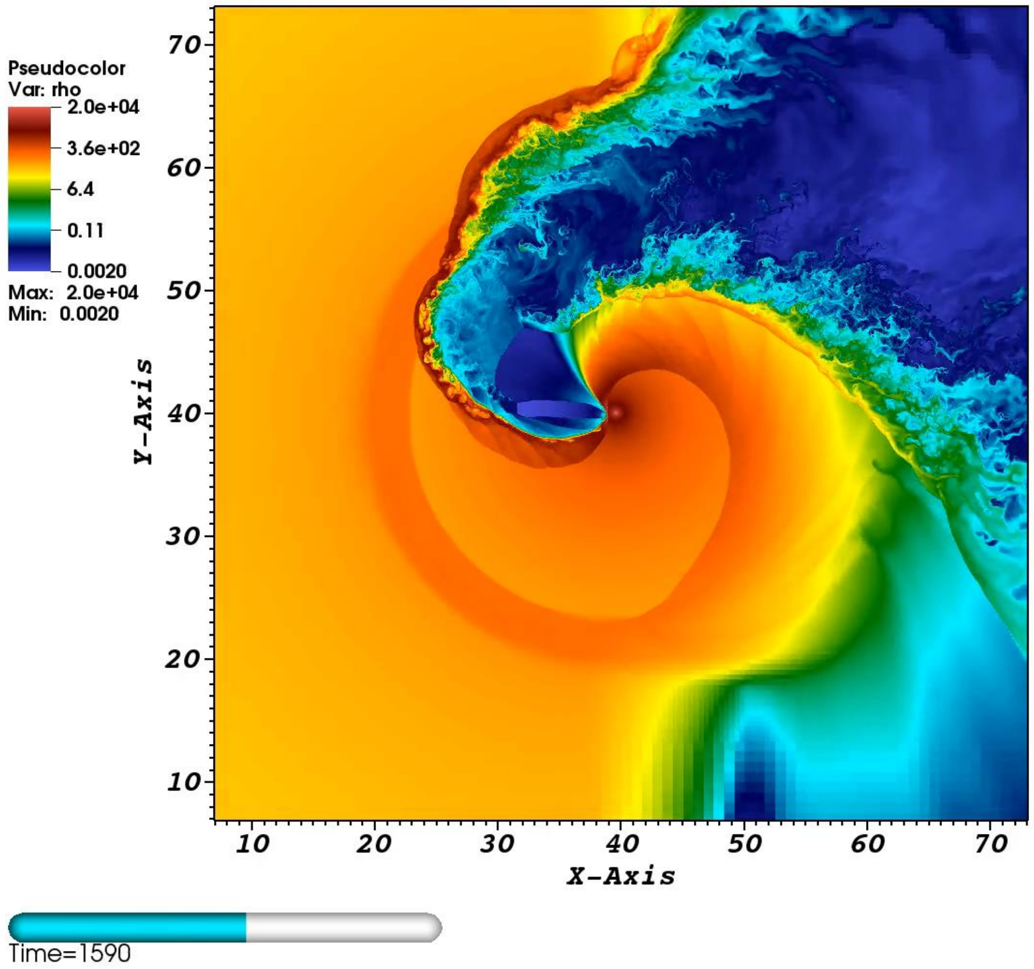

(Lamberts et al. 2013) RHD
Outflow is unstable.

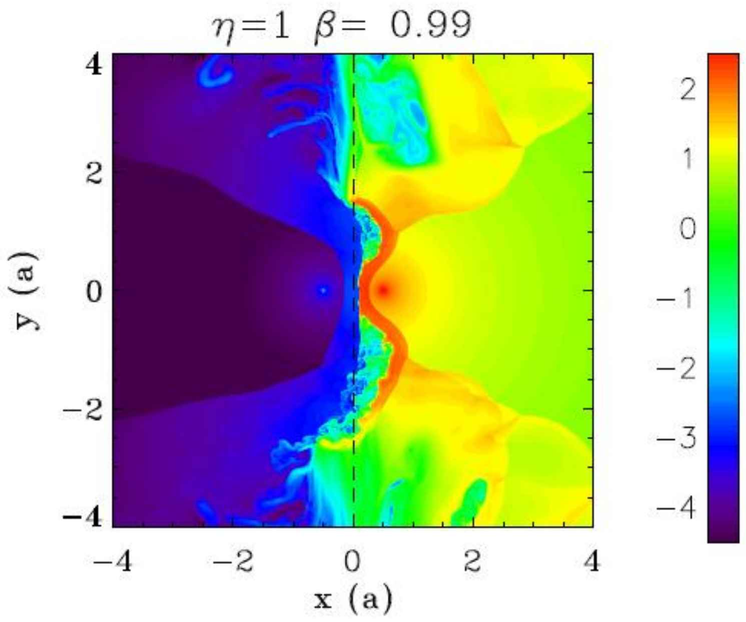

KHI in pulsar stellar wind collision region:

Density Γ= 2; η = 0.3

Density Γ= 10; η = 0.3

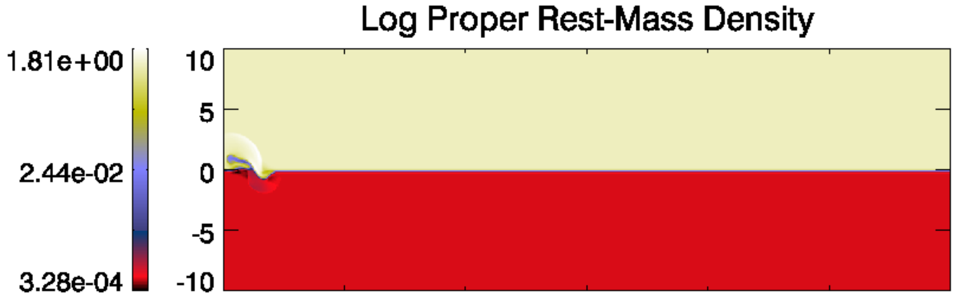

t = 2.8 s

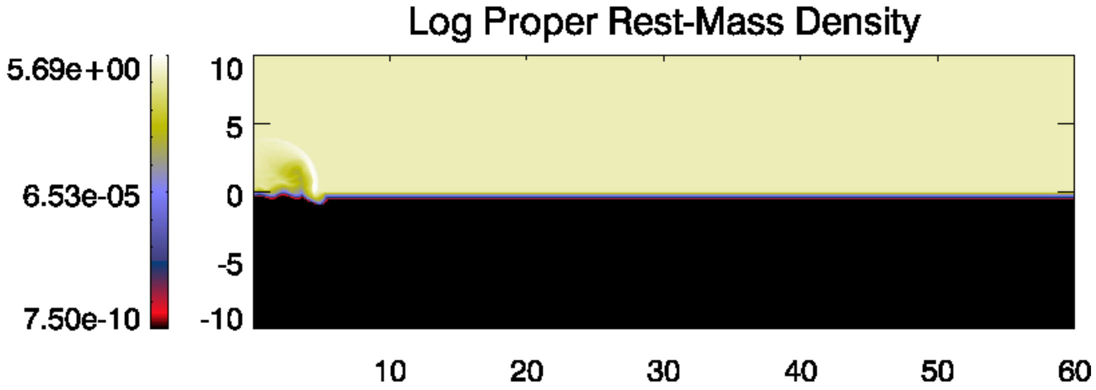

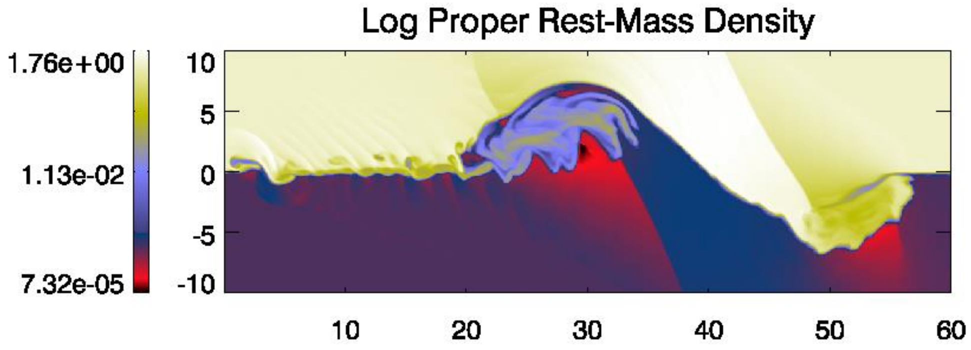

t = 34 s

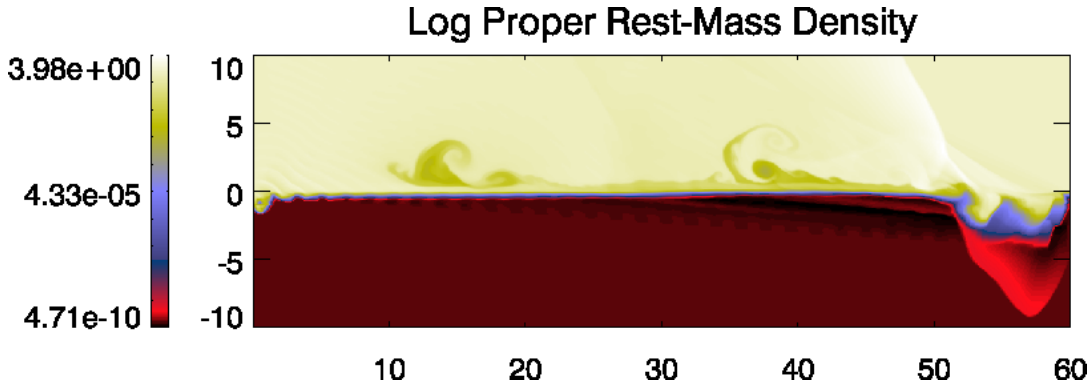

Density and velosity $\Gamma = 10$; $\eta = 0.3$

(Bosch-Ramon, MVB, Khangulyan and Perucho 2012) RHD

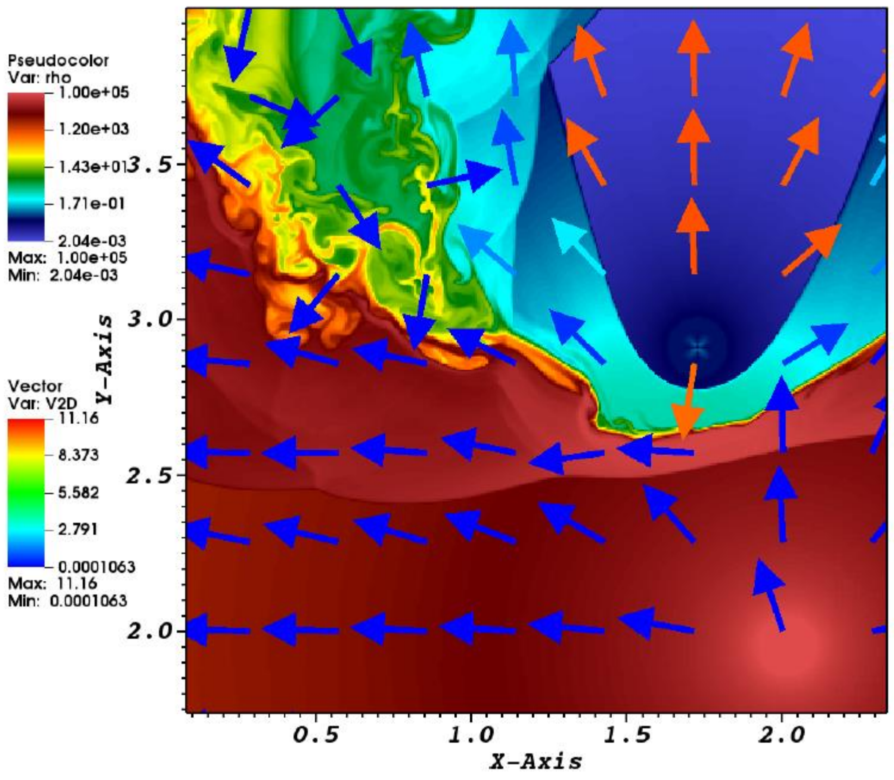

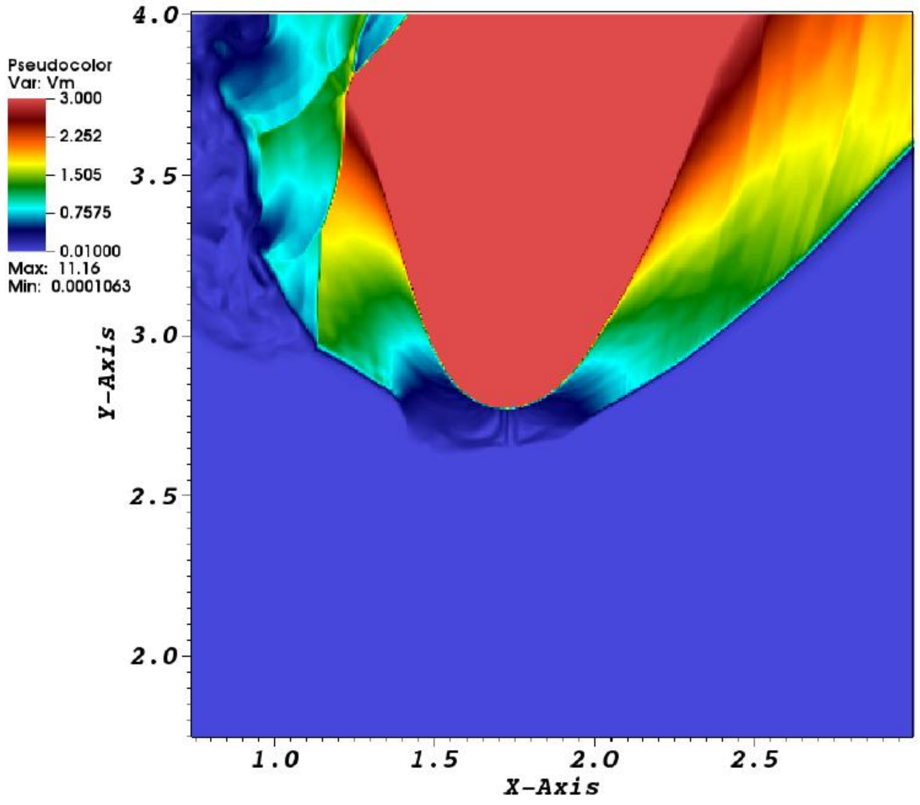

The Coriolis force trigger of RTI and RMI!

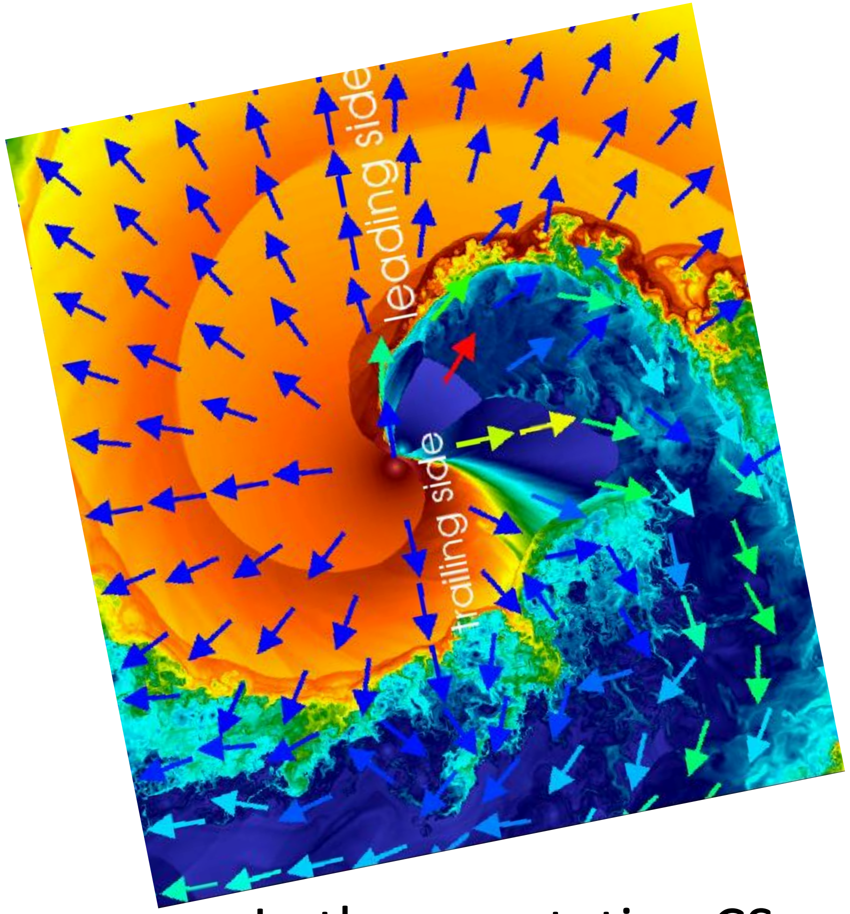

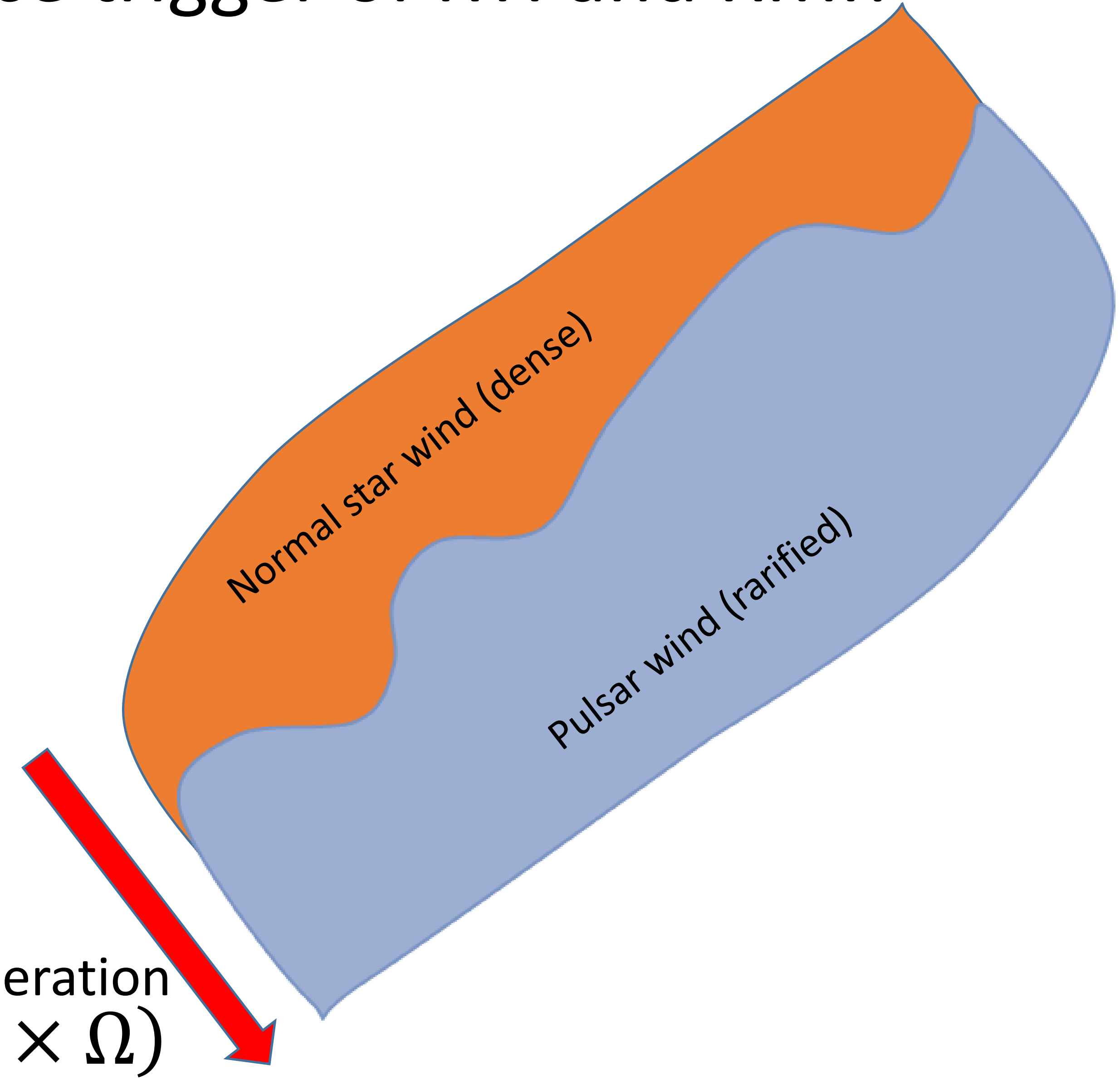

In the co rotating CS

Coriolis force produce acceleration

$$a=2(v_w \times \Omega)$$

Density $\Gamma = 2$; $\eta = 0.6$

(Bosch-Ramon, MVB, Khangulyan and Perucho 2012) RHD

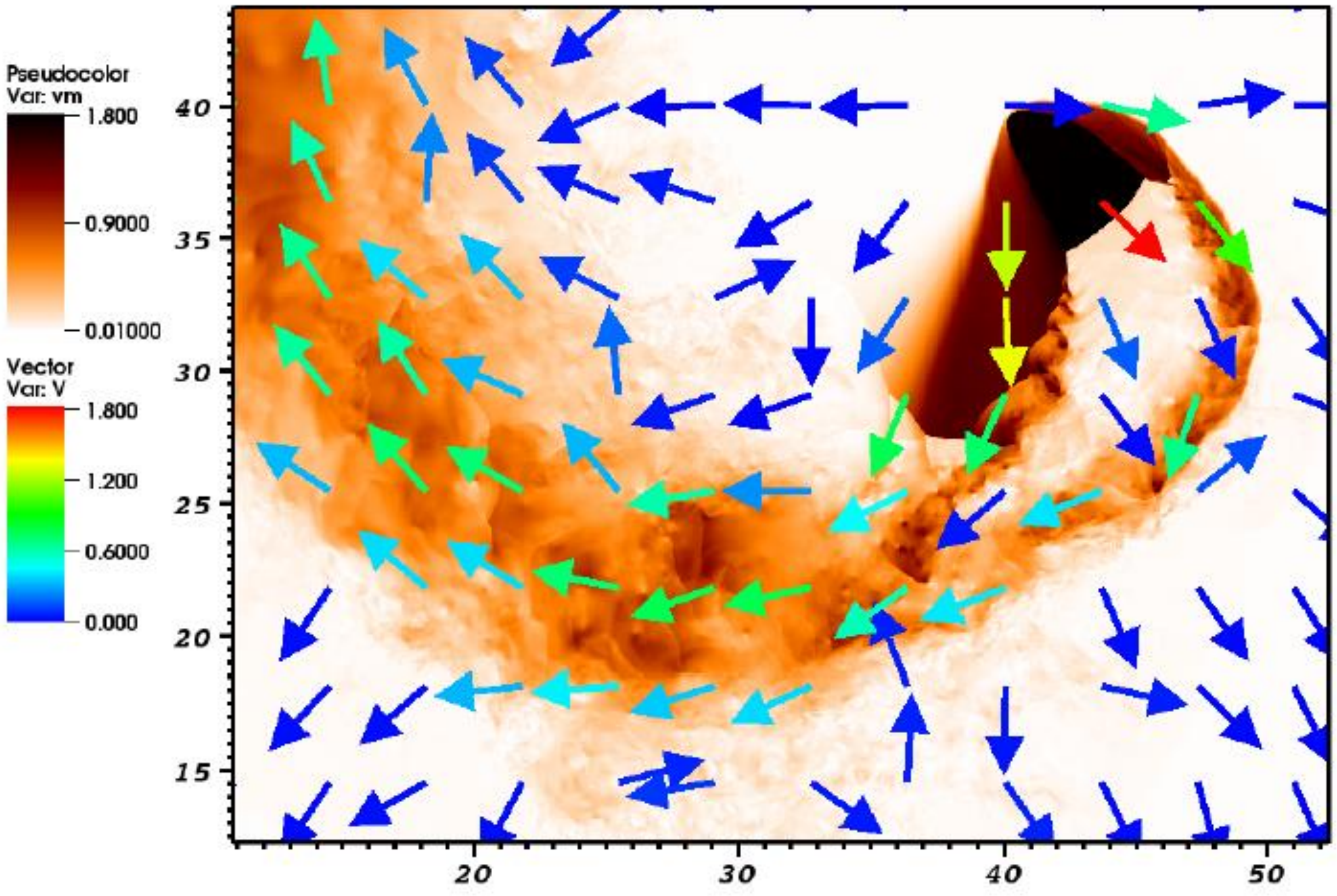

Light curve formation

(Zabalza et al 2013)

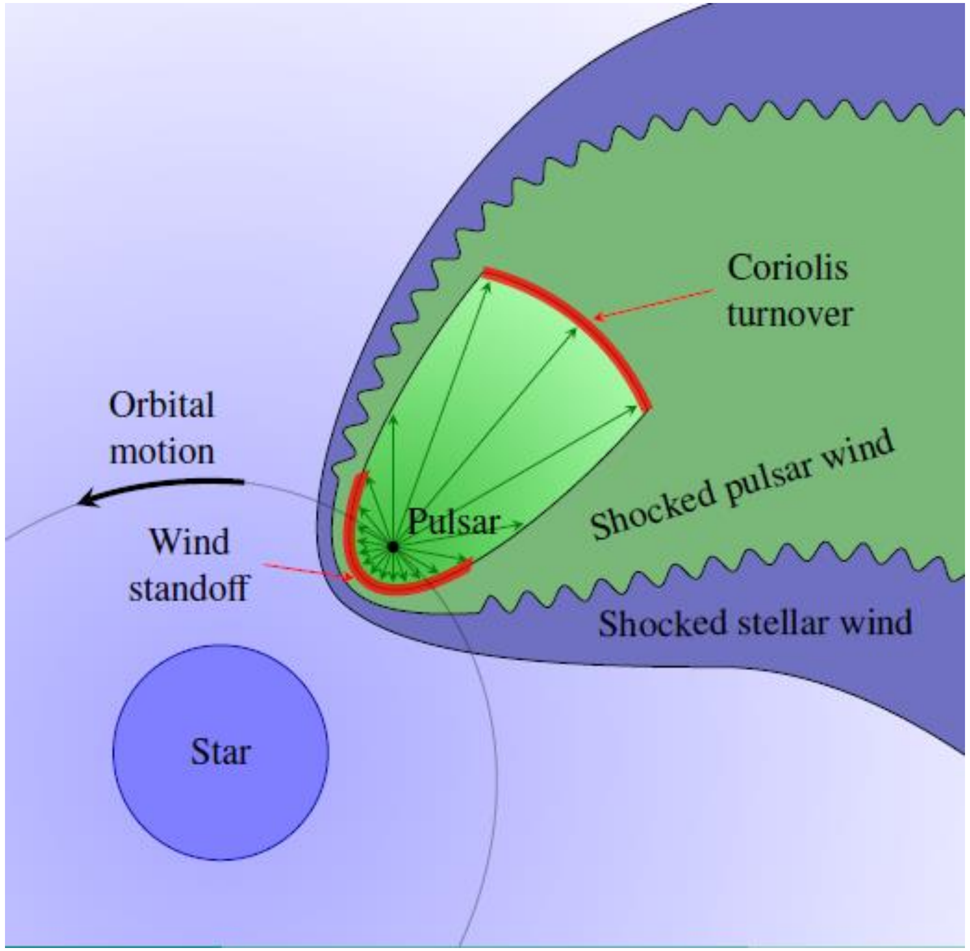

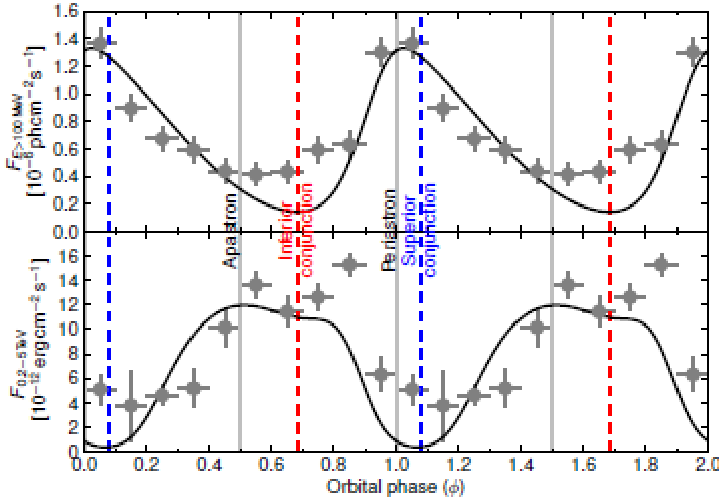

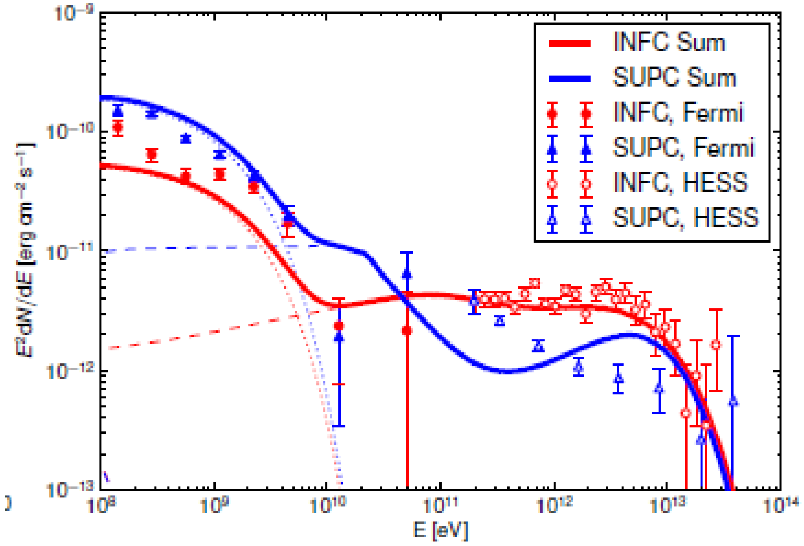

Effect of eccentric orbit

$$x \sim \frac{3\eta^{1/2} v_w}{2\Omega}$$

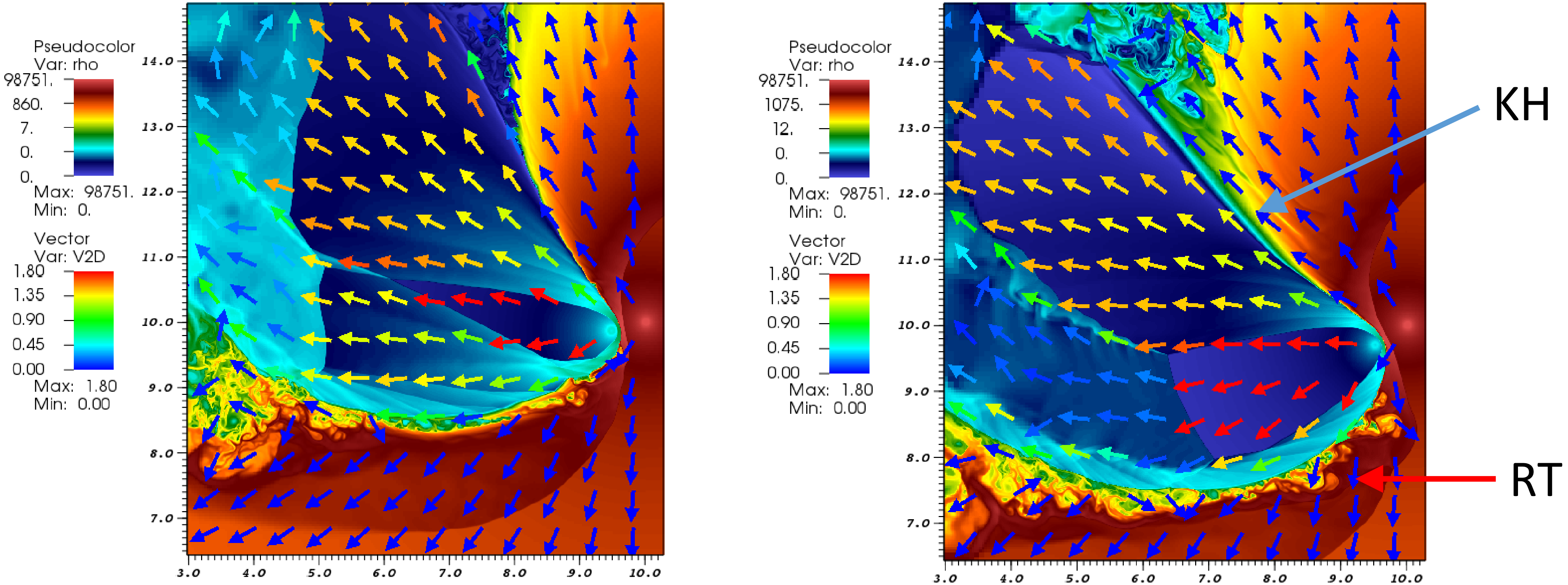

3D show time!...

3D run with Γ= 2; η = 0.1

PLUTO non uniform grid

Four velocity.

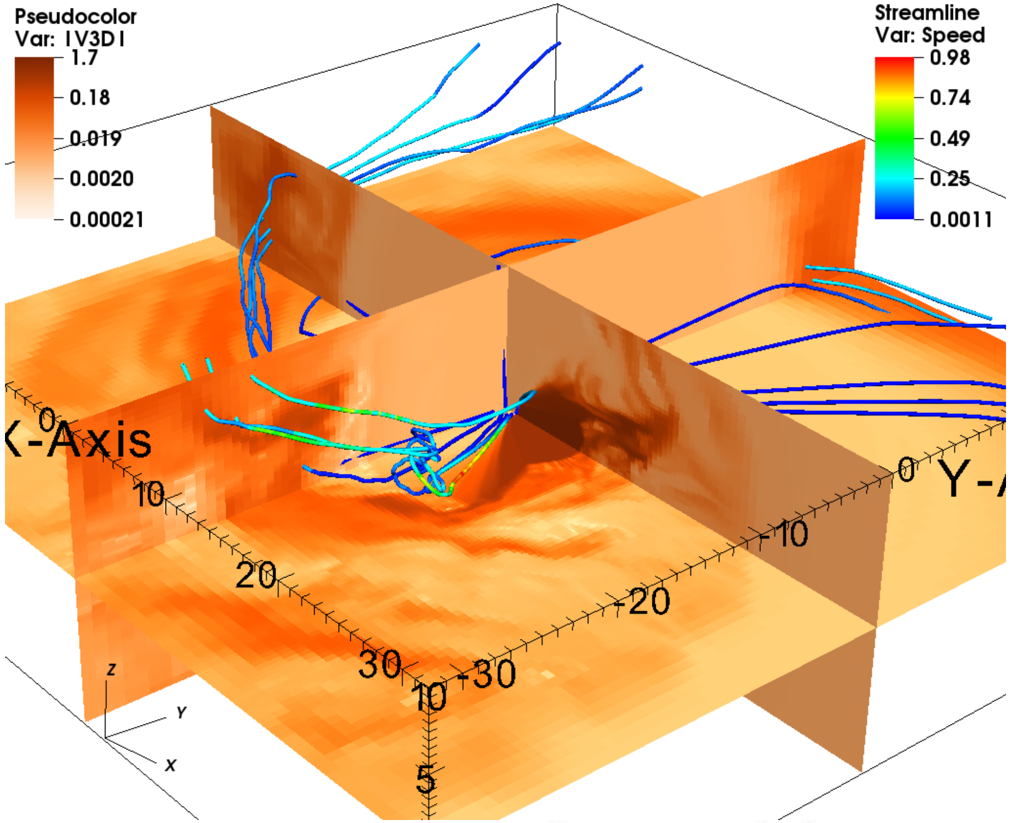

Tracer.

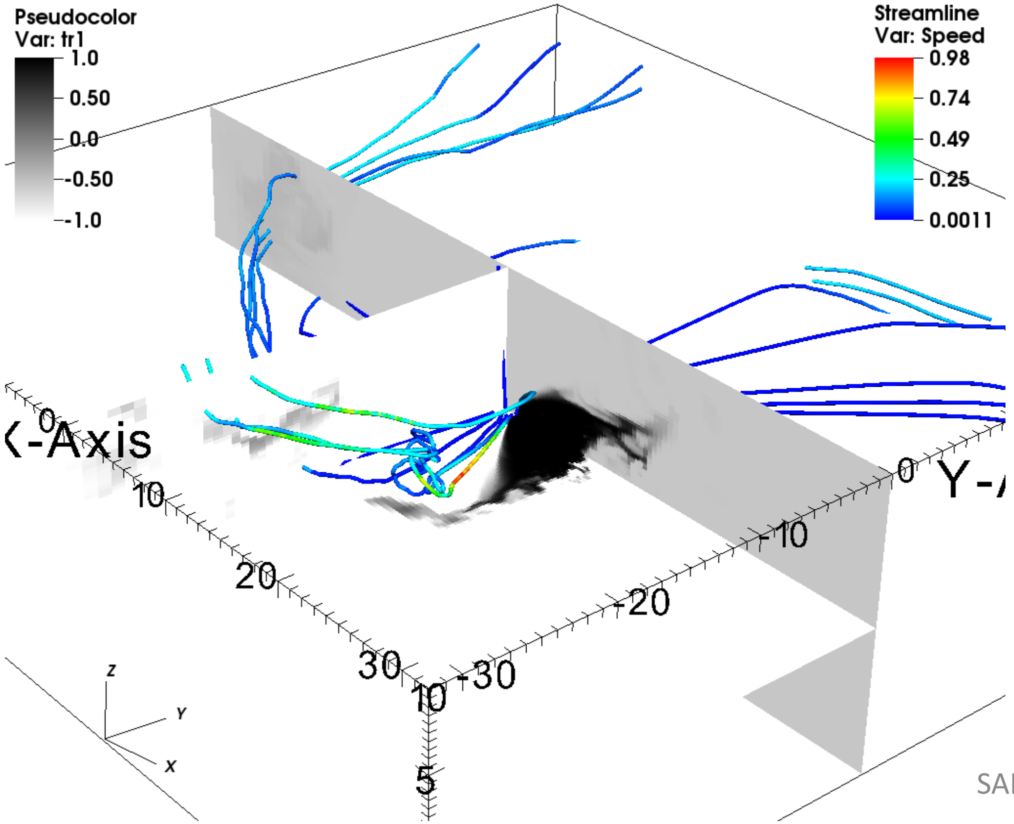

Density

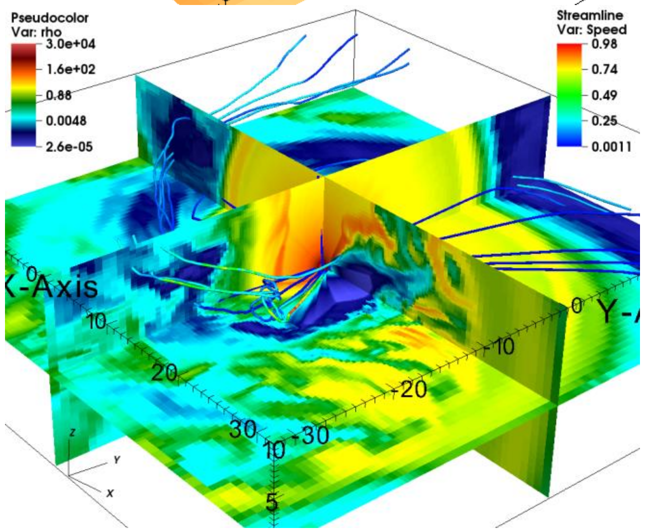

3D run $\Gamma = 2$; $\eta = 0.1$

density contours and stream lines.

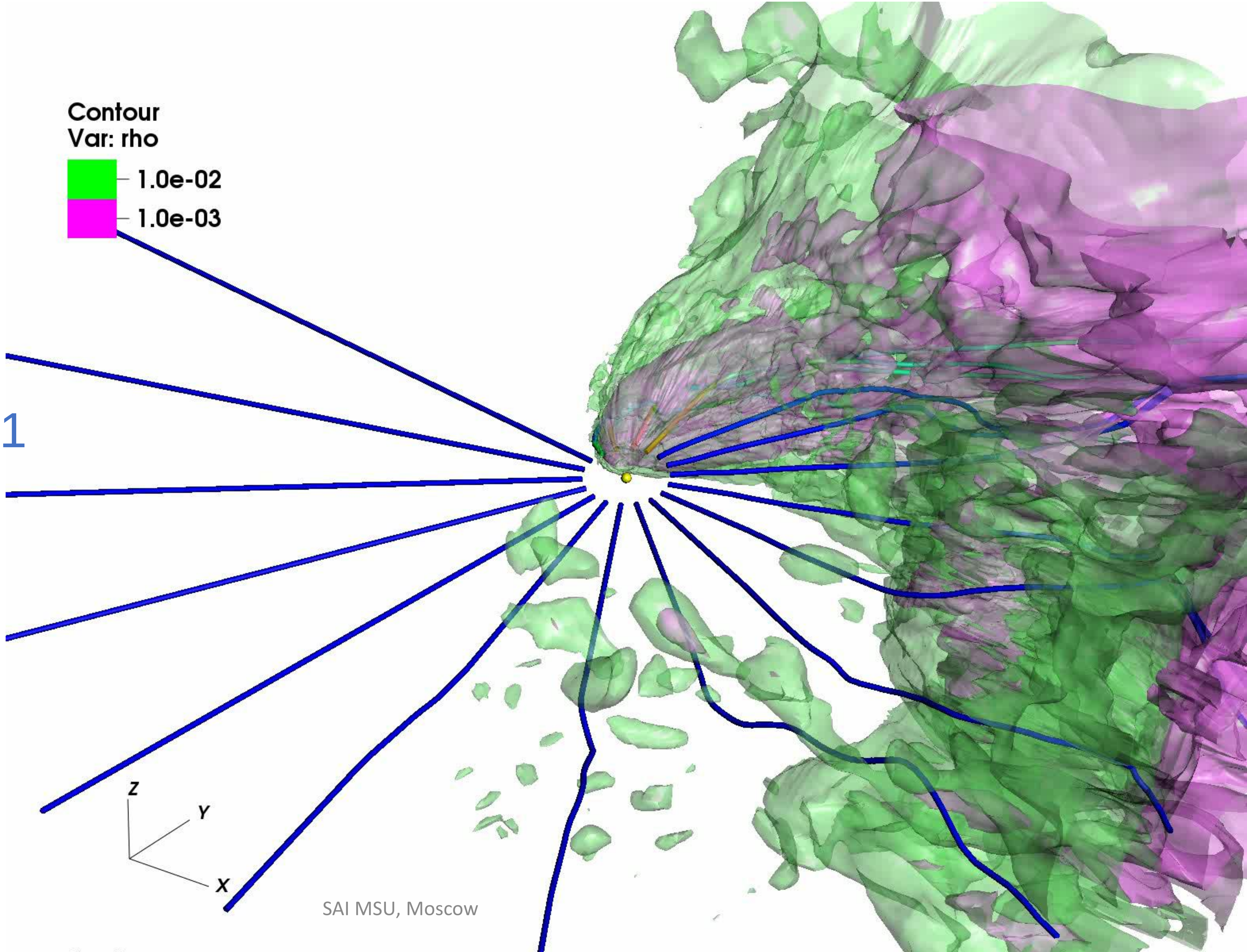

3D run $\Gamma = 2$; $\eta = 0.1$

Density and four velocity in XZ plane

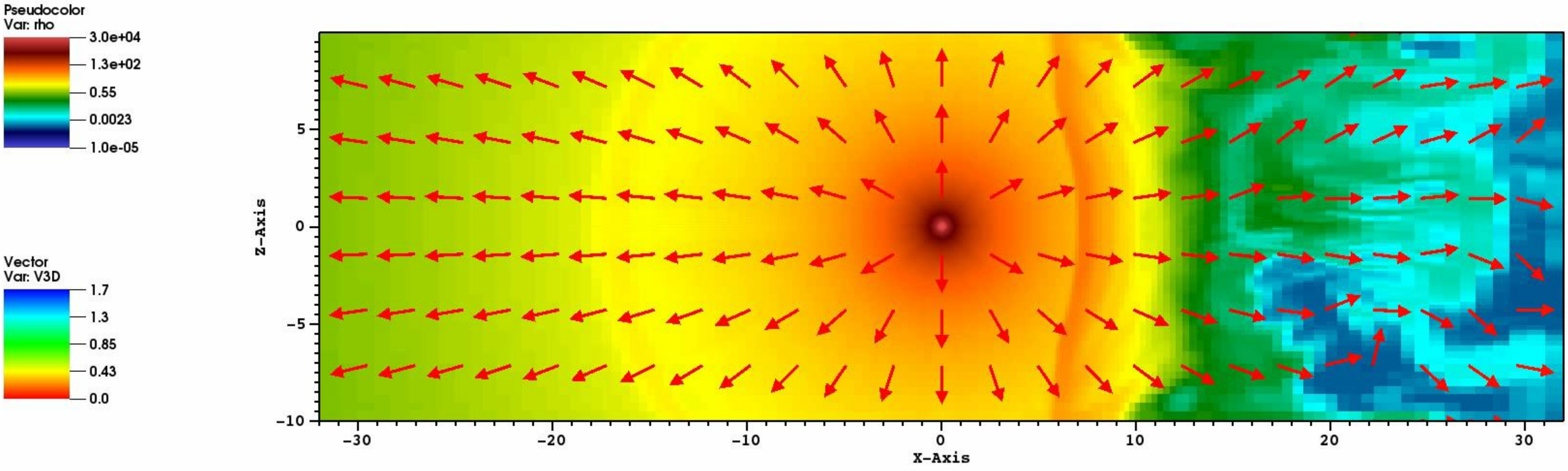

The first hydro and radiation simulations:

Dubus et al 2015

1) Artificial back shock with η=0.1.
2) Energy budget is 0.1 of observed one.

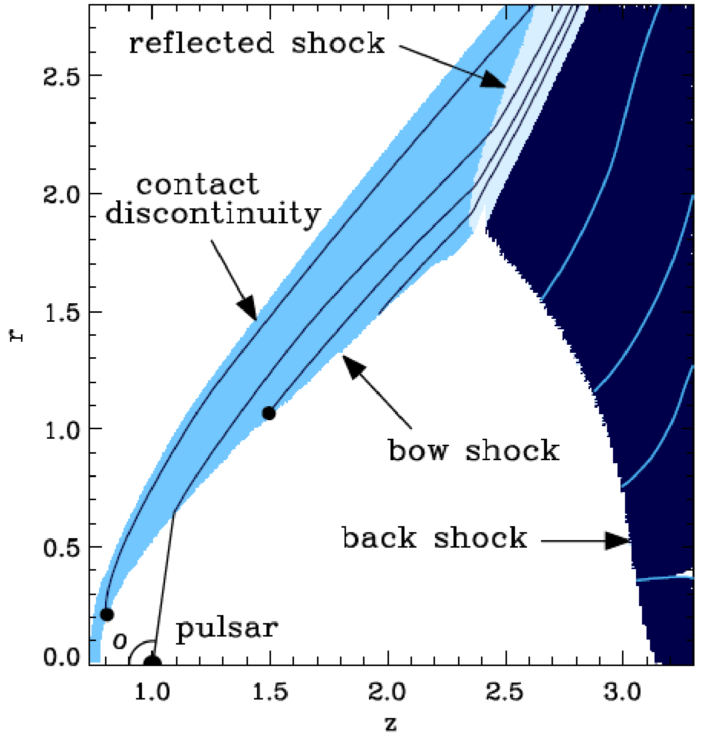

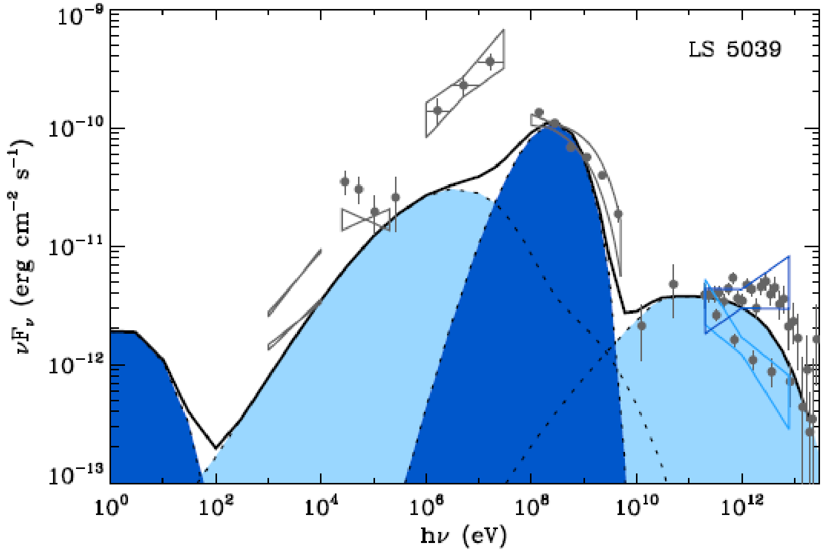

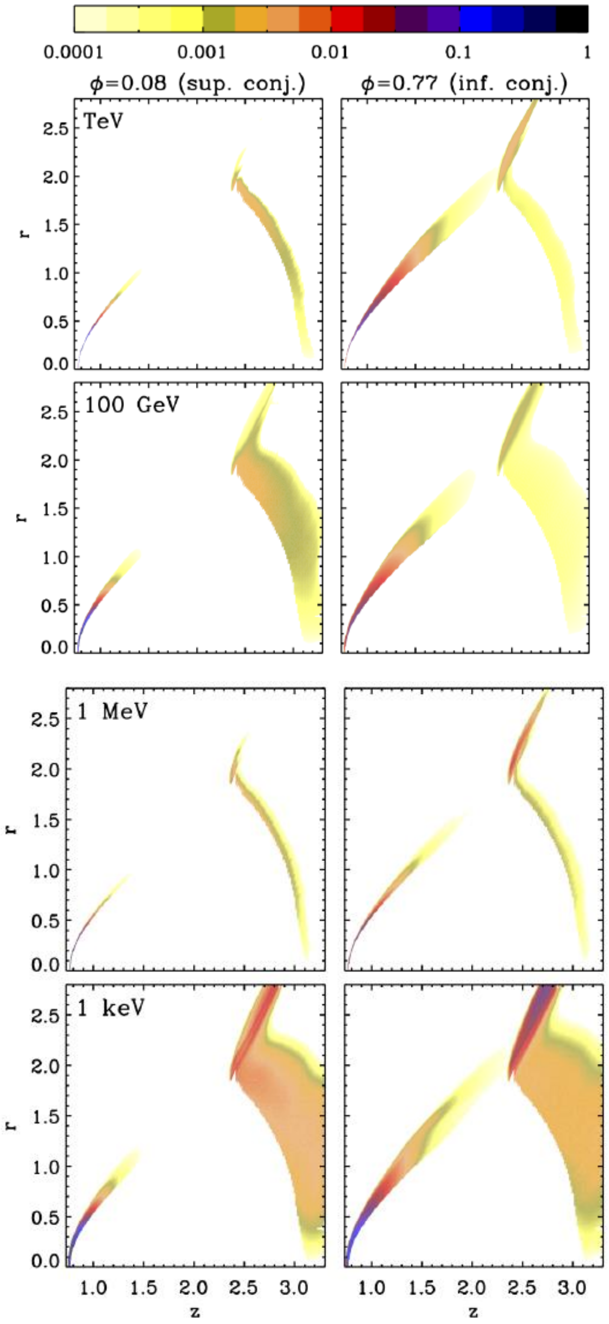

Comparison of the 3D case and 2D cases with different resolution.

Density presented in the XY plane.

3D

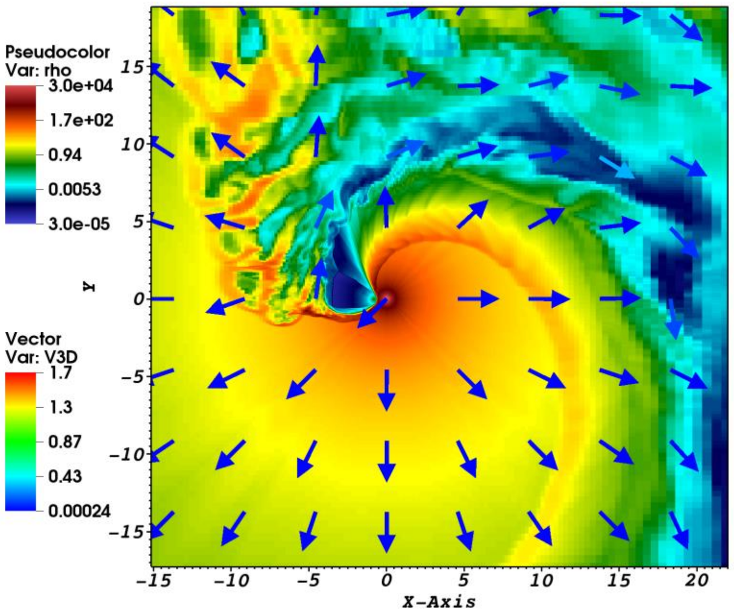

2D

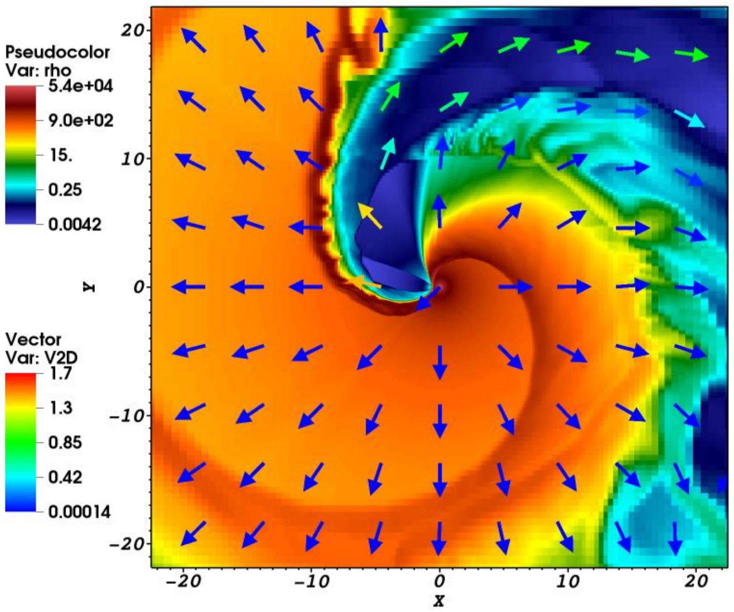

2Dx2

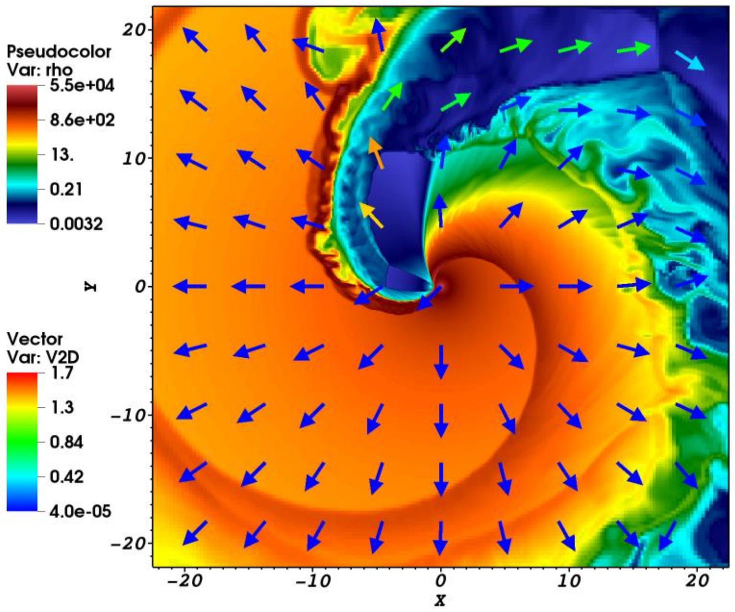

2Dx4

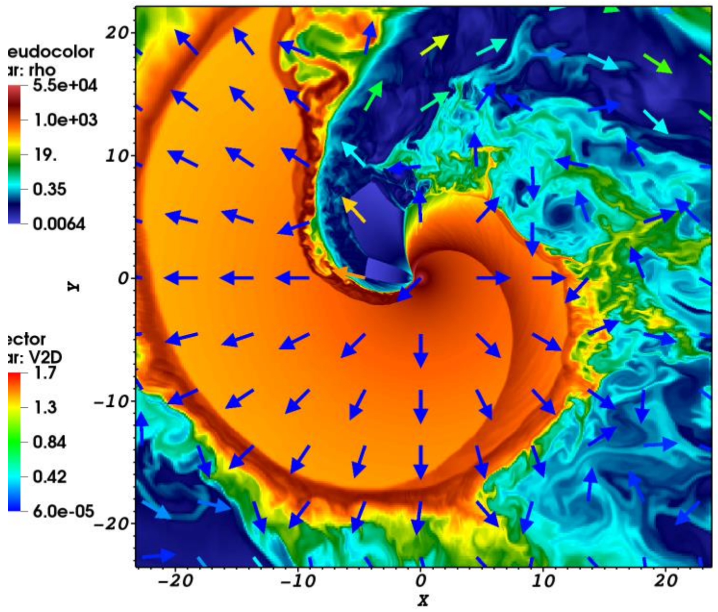

Comparison of 3D and 2D

Tracer | Four velocity | Mach

3D

vs

2D

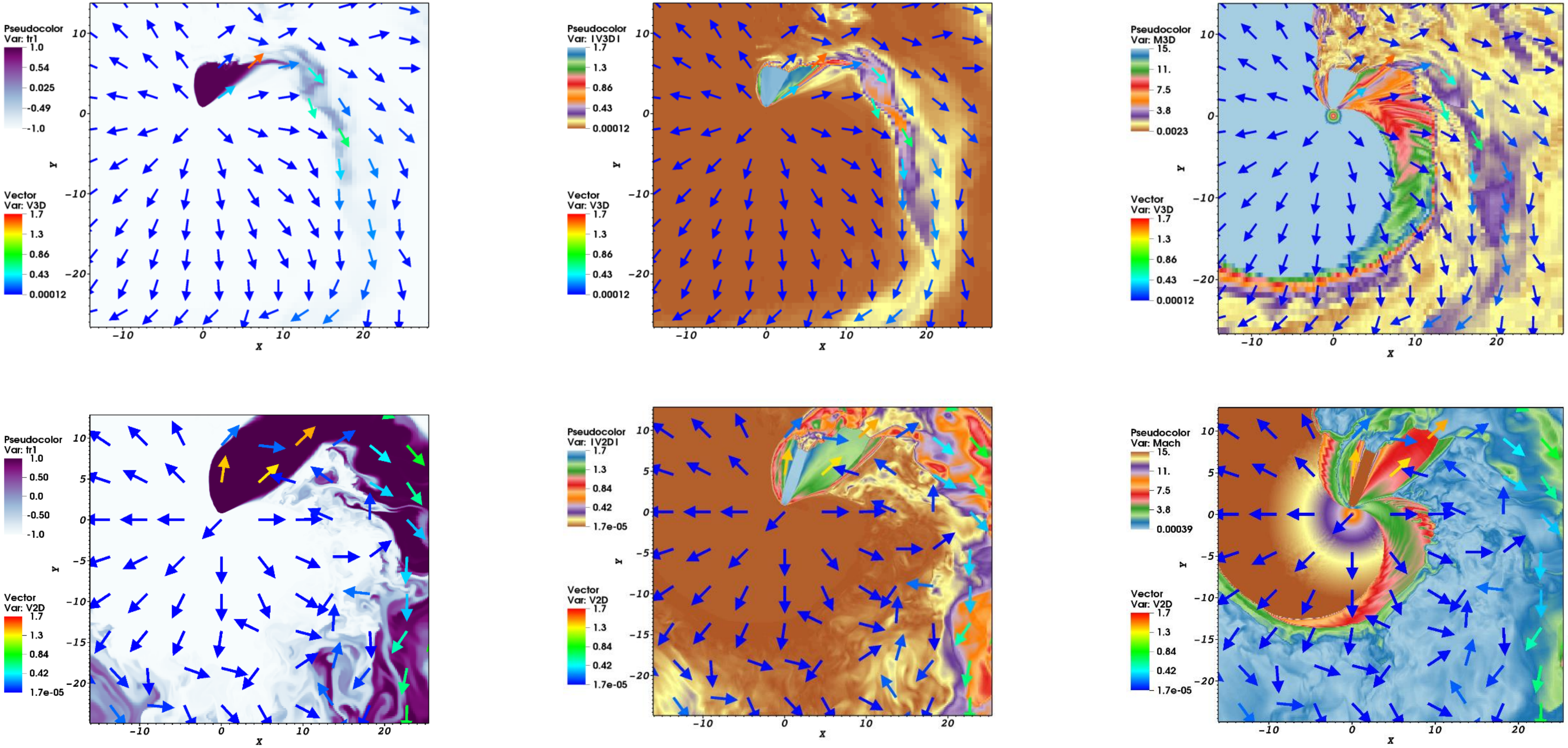

2D $\Gamma = 2$; $\eta = 0.3$ with high resolution in a large domain, density in XY plane.

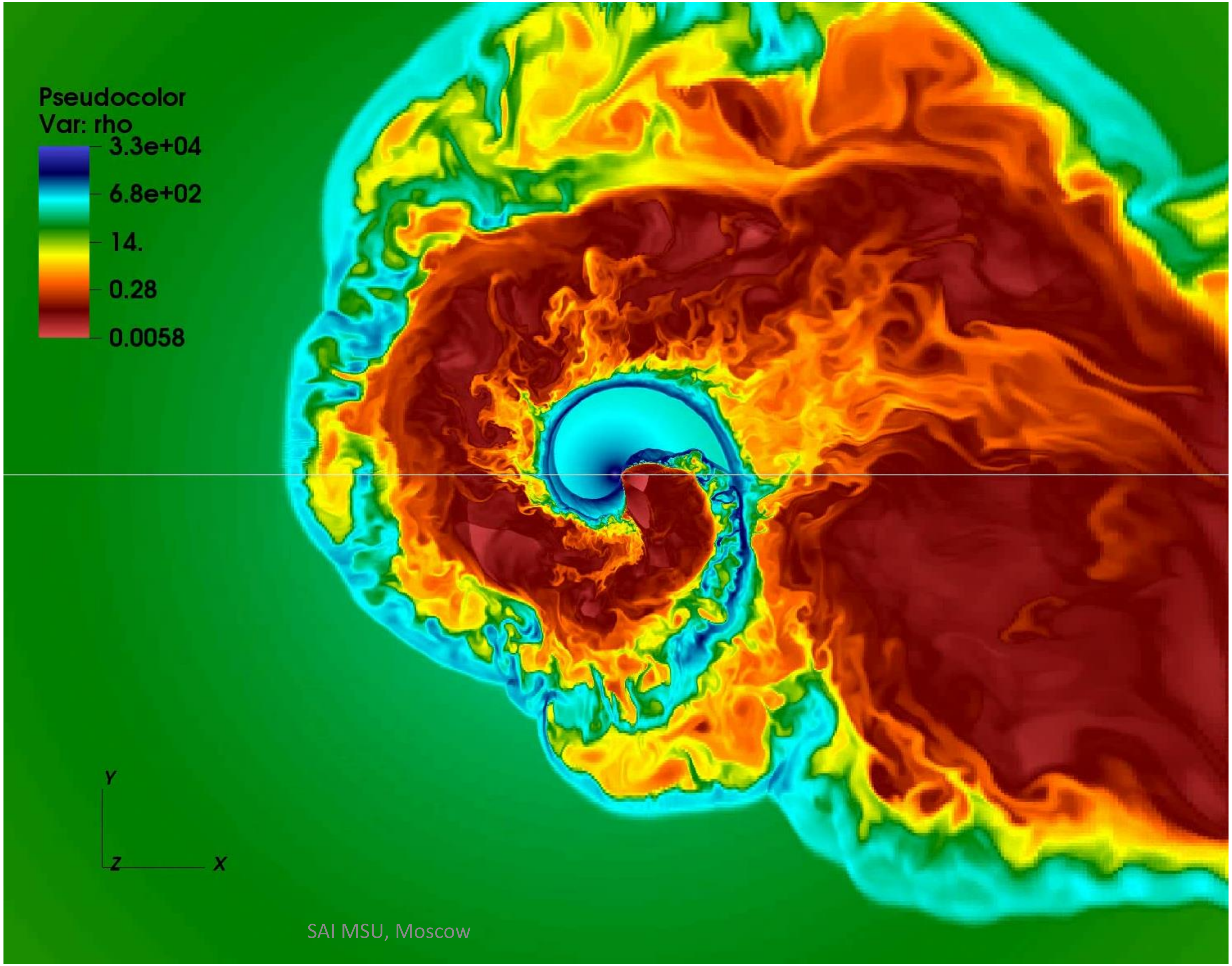

The origin of the X-ray-emitting object moving away from PSR B1259-63 in (3-1)D and more

PSR B1259-63

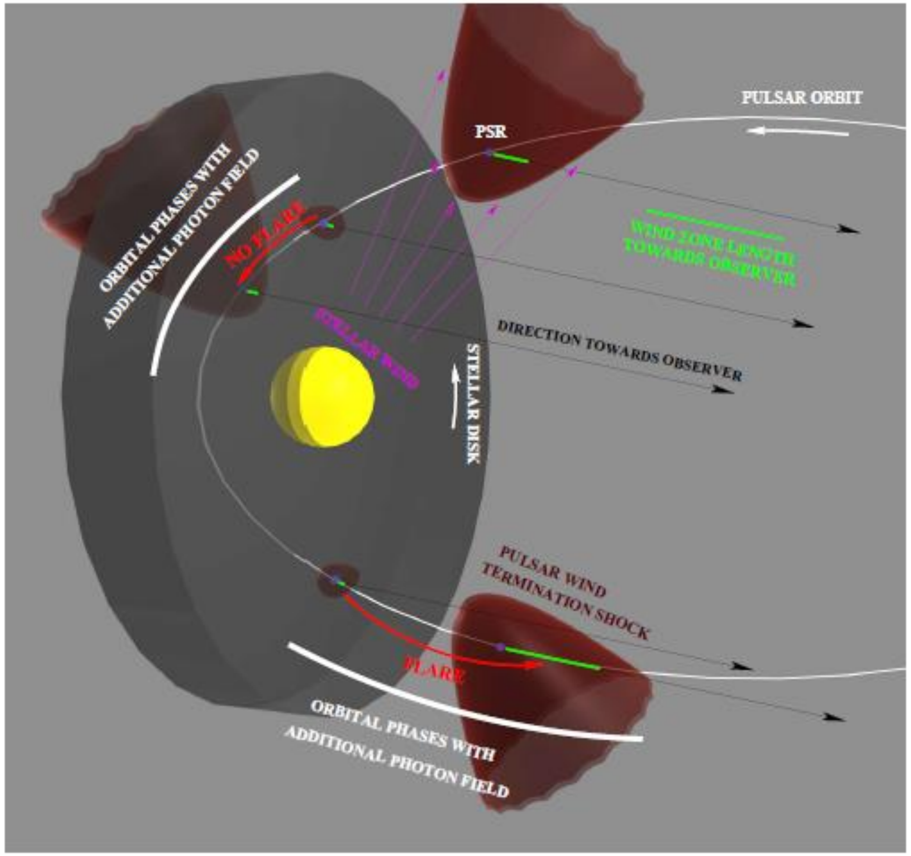

PULSAR ORBIT
PSR
ORBITAL PHASES WITH
ADDITIONAL PHOTON FIELD
NO FLARE
WIND ZONE LENGTH
TOWARDS OBSERVER
STELLAR WIND
DIRECTION TOWARDS OBSERVER
STELLAR DISK
PULSAR WIND
TERMINATION SHOCK
FLARE
ORBITAL PHASES WITH
ADDITIONAL PHOTON FIELD

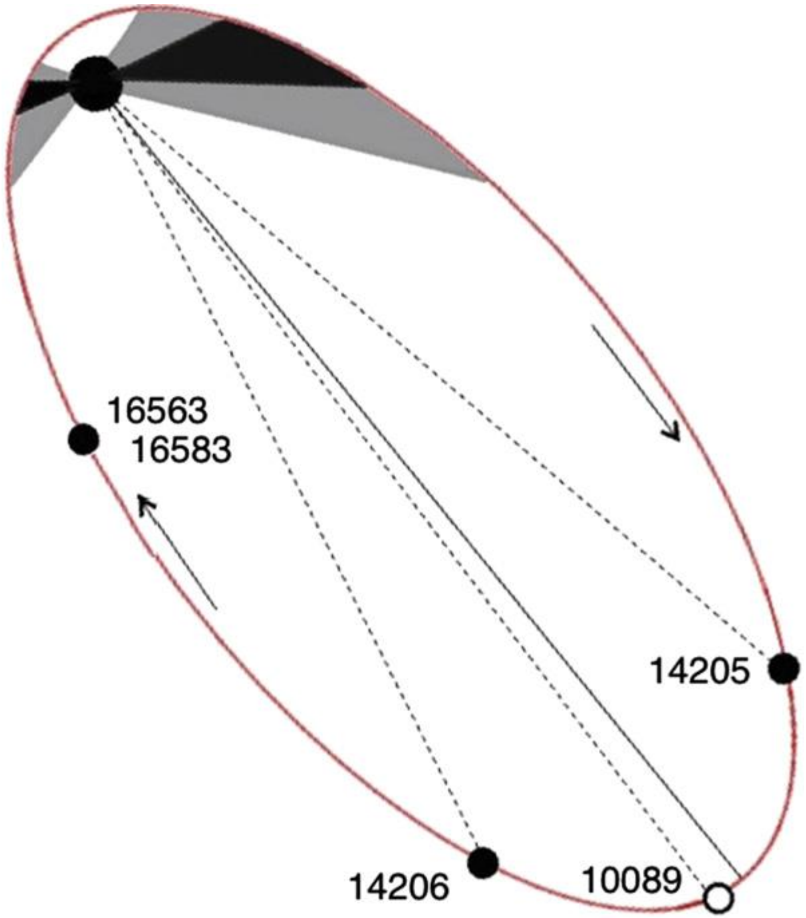

16563
16583
14205
14206
10089

The origin of the X-ray-emitting object moving away from PSR B1259-63

(Pavlov et al 2015)

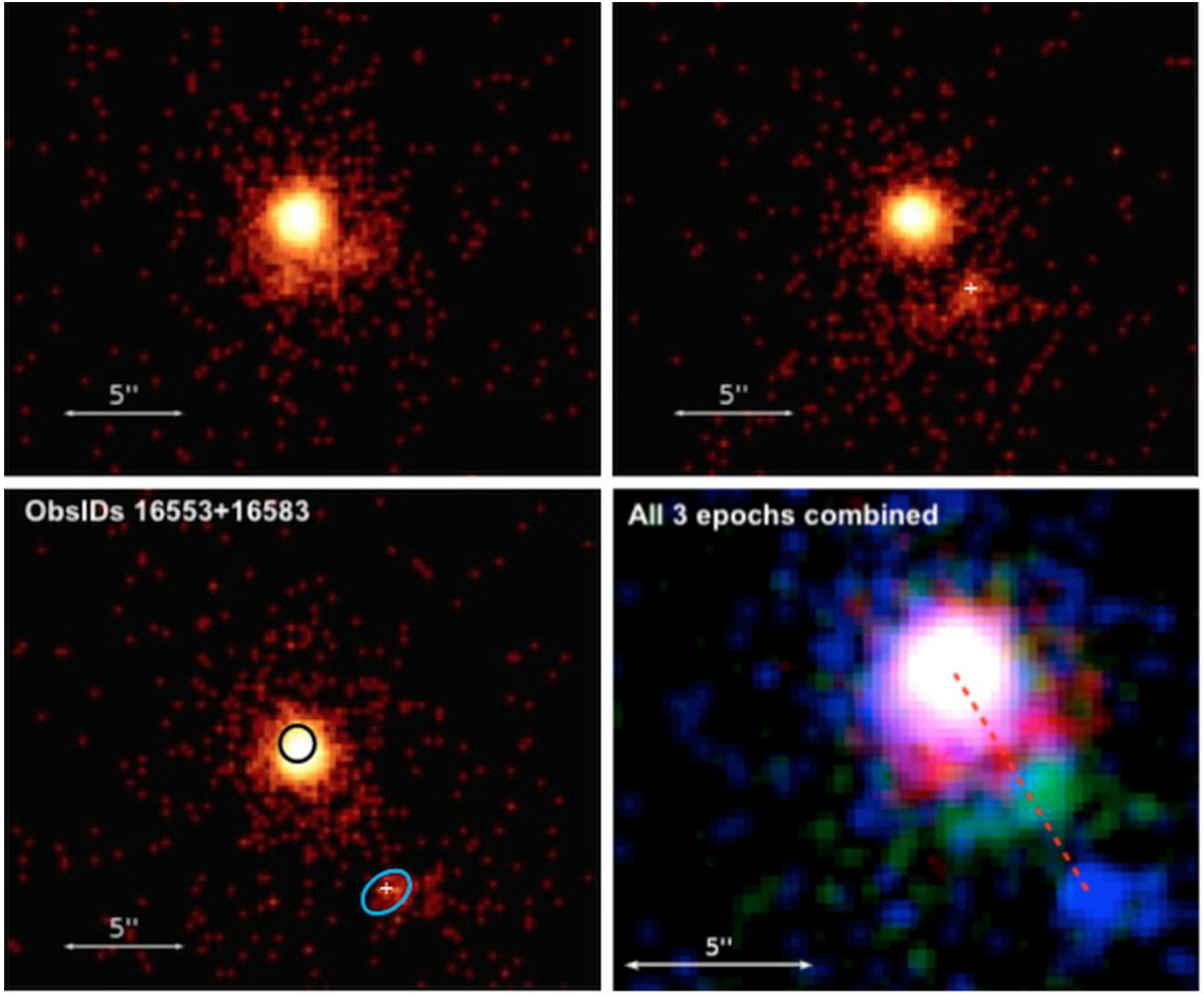

The origin of the X-ray-emitting object moving away from PSR B1259-63

(Pavlov et al 2015)

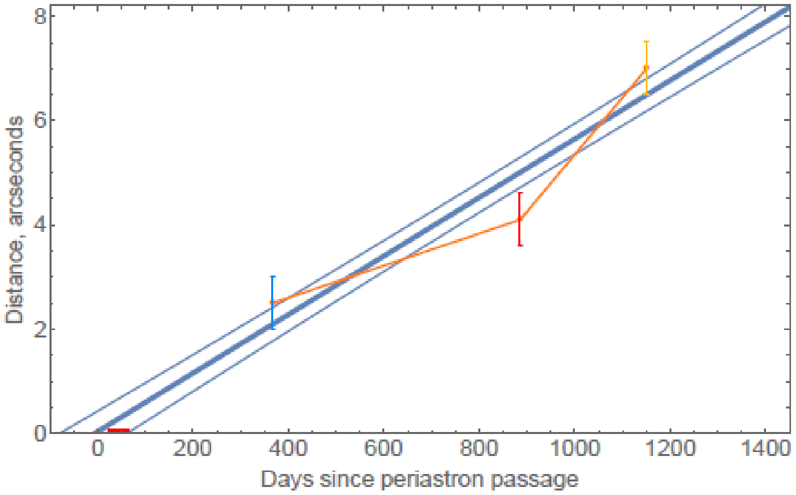

Linear fit: V = (0.07+/-0.01)c

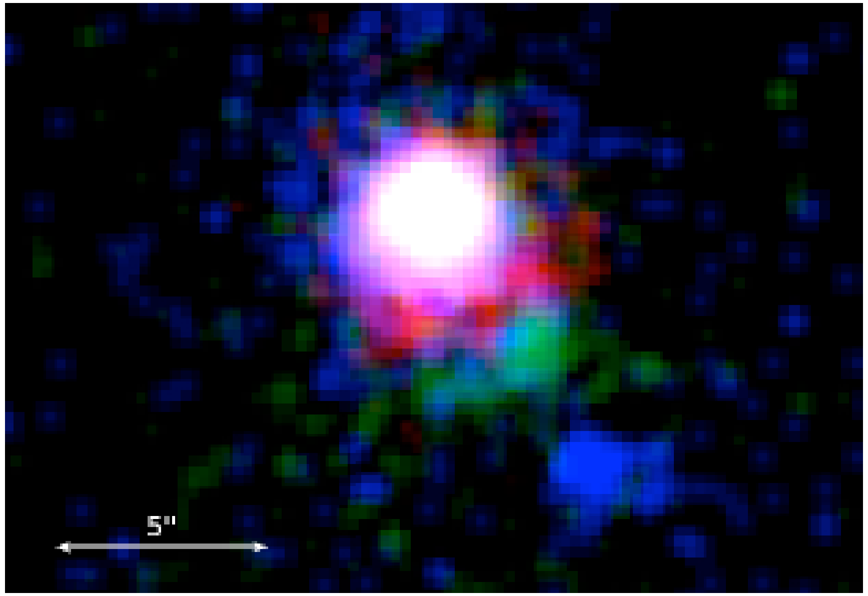

Between 3rd and 4th observations the extended structure moved by 2.5'' ±0.5''.

This corresponds to the apparent proper motion

V=(0.13±0.03)c
at d = 2.3 kpc

Apparent acceleration (?)
90±40 cm s^{-2}

Model:

$$v_{\mathrm{t}} = \sqrt{\frac{2L_{sd}(t_{\mathrm{orb}} - t_{\mathrm{pe}})}{\dot{M}\Omega t_{\mathrm{pe}}}} = \sqrt{\frac{\eta v_{\mathrm{w}} c}{\Omega}\frac{\pi - M_{\mathrm{a}}}{M_{\mathrm{a}}}}$$

$$\Omega \approx \alpha^2/4$$

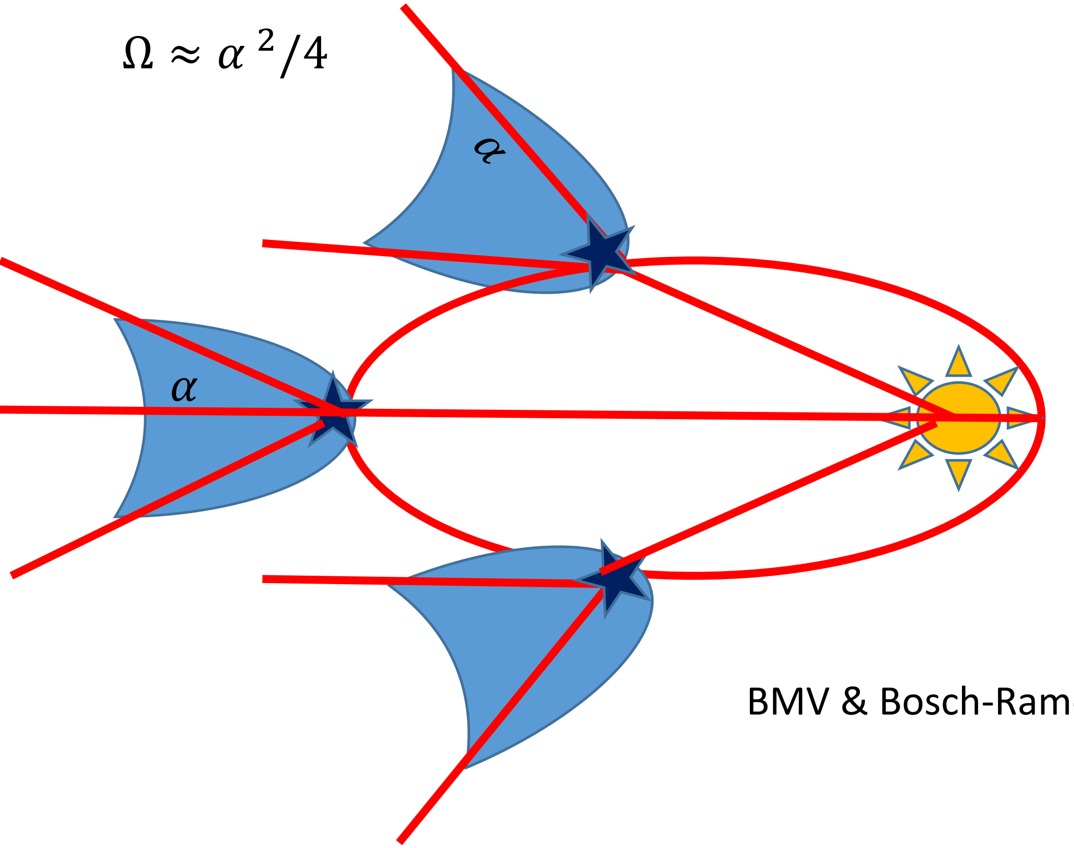

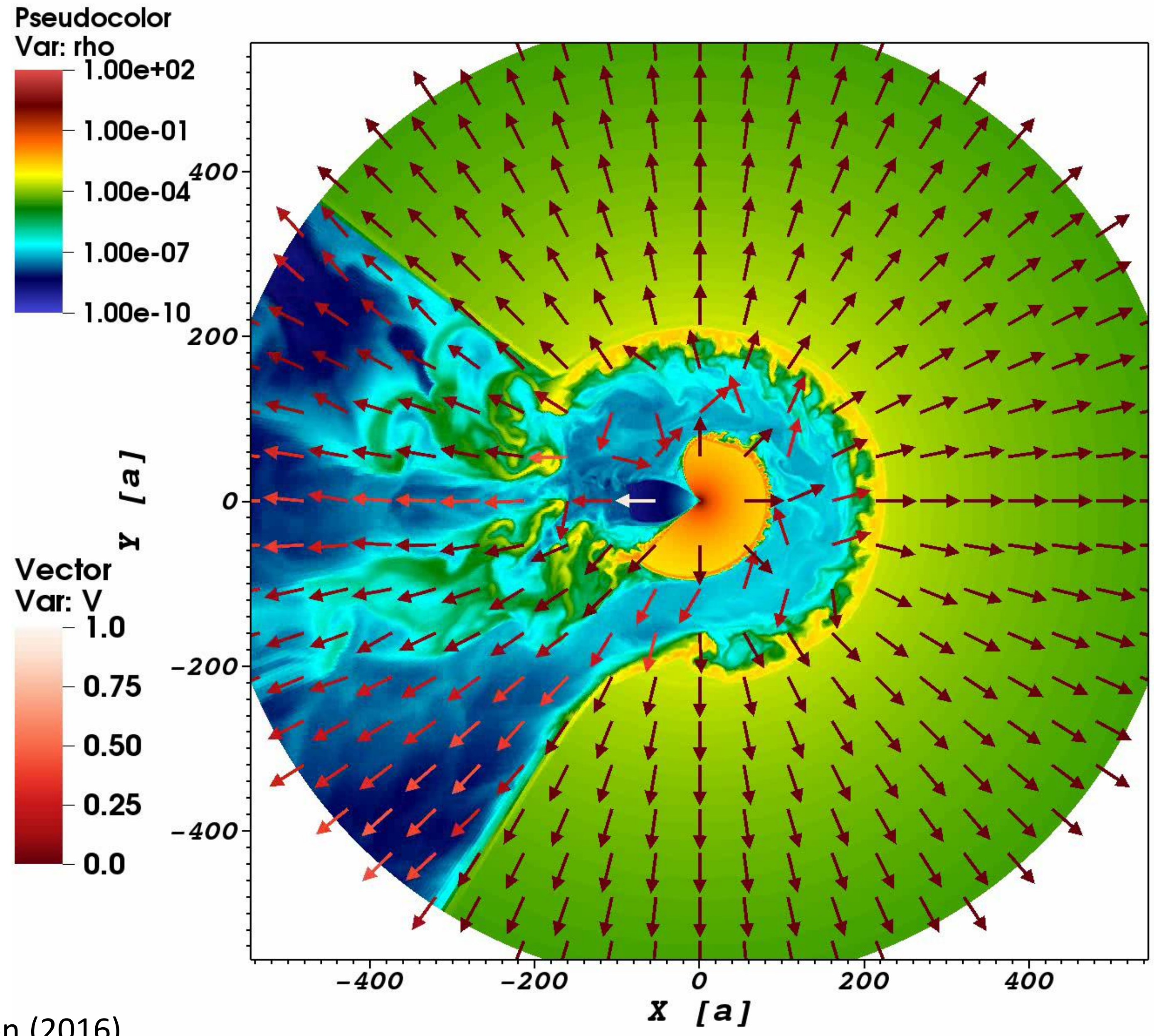

BMV & Bosch-Ramon (2016)

Results:

BMV & Bosch-Ramon (2016)

T=3.4 year
e=0.87

Pressure

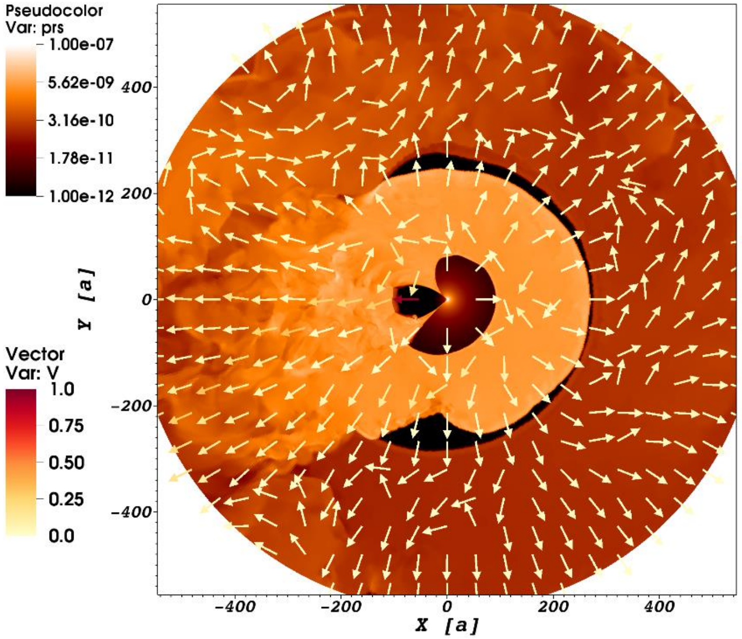

Density

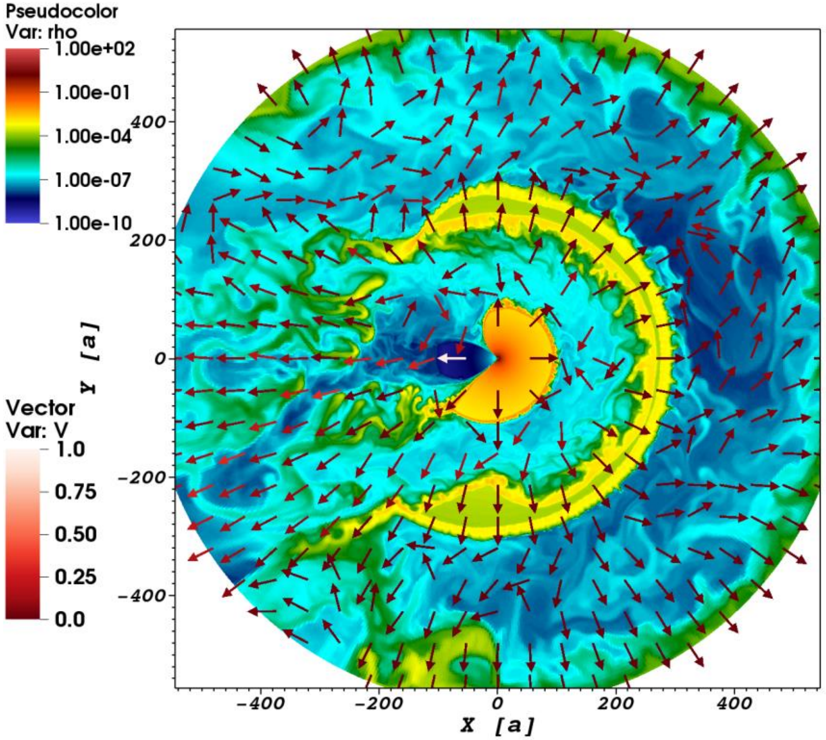

Mach number

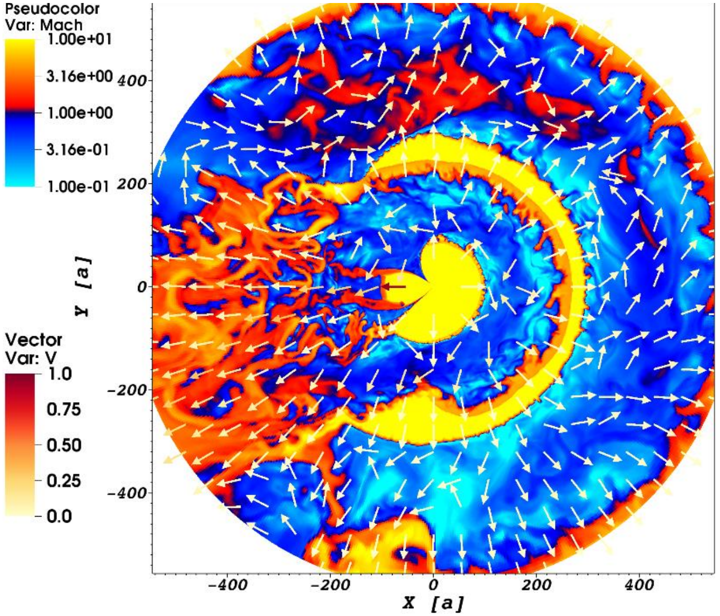

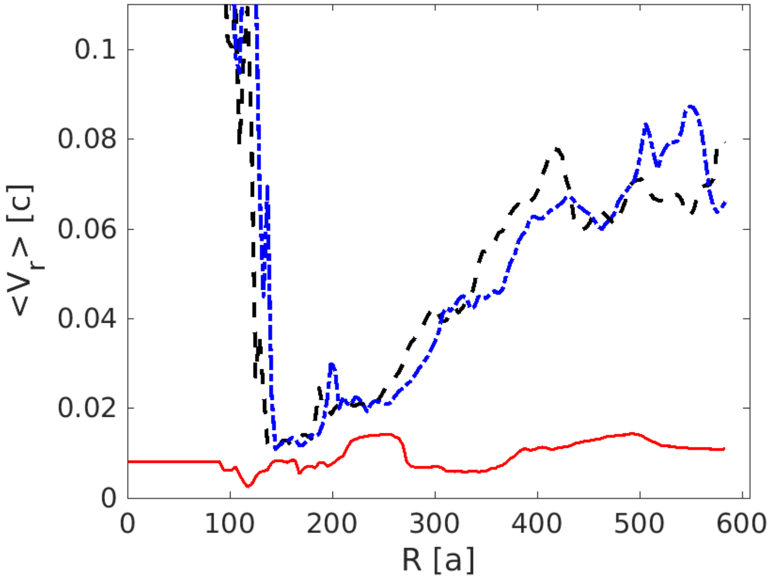

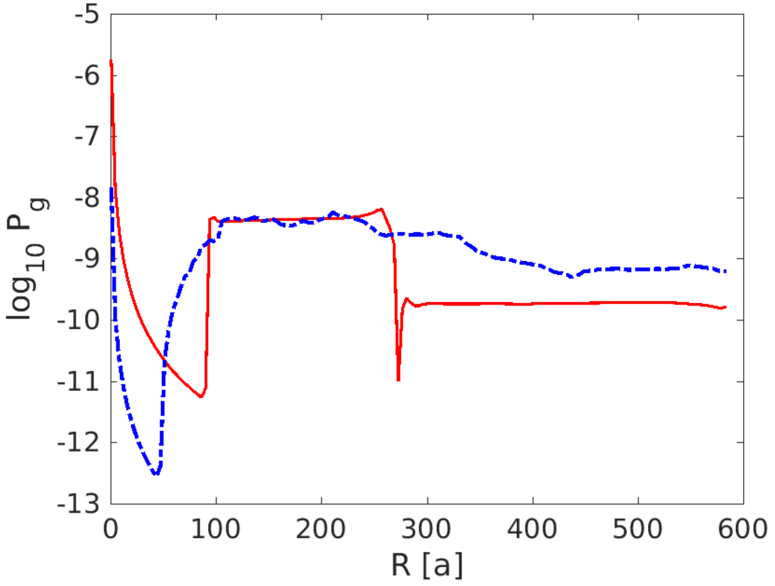

Density

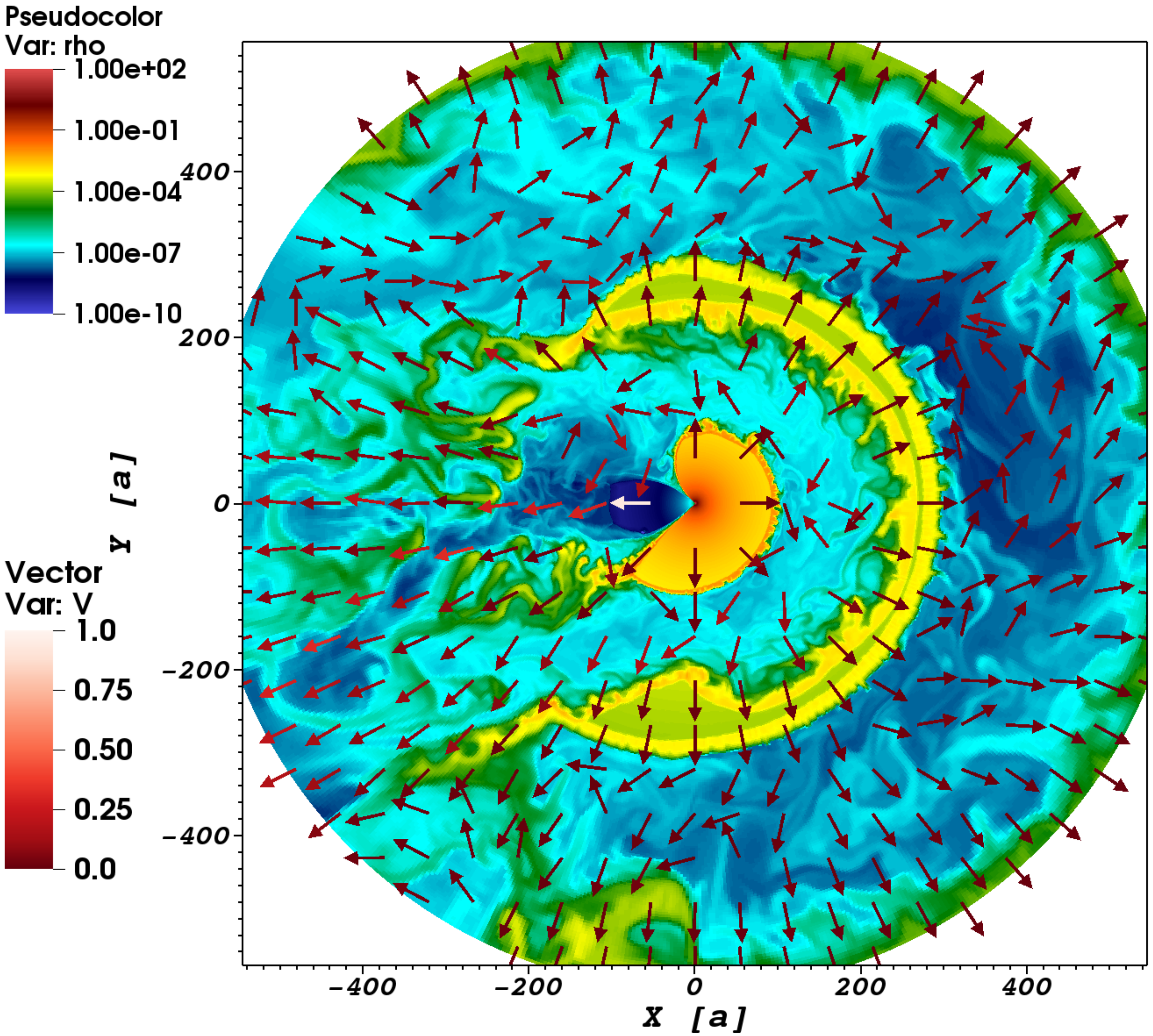

BMV & Bosch-Ramon (2016)

Jeremy Hare et al (2017)

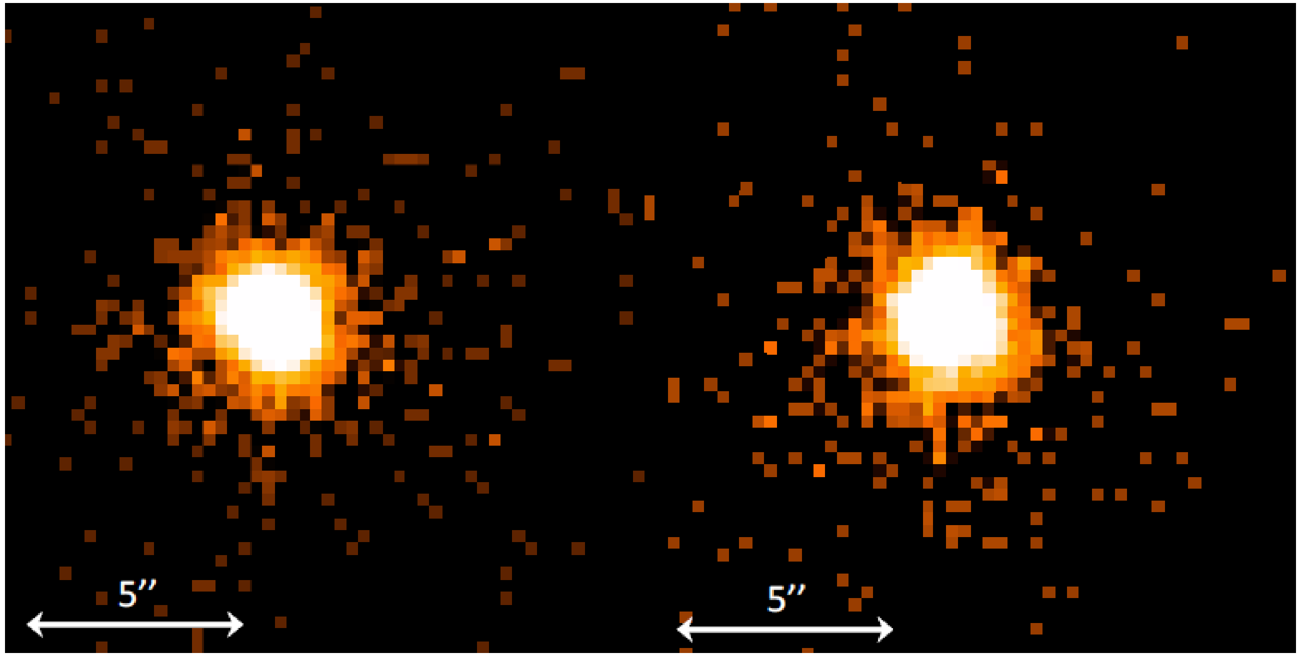

04/21/2015 01/12/2016

New clump detected moving in same direction with same velocity

Shows strange “whiskers” in Jan 2017, brightens in Apr 2017

01/06/2017 04/24/2017

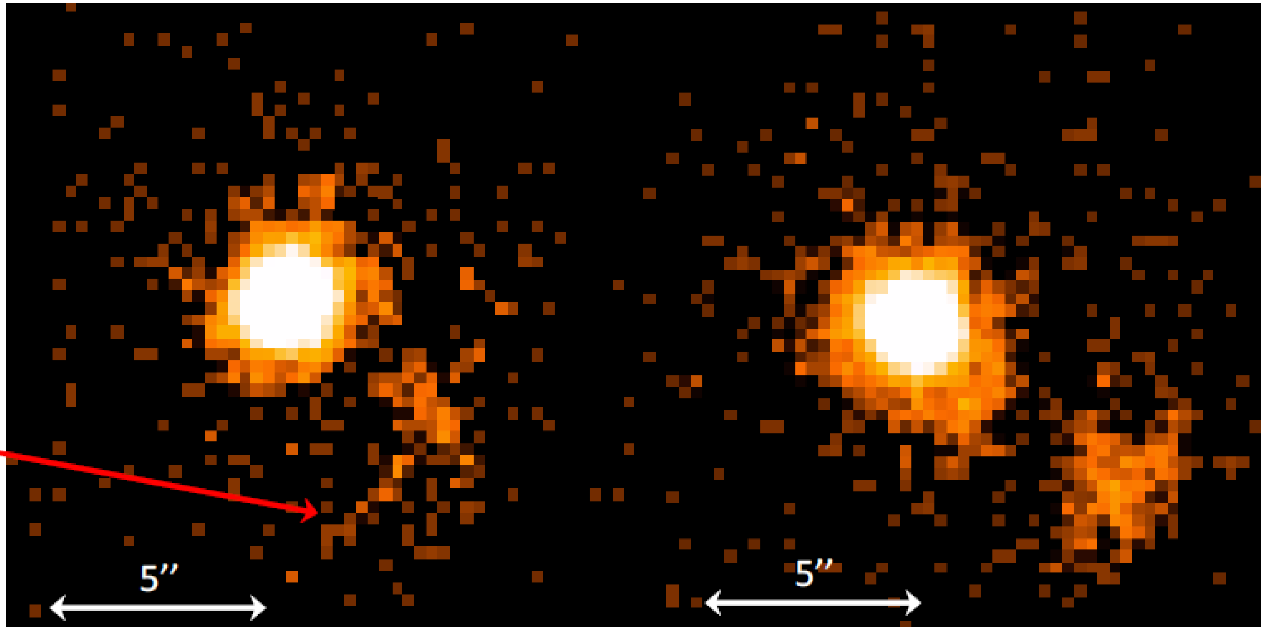

Clump separation from the binary vs time.

Jeremy Hare et al (2017)

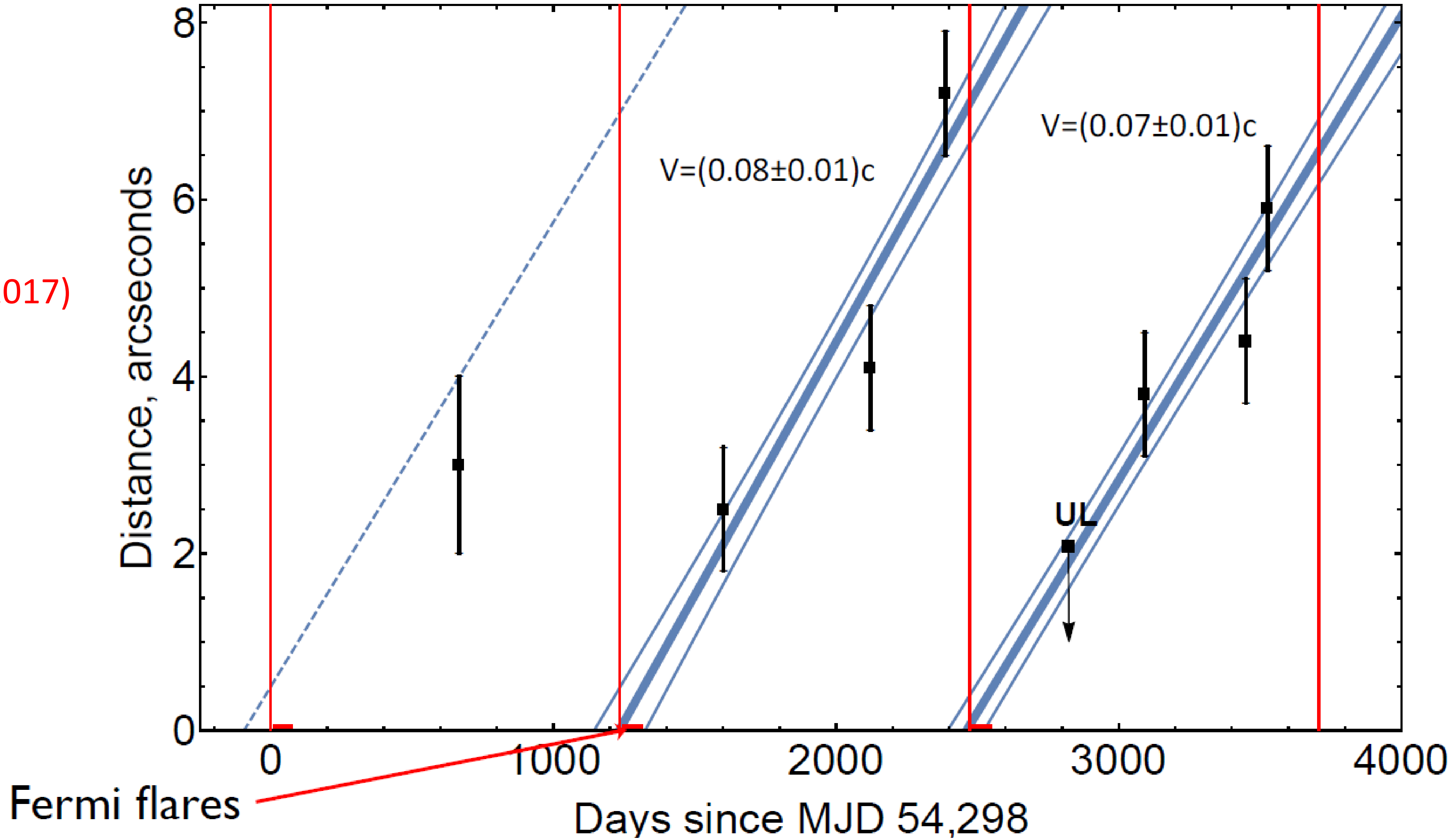

Preliminary

FGL J1086 & LSI +61 303

- T=16 day
- e=0.0

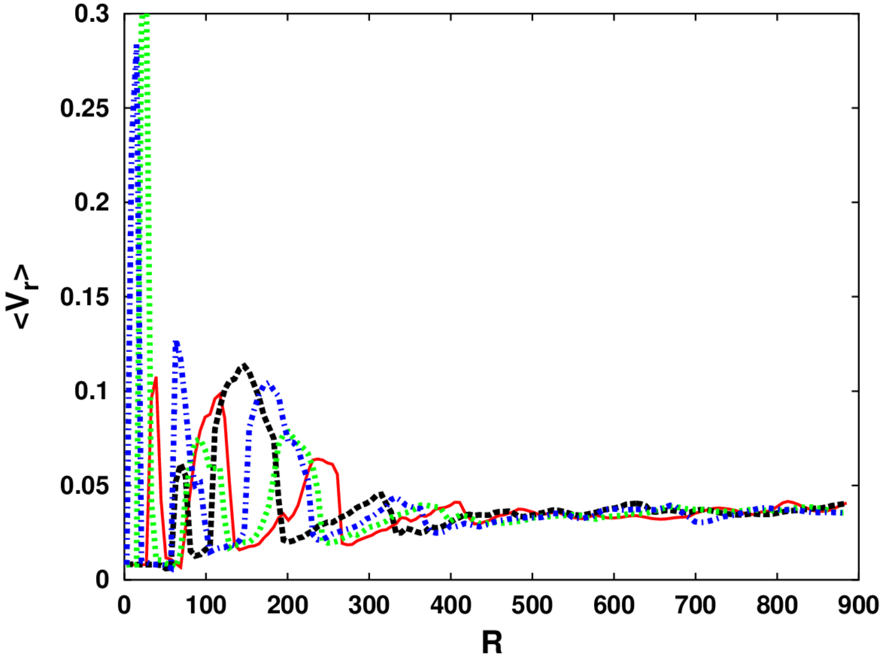

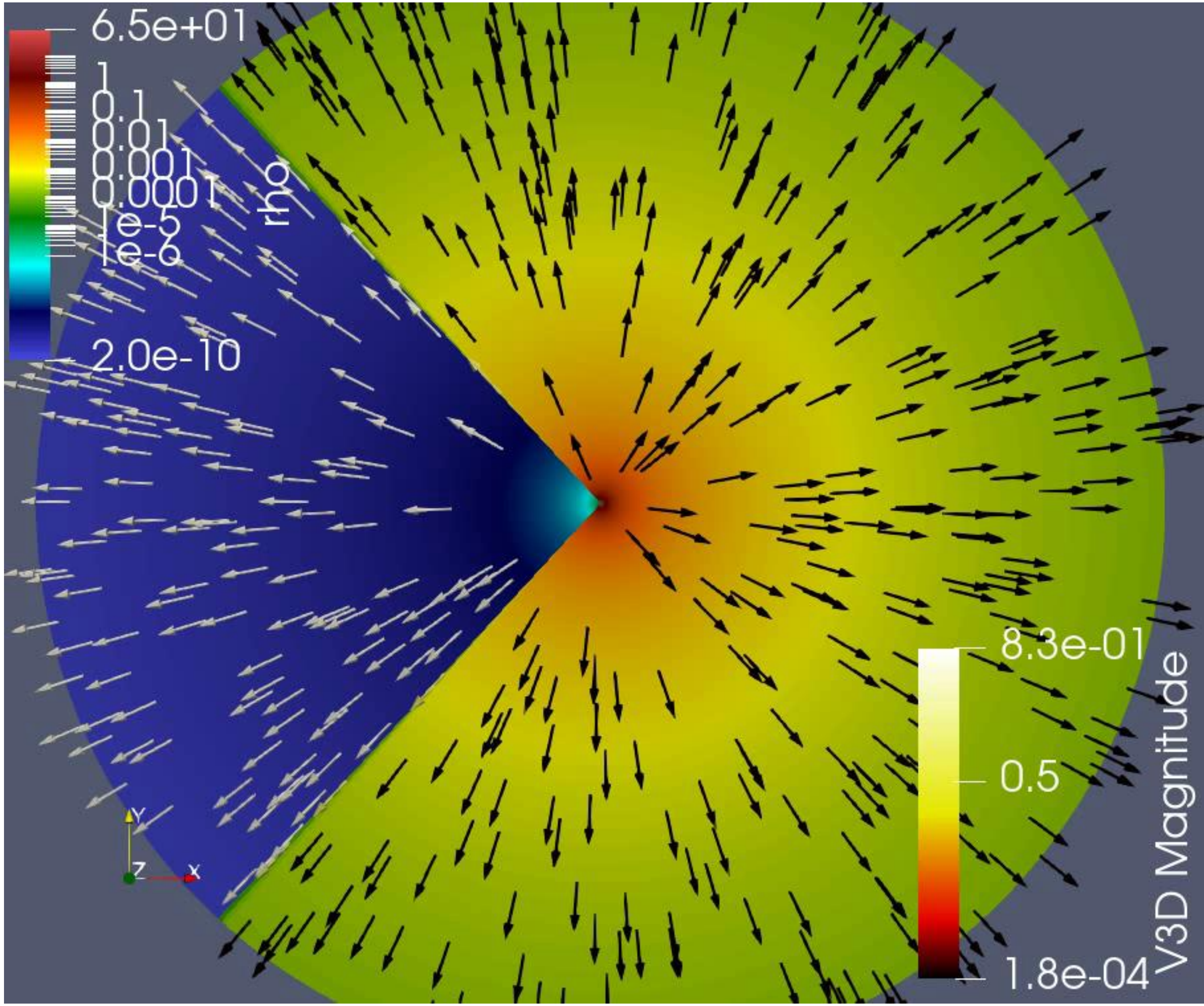

Preliminary

FGL J1086 & LSI +61 303

- T=16 day
- e=0.0

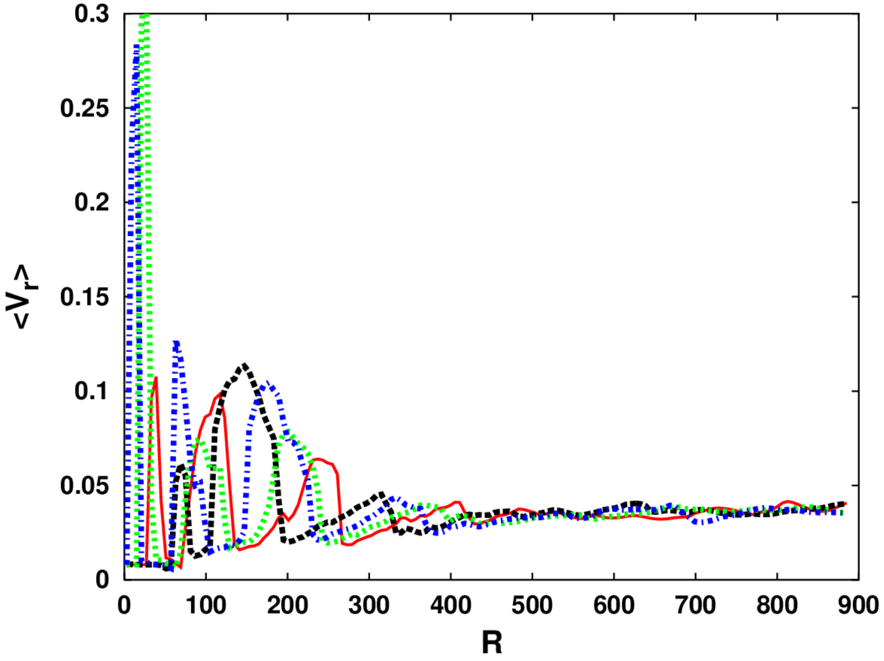

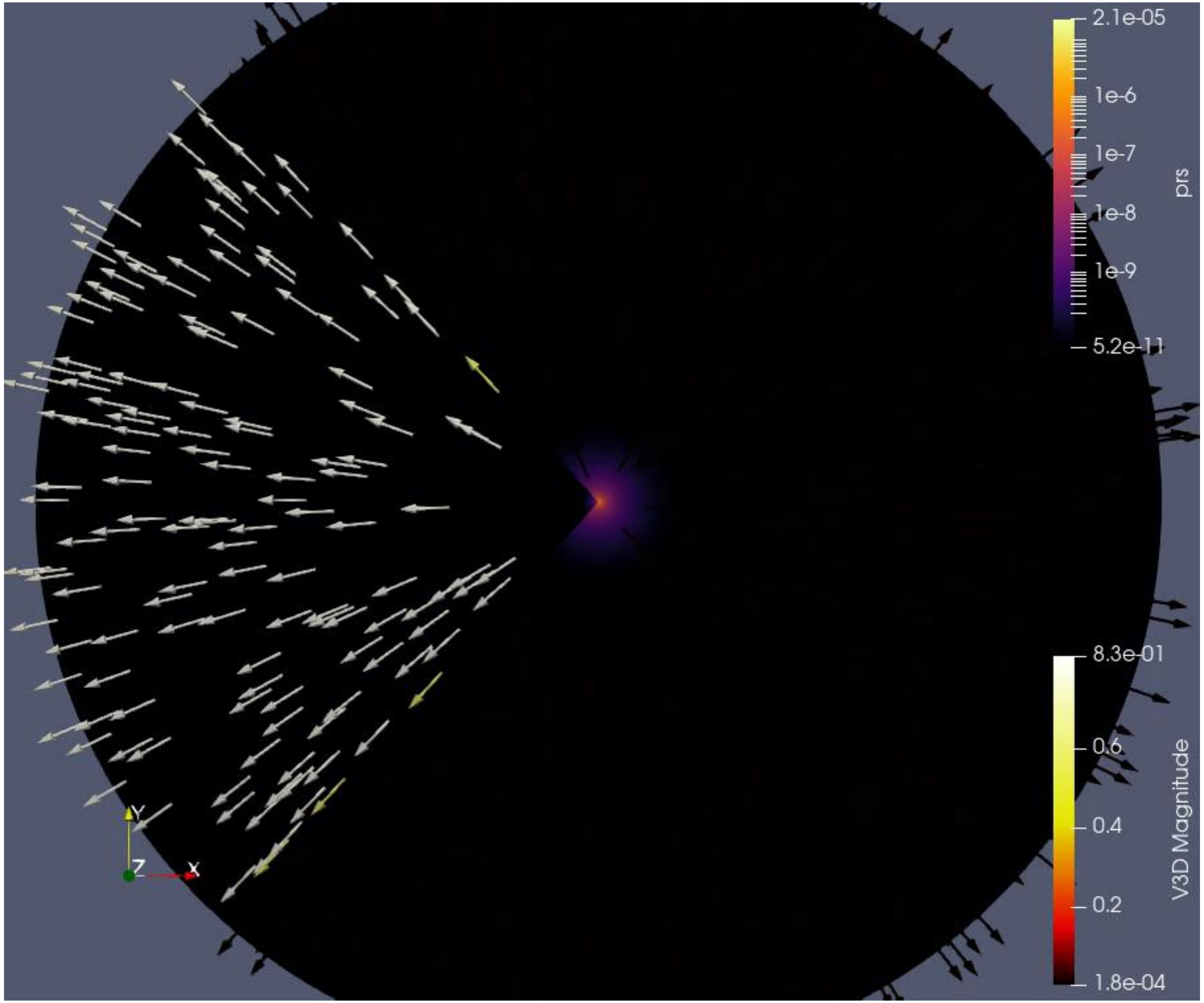

FGL J1086 & LSI +61 303

- T=16 day
- e=0.5

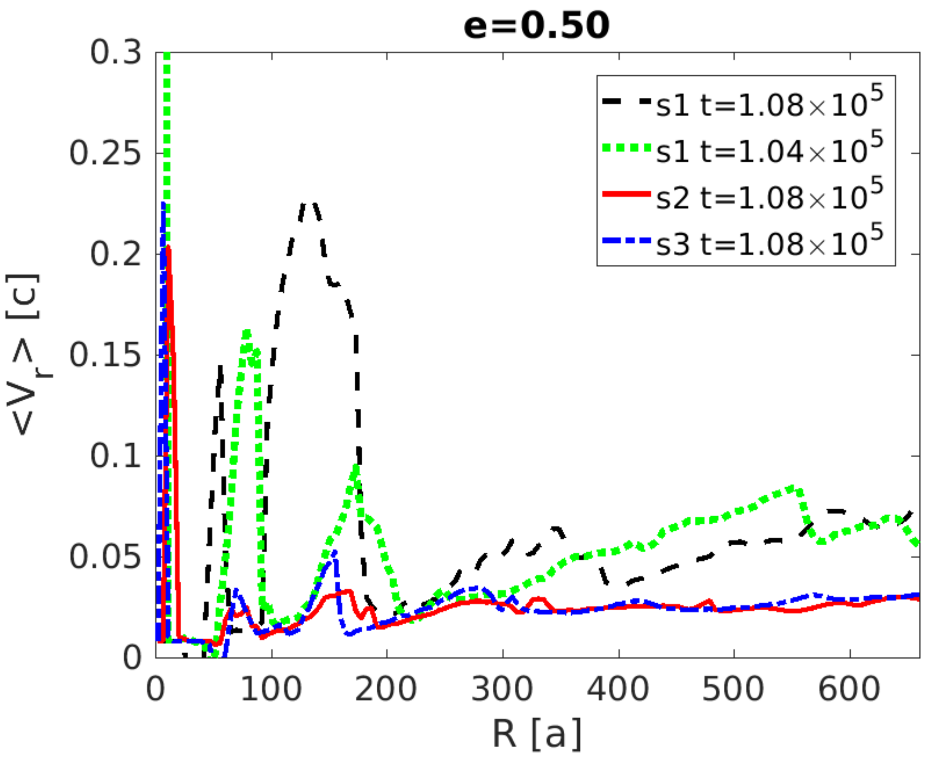

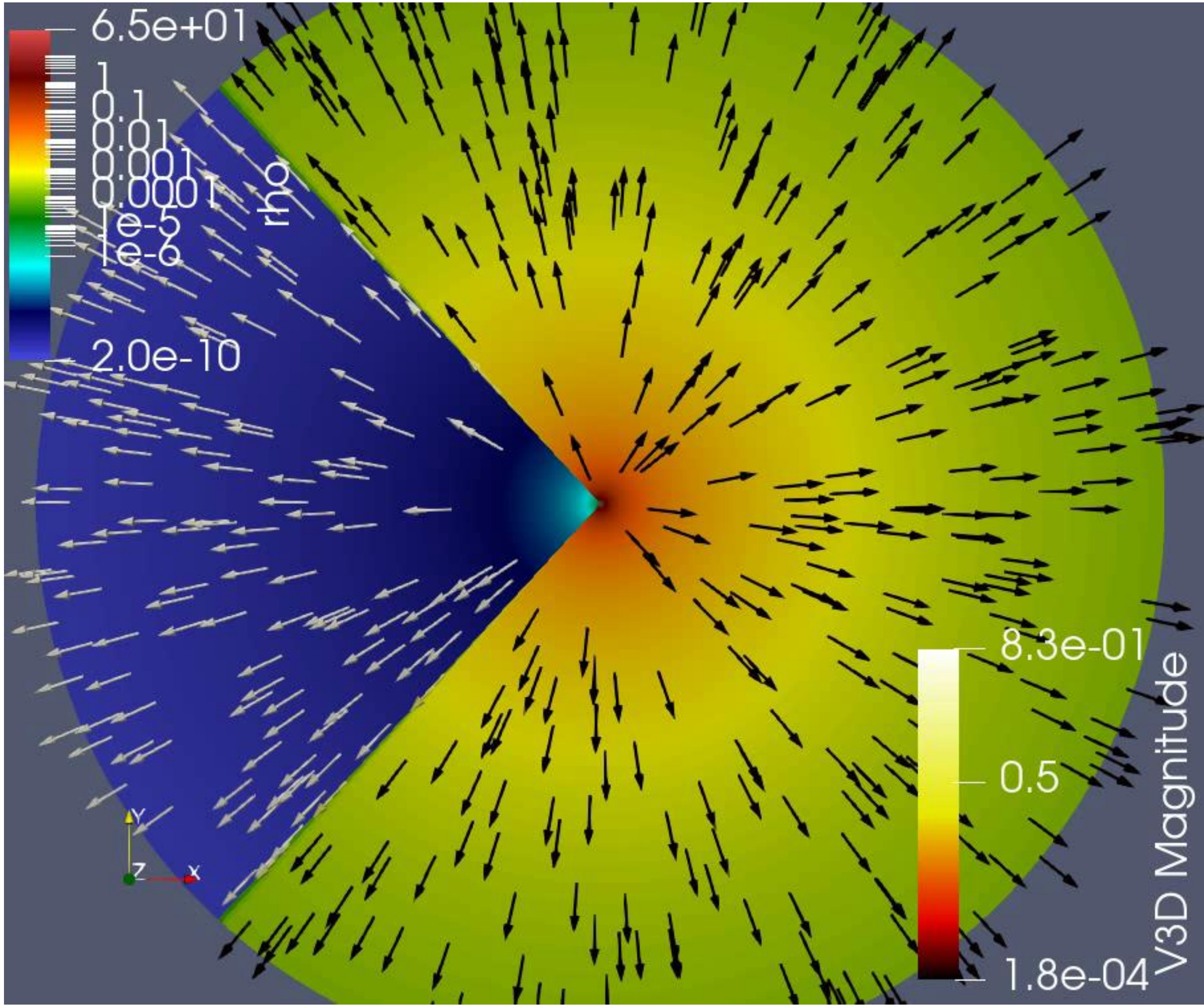

Preliminary

FGL J1086 & LSI +61 303

- T=16 day
- e=0.0-0.75

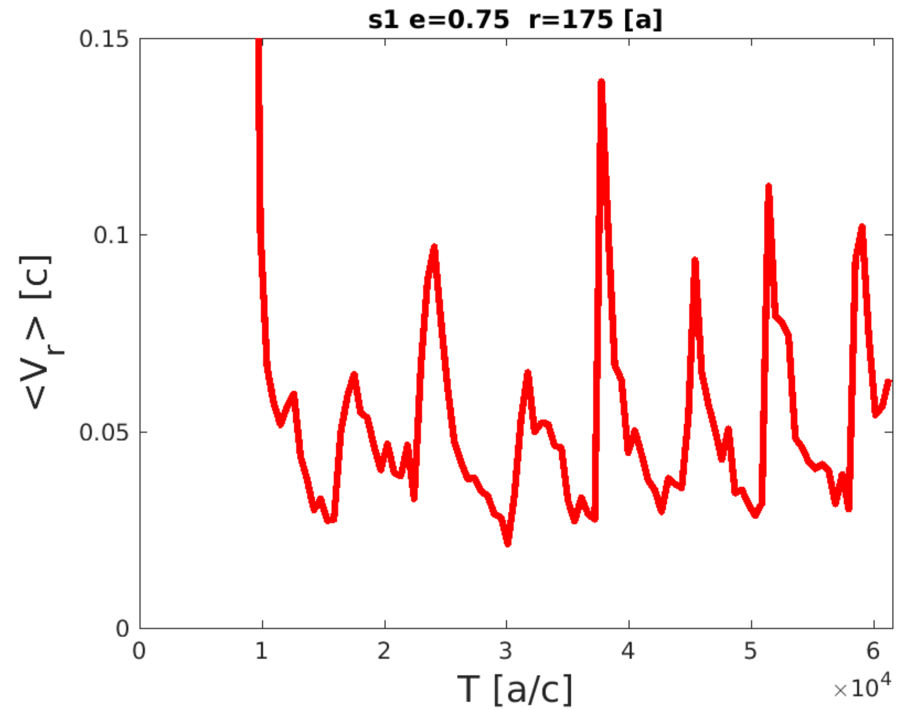

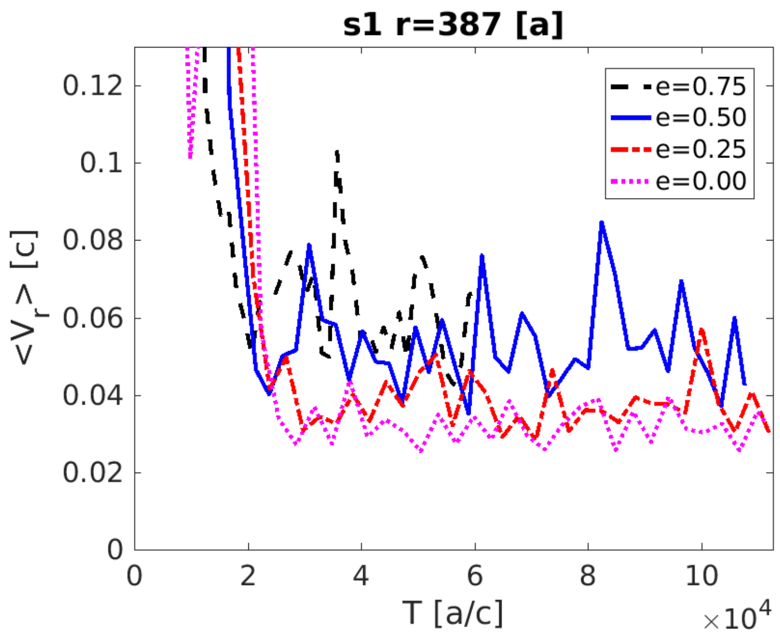

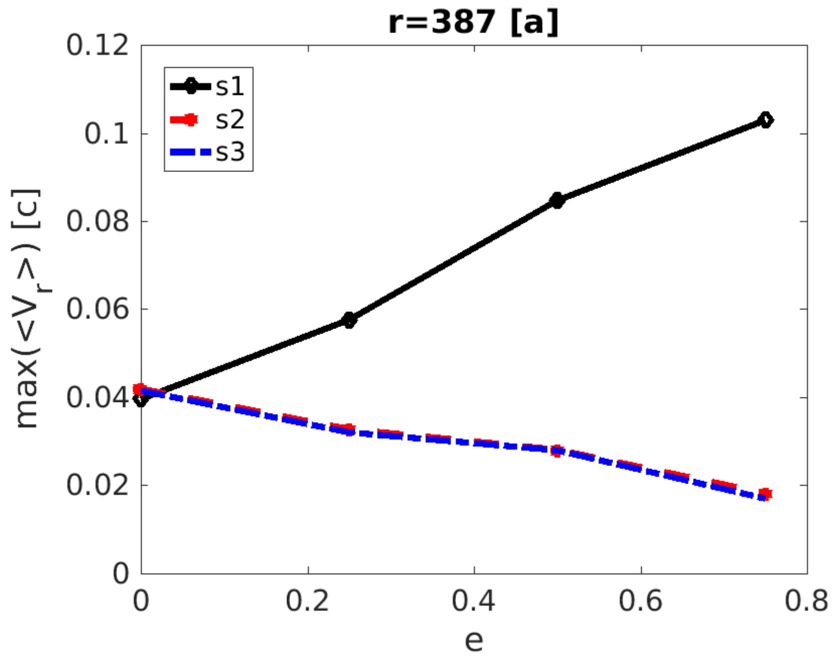

HESS J0632+57

Bosch-Ramon, Barkov, Mignone and Bordas (MNRAS 2017)

- T=321 day
- e=0.83

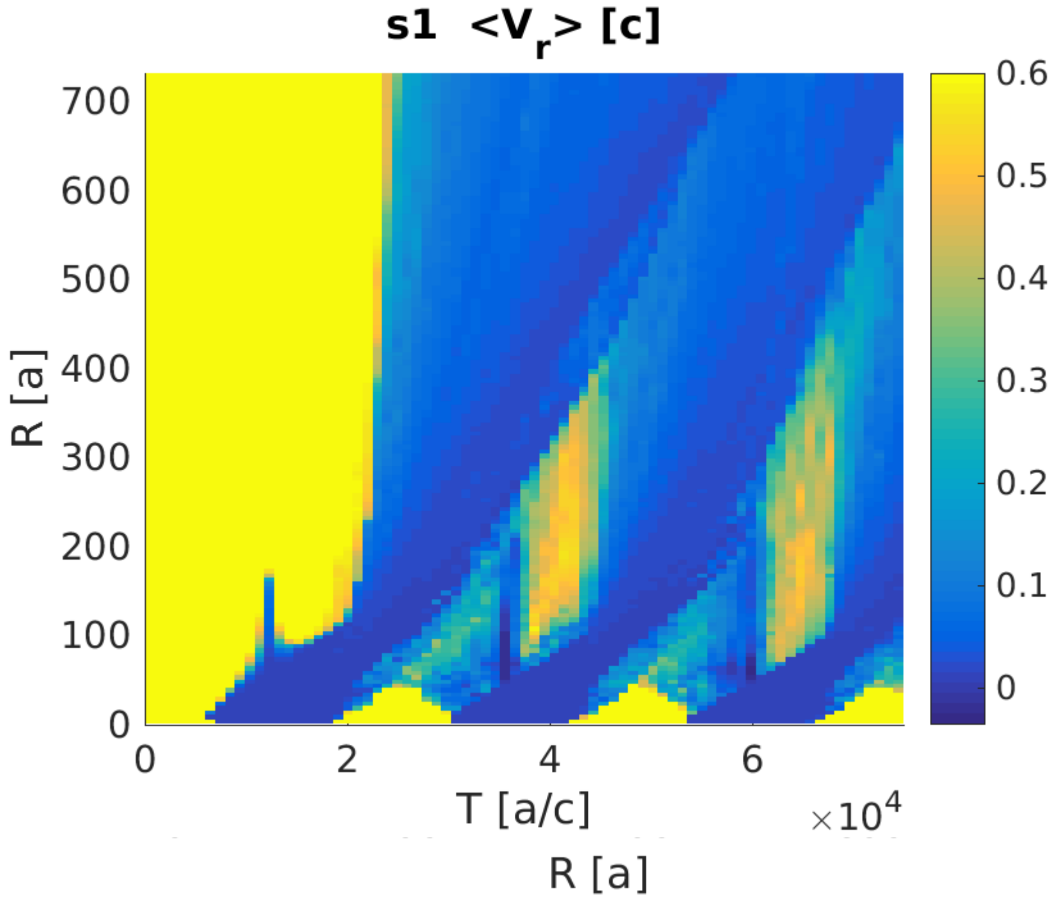

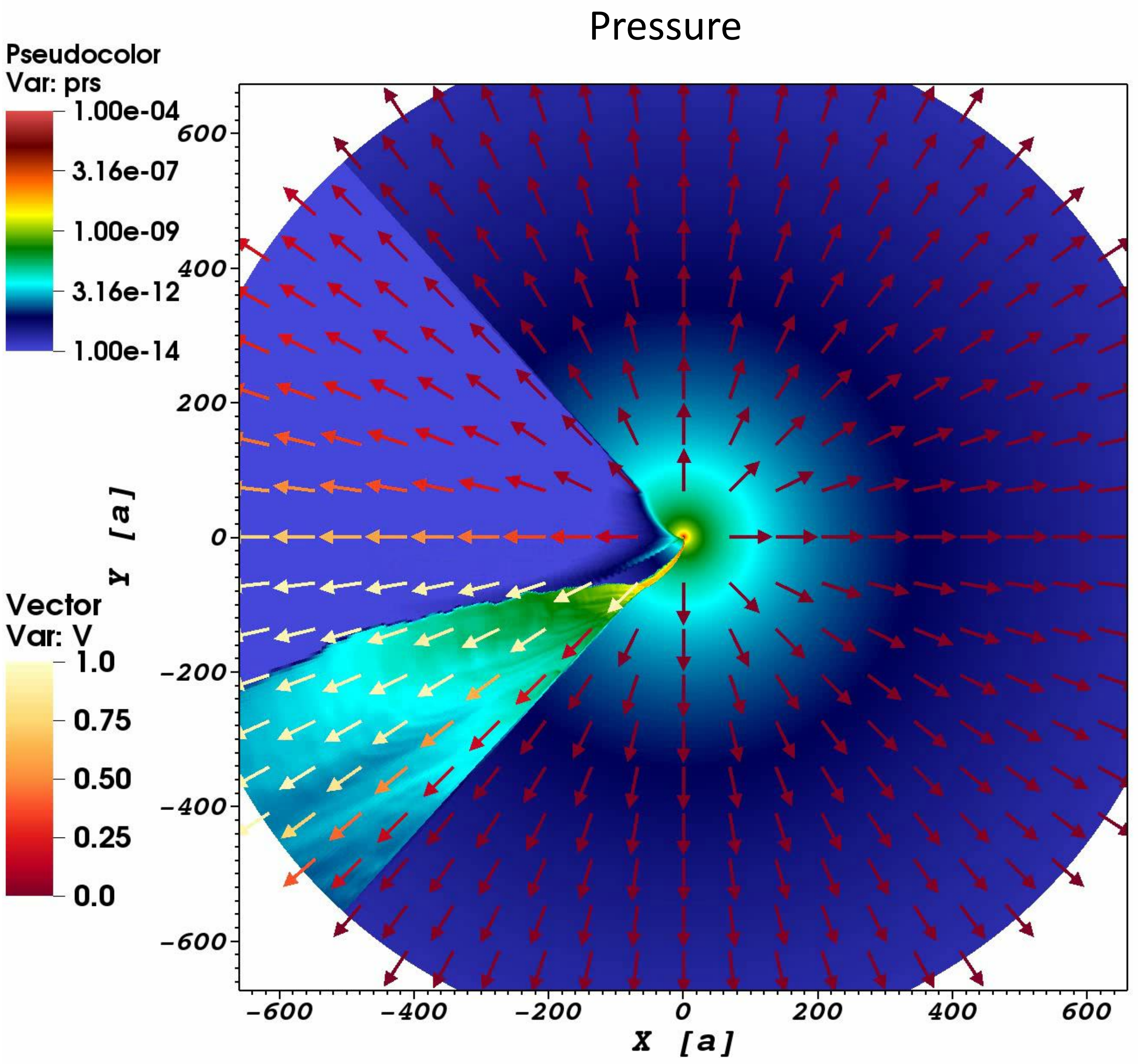

HESS J0632

Bosch-Ramon, Barkov, Mignone and Bordas (MNRAS 2017)

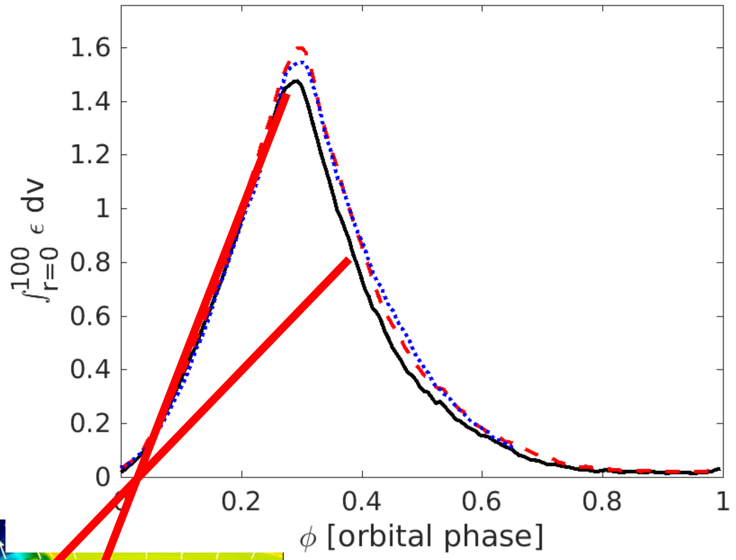

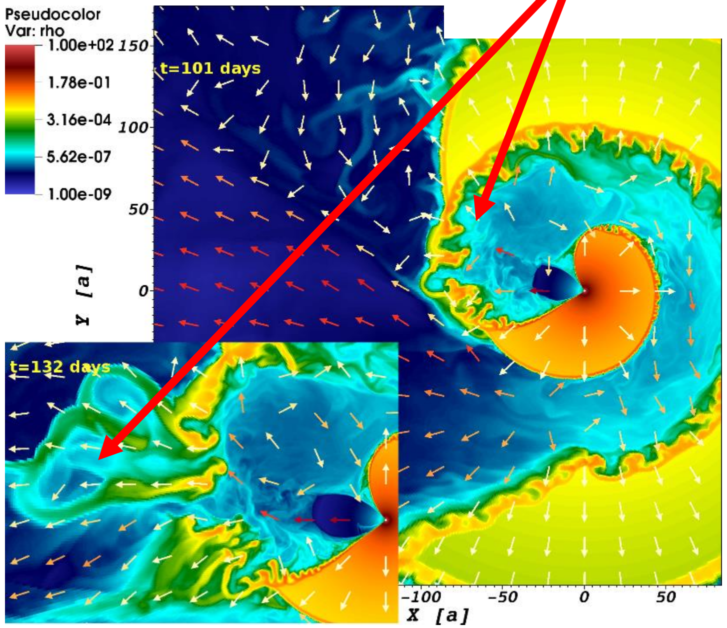

HESS J0632

X-ray

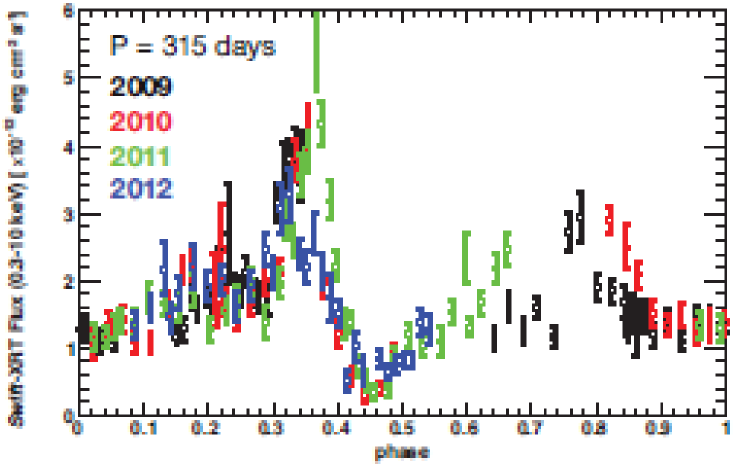

TeV

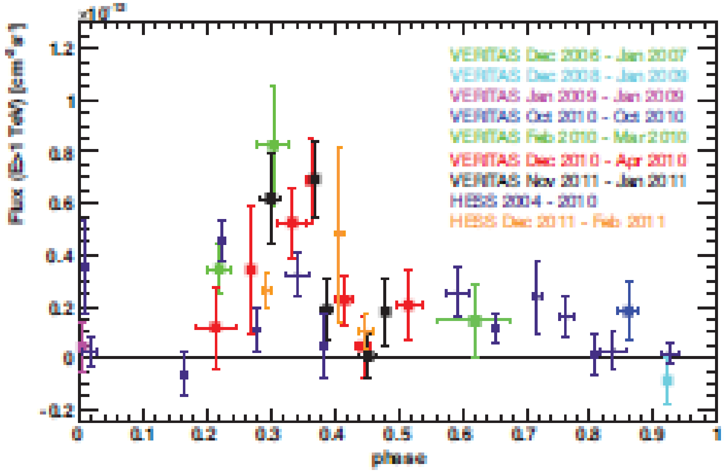

Our radiation model:

$$u_{\rm cell,NT} = \eta_{\rm NT}\, \chi_{\rm pw}\, 3P\,\Gamma$$

$$\dot\gamma_{\rm IC} = 5.5\times10^{17} T_{\rm mcc}^3 \gamma \log_{10}(1+0.55\gamma T_{\rm mcc})\times \frac{1+\frac{1.4\gamma T_{\rm mcc}}{(1+12\gamma^2 T_{\rm mcc}^2)}}{1+25\gamma T_{\rm mcc}} \left(\frac{R_*}{r}\right)^2$$

$$T_{\rm mcc} = kT_*/m_e c^2$$

Khangulyan et al. 2014

$$E_{\rm sync} \approx 0.2\left(\frac{\epsilon_{\gamma,keV}}{B\,[G]}\right)^{1/2}\ {\rm erg}$$

$$t_{\rm sync} \approx \frac{6\times10^2}{B^2\, E_{\rm sync}}\ {\rm s}$$

$$t_{\rm IC} = \gamma/\dot\gamma_{\rm IC}$$

$$t_{\rm nonrad} \sim r/v_{\rm f}$$

$$B = \sqrt{\epsilon_B 8\pi P}$$

$$f \sim \min(1, t_{\rm rad}/t_{\rm nonrad})$$

$$L_{\rm IC/sync} \sim a_{\rm Band}\int_V \frac{f\, u_{\rm cell,NT}}{t_{\rm IC/sync}}\, dV$$

Barkov & Bosch-Ramon (2018)

Barkov & Bosch-Ramon (2018)

HESS J0632

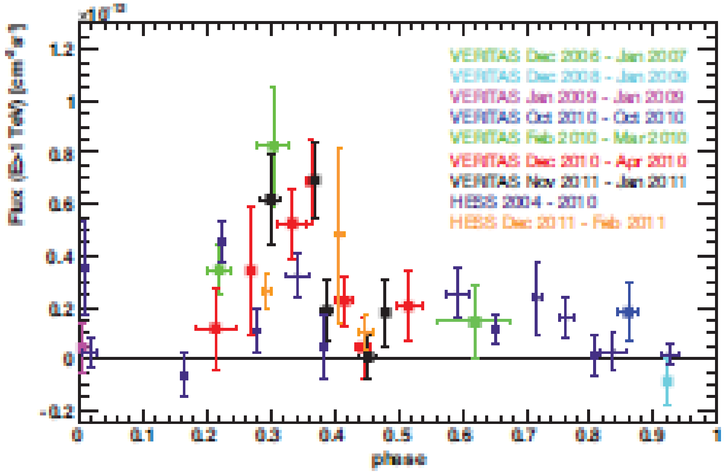

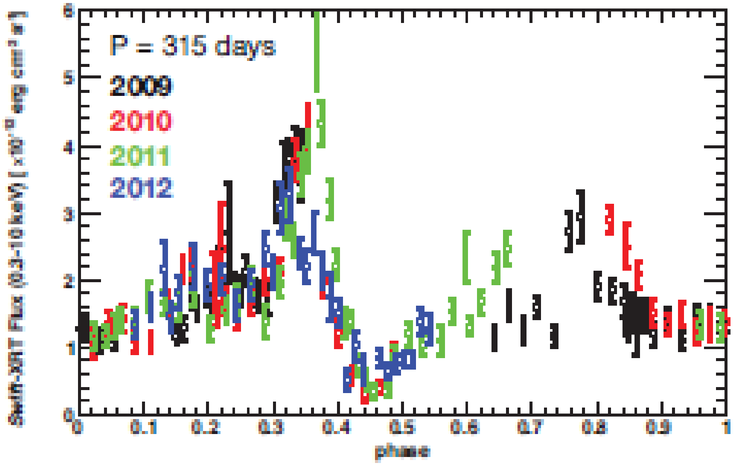

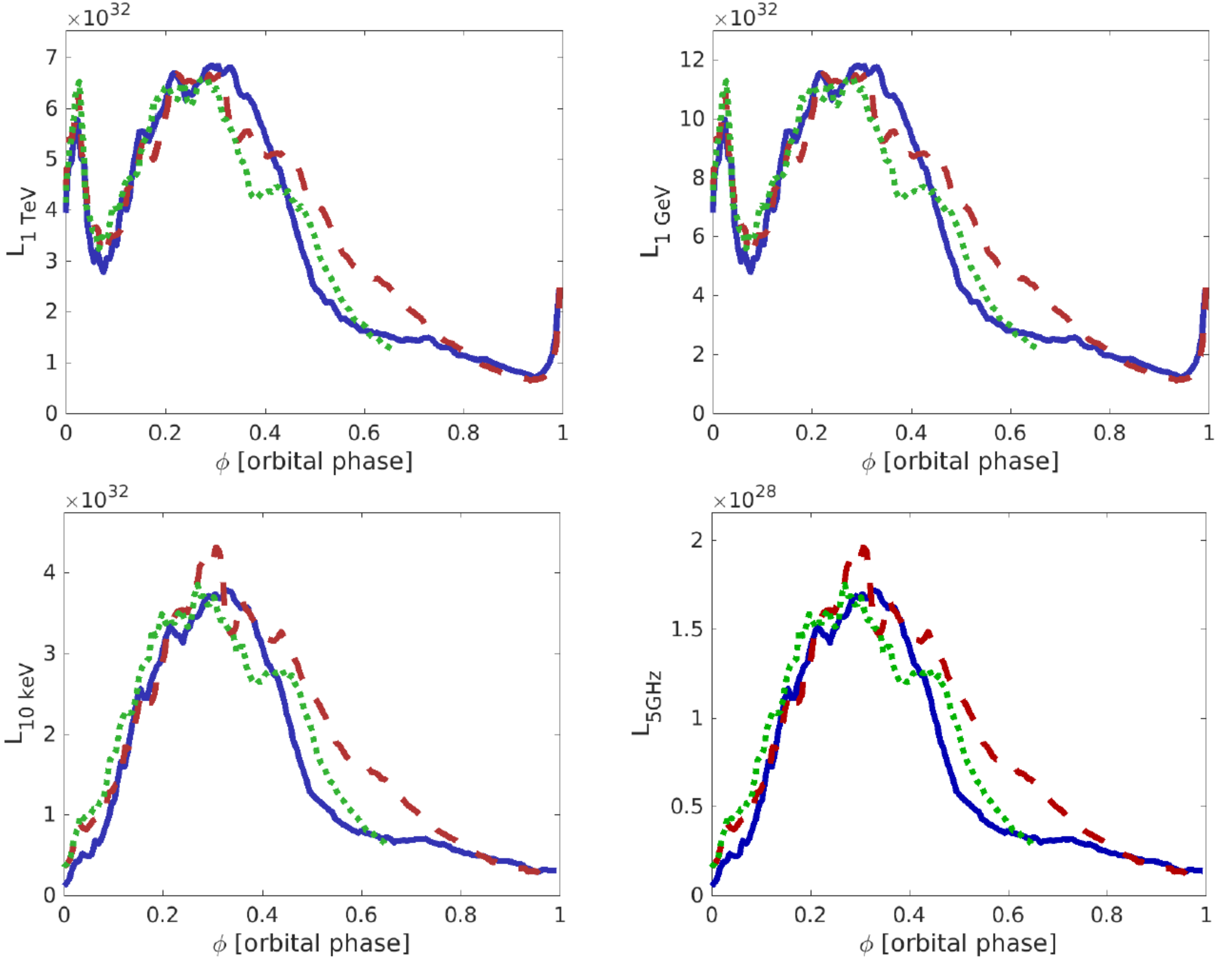

HESS J0632

Displacement on the radio maps.

Moldon et al (2011)

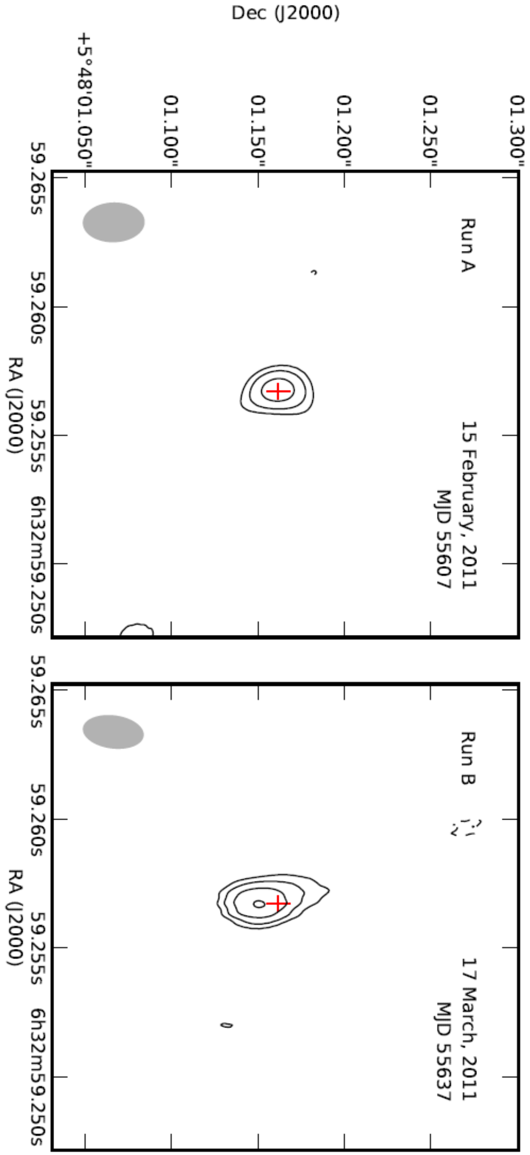

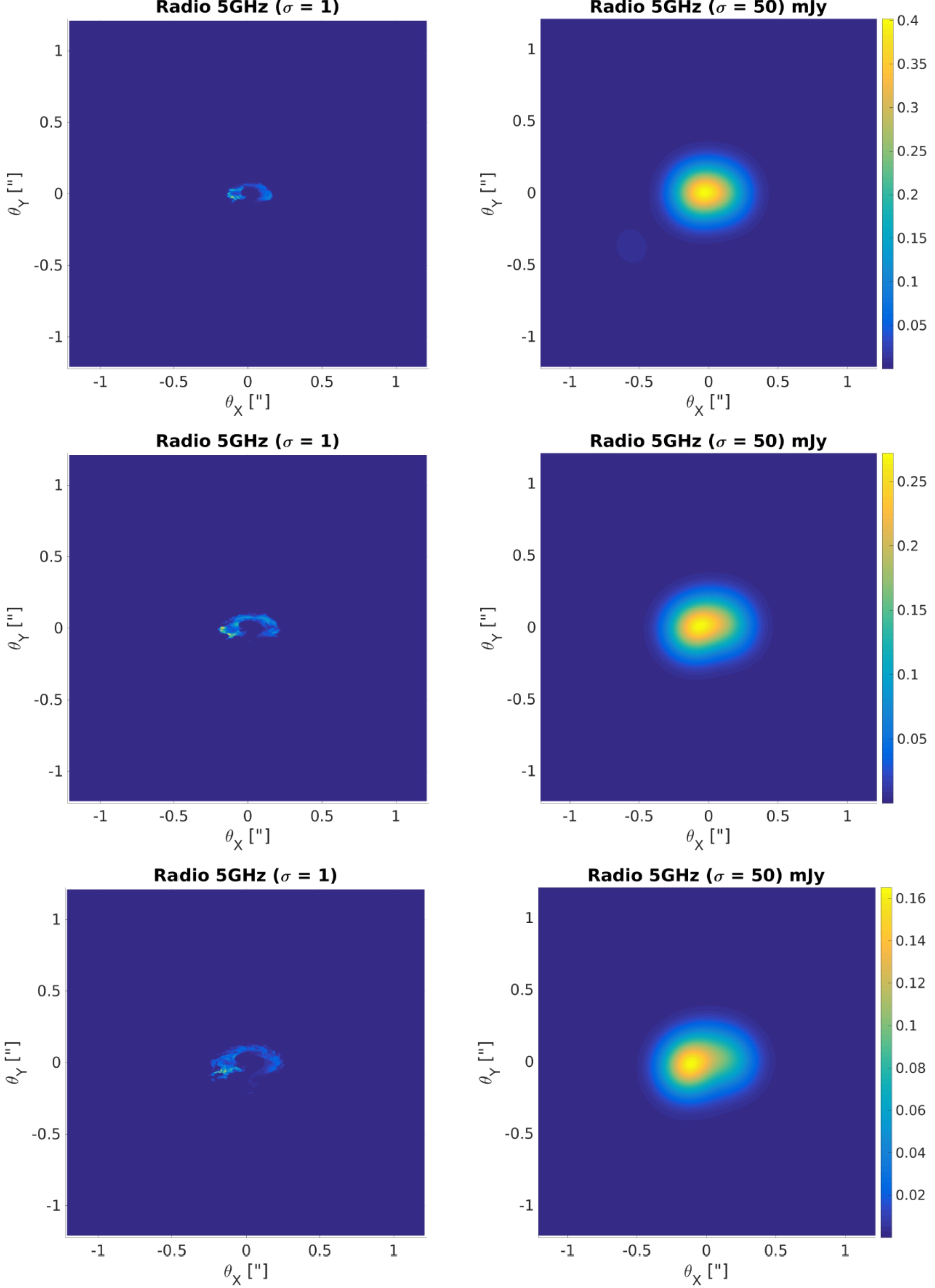

Barkov & Bosch-Ramon (2018)

Binary Systems in VHE Regime

Object	PSR B1259	LS 5039	J0632	J2032	J1086	LS I +61 303	Cyg X-1
Type	O8+Pulsar	O6+?	Be+Pulsar?	B0+Pulsar	O6+?	Be+?	O9+BH
L_s, erg/s	3×10^{37}	7×10^{38}	10^{38}	10^{38}	7×10^{38}	10^{38}	1.3×10^{39}
Orbit Size, cm	$10^{13} - 10^{14}$	$10^{12} - 3 \times 10^{12}$	$10^{13} - 7 \times 10^{13}$	$10^{13} - 5 \times 10^{14}$	$\sim 10^{13}$	$2 \times 10^{12} - 10^{13}$	3×10^{12}
Eccentricity	0.87	0.31	0.83	0.97	0.25?	0.72	0
Inclination	35	10-75	10?	50	???	~30	~30
HE Instrument	EGRET Fermi	EGRET Fermi	Fermi	Fermi	Fermi	EGRET Fermi	AGILE
GeV detection	LC+Spctr	LC+Spctr	LC+Spctr	LC+Spectr	LC+Spctr	LC+Spctr	Point
VHE Instrument	HESS	HESS	HESS, MAGIC VERITAS	VERITAS, MAGIC	HESS	MAGIC VERITAS	MAGIC HESS
TeV detection	$\sim 20\sigma$	$\sim 100\sigma$	$\sim 50\sigma$	$\sim 20\sigma$	$\sim 10\sigma$	$\sim 10\sigma$	4σ
signal	periodic	Periodic, variable	periodic	flare	periodic	Periodic, variable	flare

Conclusions:

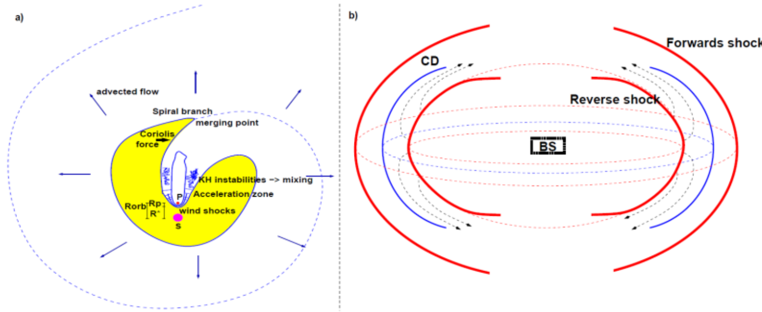

- First 3D RHD simulations of stellar and pulsar wind collision confirm that the interaction of stellar and pulsar winds yields structures that evolve non-linearly and get strongly entangled.
- Large scale simulations show that spiral arms loose their integrity on scales about 300a.
- Orbital eccentricity leads to variation of the Coriolis turnover tail size.
- $x \sim \frac{3\eta^{1/2} v_w}{2\Omega}$
- The X-ray transient observed in PSR 1259 can be explained as result of pulsar and stellar winds interaction on the eccentric binary system.
- the non-thermal activity before and around apastron can be linked to the accumulation of non-thermal particles in the vicinity of the binary, and the sudden drop of the emission before apastron is produced by the disruption of the two-wind interaction structure.

BMV, Lyutikov, Klingler and Bordas (2018)

Pulsar and ISM interaction

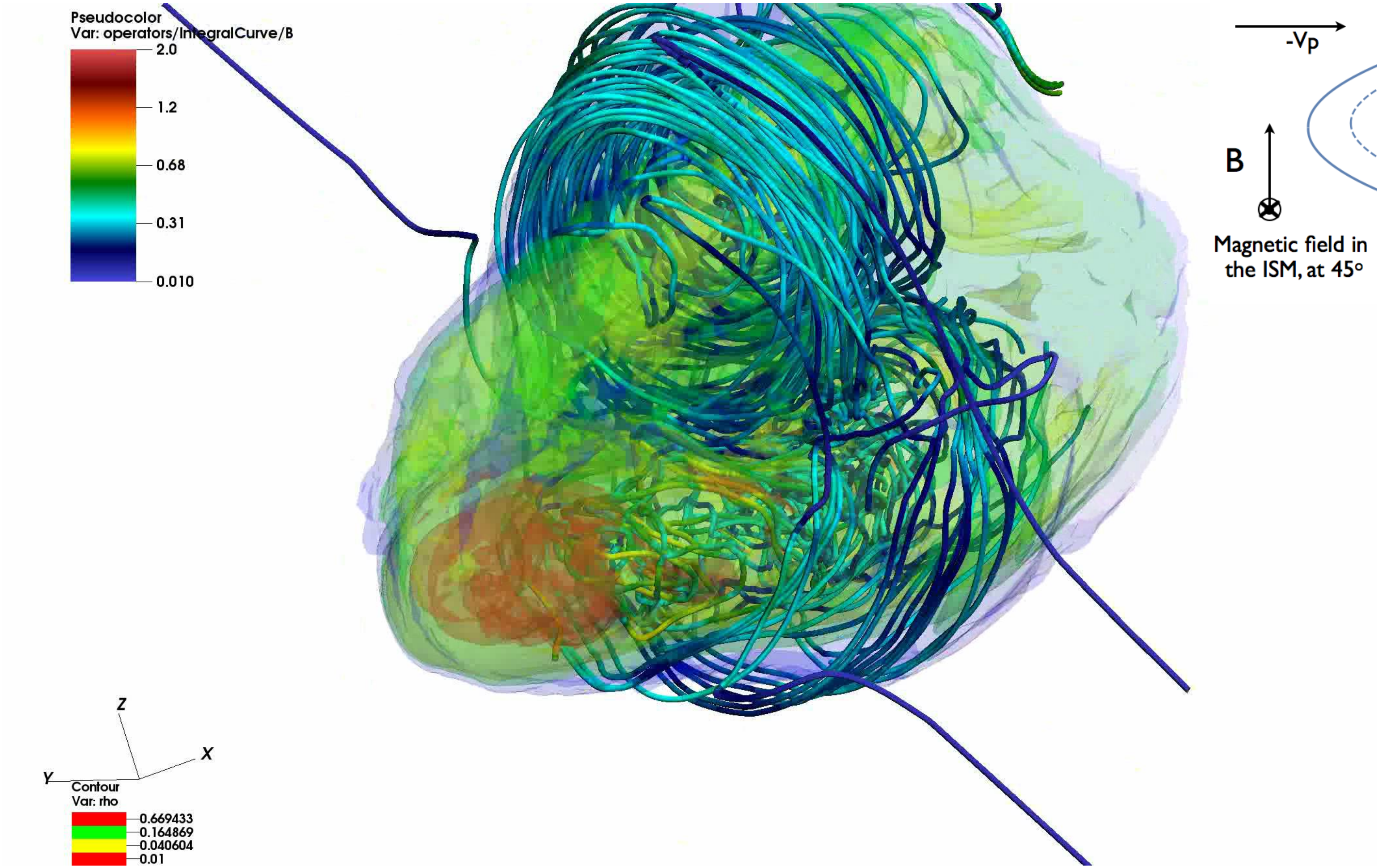

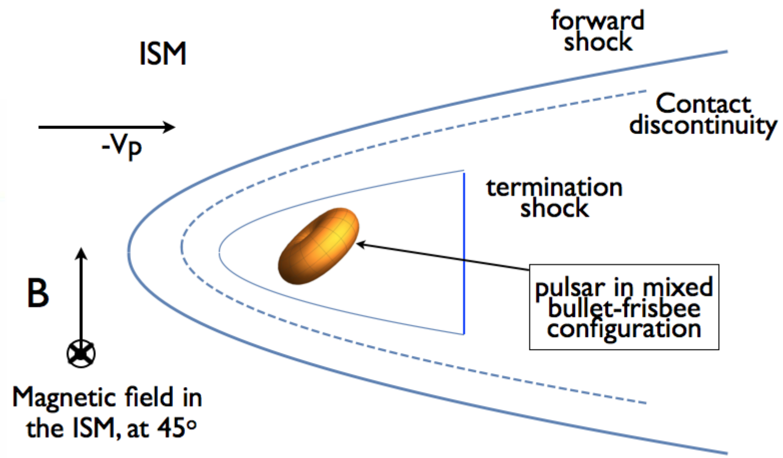

LS I +61 303

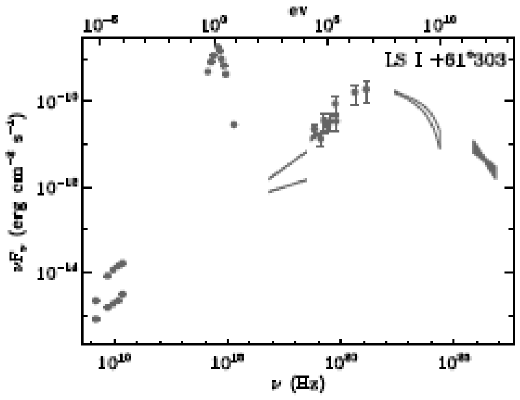

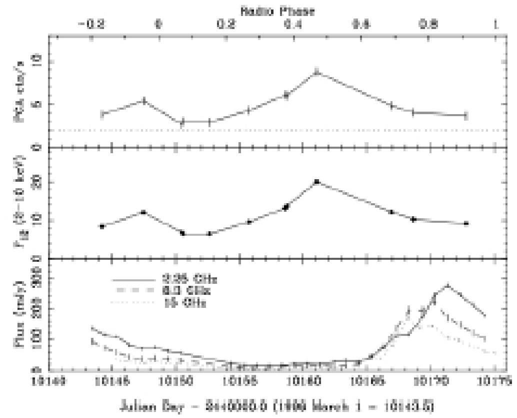

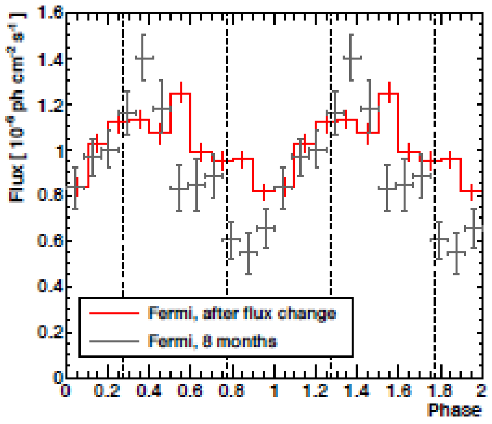

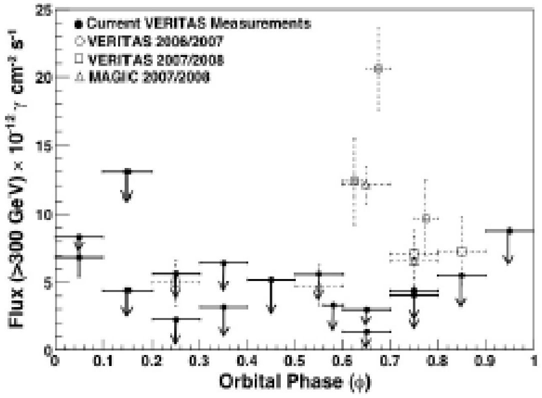

HESS J0632

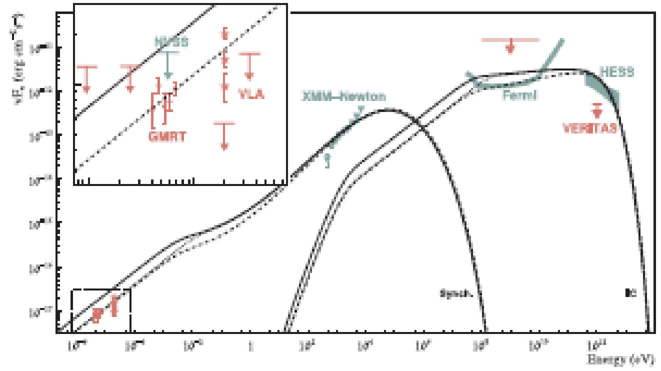

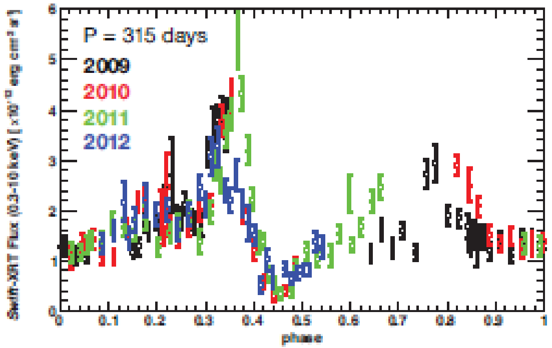

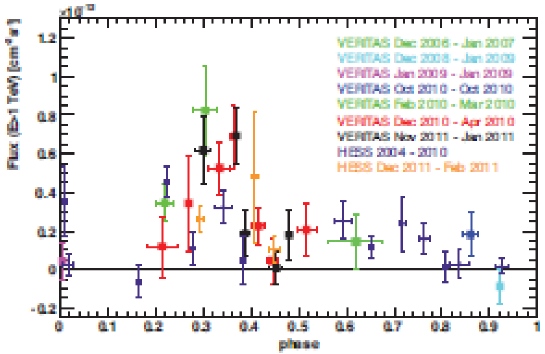

1FGL J1018

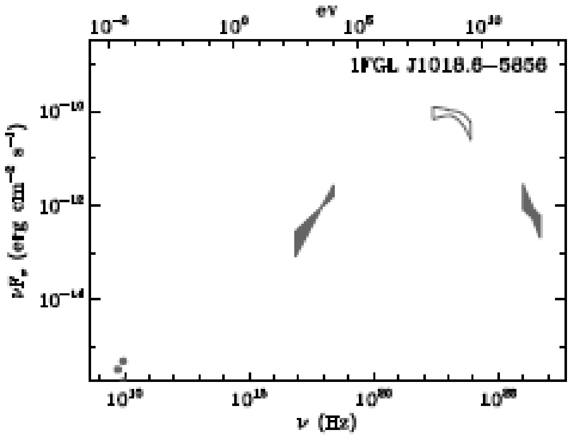

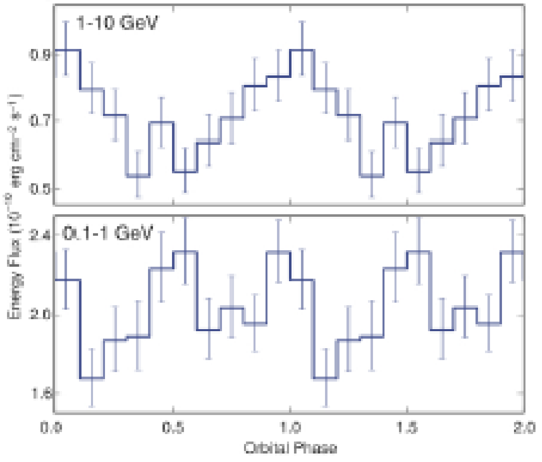

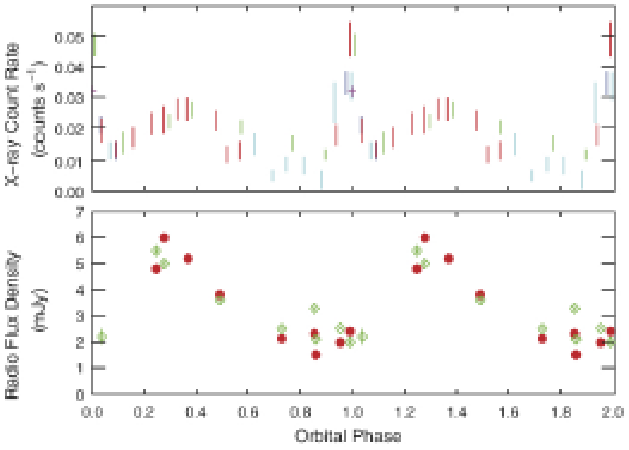

PSR 1259